Characterization of a recombinant Modified Vaccinia virus Ankara expressing the severe acute respiratory syndrome virus 2 spike protein

von Alina Tscherne, M.Sc.

Inaugural-Dissertation zur Erlangung der Doktorwürde

(Dr. rer. biol. vet.)

der Tierärztlichen Fakultät der Ludwig-Maximilians-Universität München

Characterization of a recombinant Modified Vaccinia virus Ankara expressing the severe acute respiratory syndrome virus 2 spike protein

von Alina Tscherne, M.Sc.

aus Voitsberg (Österreich)

München 2021

Aus dem Veterinärwissenschaftlichen Department der

Tierärztlichen Fakultät der Ludwig-Maximilians-Universität München

Lehrstuhl für Virologie

Arbeit angefertigt unter der Leitung von:

Univ.-Prof. Dr. Gerd Sutter

Mitbetreuung durch:

Univ.-Prof. Dr. Asisa Volz

Gedruckt mit Genehmigung der Tierärztlichen Fakultät der

Ludwig-Maximilians-Universität München

Dekan: Univ.-Prof. Dr. Reinhard K. Straubinger, Ph.D.

Berichterstatter: Univ.-Prof. Dr. Gerd Sutter

Korreferentin: Priv.-Doz. Dr. Simone M.-L. Renner

Tag der Promotion: 17. Juli 2021

Für meine Familie

Die vorliegende Dissertationsschrift enthält wissenschaftliche Daten, die im Journal *Proceedings of the National Academy of Sciences of the United States of America* (PNAS) veröffentlicht wurden:

Alina Tscherne, Jan Hendrik Schwarz, Cornelius Rohde, Alexandra Kupke, Georgia Kalodimou, Leonard Limpinsel, Nisreen M.A. Okba, Berislav Bošnjak, Inga Sandrock, Sandro Halwe, Lucie Sauerhering, Katrin Brosinski, Liangliang Nan, Elke Duell, Sylvia Jany, Astrid Freudenstein, Jörg Schmidt, Anke Werner, Michelle Gellhorn Sera, Wolfgang Guggemos, Michael Seilmaier, Clemens-Martin Wendtner, Reinhold Förster, Bart L. Haagmans, Stephan Becker, Gerd Sutter, Asisa Volz

"Immunogenicity and efficacy of the COVID-19 candidate vector vaccine MVA-SARS-2-S in preclinical vaccination", erschienen am 13.07.2021 (doi: 10.1073/pnas.2026207118.)

TABLE OF CONTENTS

I. ABBREVIATIONS

ACE2	angiotensin-converting enzyme 2
ADE	antibody-dependent enhancement
APC	antigen-presenting cell
ARDS	acute respiratory distress syndrome
Bcl-2	B-cell lymphoma 2
BSA	bovine serum albumin
CAM	chorioallantois membranes
CD	cluster of differentiation
CDC	Centers for Disease Control and Prevention
CEF	chicken embryonic fibroblasts
CO_2	carbon dioxide
COVID-19	coronavirus disease 2019
CSG	*Coronaviridae* Study Group
DAI	double-stranded RNA activated inhibitor of translation
DAPI	4′,6-Diamidin-2-phenylindol
ddH_2O	double-distilled water
DMEM	Dulbecco`s modified Eagle`s medium
DMSO	dimethyl sulfoxide
DNA	deoxyribonucleic acid
dNTP	deoxynucleosidtriphosphate
DPBS	Dulbecco`s phosphate buffered saline
dsRNA	double-stranded RNA
EBV	Epstein–Barr virus
EDTA	ethylene-diamine tetraacetate
eIF2α	eukaryotic initiation factor-2α
ELISA	enzyme-linked immunosorbent assay
ELISpot	enzyme-linked immunosorbent spot assay
ER	endoplasmic reticulum
ERD	enhanced respiratory infection
ERGIC	endoplasmic reticulum Golgi intermediate complex
EV	extracellular virion
FACS	fluorescence-activated cell sorting
FBS	fetal bovine serum
FDA	Food and Drug Agency

FP	fusion protein
GPT	glutamate-pyruvate-transaminase
hpi	hours post infection
HA	hemagglutinin
HEPES	N-(2-Hydroxyethyl)-piperazin-N′-(2-ethansulfonsäure)
HIV	human immunodeficiency virus
HR	heptat repeat
HRP	horseradish peroxidase
IC_{50}	half maximal inhibitory concentration
ICS	intracellular cytokine staining
ICU	intensive care unit
IEDB	Immune Epitope Database
i.m.	intramuscular
IMV	intracellular mature virus
IFA	Immunofluorescence assay
IFN	interferon
Ig	immunoglobulin
IL	interleukin
IRF	interferon regulatory factor
I.T.	intracellular tail
kDa	kilodalton
kb	kilo base pairs
LB	lysogeny broth
l	liter
M	Mol
MEM	minimal essential medium
MHC	major histocompatibility complex
mg	milligram
min	minute
ml	milliliter
mM	millimol
MOI	multiplicity of infection
MVA	Modified Vaccinia virus Ankara
MVA-SARS-CoV-2-S/ MVA-S	Modified Vaccinia virus Ankara expressing severe acute respiratory syndrome coronavirus 2 spike protein
NF-κB	nuclear factor kappa-light-chain-enhancer of activated B cells

nsp	non-structural protein
NTD	*N*-terminal domain
OD	optical density
o/n	over night
PBS(T)	phosphate buffered saline (tween20)
PCR	polymerase chain reaction
PFU	plaque-forming units
PMA	phorbol 12-myristate 13-acetate
PNGase F	peptide-N-glycosidase F
PUMA	p53 upregulated modulator of apoptosis
RBD	receptor-binding domain
RdRp-complex	RNA-dependent RNA polymerase complex
RNA	ribonucleic acid
rpm	revolutions per minute
RPMI	Roswell Park Memorial Institute
RPV	Rinderpest virus
RT	room temperature
RT-PCR	reverse transcription polymerase chain reaction
SARS-CoV-2	severe acute respiratory syndrome coronavirus 2
SDS-PAGE	sodium dodecyl sulfate polyacrylamide gel electrophoresis
sec	second
SFC	spot-forming cells
T.A.	transmembrane anchor
TAE	tris-acetate-EDTA
TBS	tris-buffered saline
$TCID_{50}$	tissue culture infection dose 50
TCR	T cell receptor
Th	T helper
TMB	3,3′,5,5′-Tetramethylbenzidin
TNF-α	tumor necrosis factor alpha
UV	ultraviolet
V	volt, volume
VNT	virus neutralization assay
VP-SFM	virus production serum-free medium
VSV	vesicular stomatitis virus
WB	Western Blot
WHO	World Health Organization

II. INTRODUCTION

The severe acute respiratory syndrome coronavirus 2 (SARS-CoV-2) is the causative pathogen of the global pandemic coronavirus disease 2019 (COVID-19). Due to an extremely efficient human-to-human transmission, a global spread of SARS-CoV-2 occurred within months, since affecting the daily life of millions of individuals. Many infections are asymptomatic or show mild symptoms and the estimated case fatality rate of 2-5% is lower than for infections with other coronaviruses, such as SARS-CoV-1 (~10%) (WHO 2021c) or MERS-CoV (~34 %) (WHO 2019). Nevertheless, cases of long-lasting diseases following a COVID-19 infection (long-COVID, post-COVID or chronic COVID) are described, affecting symptomatic and asymptomatic patients. The use of vaccines is the best option to halt the global threat of SARS-CoV-2 and vaccine research started at an unprecedented speed. One year after the emergence of COVID-19, more than 65 SARS-CoV-2 specific vaccine candidates are in clinical trials. By the end of February 2021, two mRNA-based vaccines and one replication-deficient adenoviral vector vaccine are already licensed for immunization in Europe. Herby, the SARS-CoV-2 spike (S) protein is the key antigen for vaccine development. Efficient activation of humoral and cell-mediated immune responses is the expected basis of protective vaccination.

The aim of this project was the generation and characterization of recombinant Modified Vaccinia virus Ankara (MVA) as a new COVID-19 candidate vaccine. In cell culture infections, the recombinant virus demonstrated high levels of genetic stability, efficient synthesis of SARS-CoV-2 S protein and a growth capacity suitable for vaccine production at industrial scale. S protein-specific humoral and cell-mediated immune responses were activated in BALB/c mice following vaccination with two different doses and two different vaccination schedules. These results contributed to a better understanding of spike antigen specific immune responses and strongly supported the further development of recombinant MVA as vaccine against SARS-CoV-2.

III. LITERATURE REVIEW

1. SARS-CoV-2: an emerging pathogen

1.1. Year 2020: Beginning of a global pandemic

On December 13th, 2019, a novel virus invaded the human population (VOLZ et al. 2020), leading to a global pandemic within a few months. The first confirmed cases were reported at a seafood market in Wuhan (China) and the new agent spread throughout the world by travelers and community-based contacts (LI et al. 2020; ZHU et al. 2020). On February 11th, 2020, the new virus was named severe acute respiratory syndrome coronavirus 2 (SARS-CoV-2) by the *Coronaviridae* Study Group (CSG) of International Committee on Taxonomy of Viruses (CORONAVIRIDAE STUDY GROUP OF THE INTERNATIONAL COMMITTEE ON TAXONOMY OF VIRUSES. 2020; HU et al. 2020). The disease caused by this agent was named coronavirus infectious disease 2019 (COVID-19) (SUN et al. 2020b) and on March 11th, 2020, COVID-19 was declared as a global pandemic by the World Health Organization (WHO) (SONG et al. 2020). Phylogenetic analysis showed relations to severe acute respiratory syndrome corona virus 1 (SARS-CoV-1) and Middle East respiratory syndrome coronavirus (MERS-CoV), both leading to smaller outbreaks in 2003 and 2012, respectively (DROSTEN et al. 2003; ZAKI et al. 2012; ZHONG et al. 2003; KSIAZEK et al. 2003). By the end of February 2021, one year after the first outbreak of COVID-19, more than 100 million global cases were confirmed with more than 2 million deaths. Globally, the United States, India and Brazil are the countries with the highest number of confirmed cases (JHU 2021).

1.2. Taxonomy and viral life cycle

SARS-CoV-2 is an enveloped, single-stranded RNA virus with a genome size of about 26 to 32 kb (CORONAVIRIDAE STUDY GROUP OF THE INTERNATIONAL COMMITTEE ON TAXONOMY OF VIRUSES. 2020; LU et al. 2020). The new virus is classified as a member of the order *Nidovirales*, family *Coronaviridae*, and subfamily *Orthocoronavirinae* (LAI et al. 2020; LU et al. 2020; WOO et al. 2012) **(Figure 1)**. Coronaviruses are found commonly

among mammals (including humans) and birds causing a variety of different infectious diseases such as respiratory, gastro-intestinal, hepatic or neurological disorders (GUY et al. 2000; SIDDELL et al. 2008). Since 2020, seven different coronavirus species are known to cause illnesses in humans.

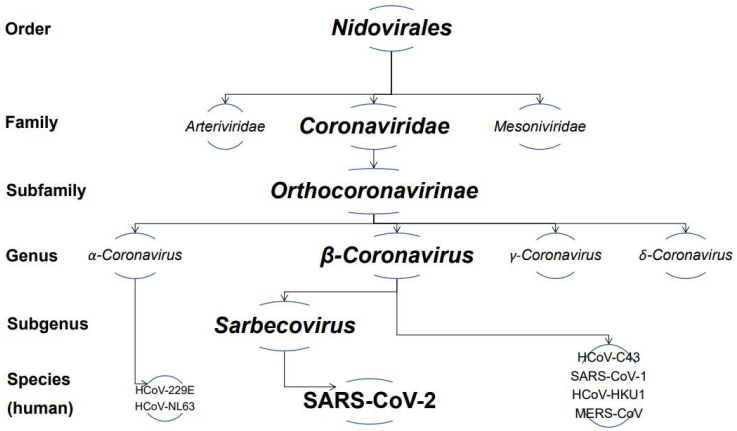

Figure 1: Classification of the seven human pathogenic coronaviruses. New SARS-CoV-2 belongs to the order *Nidovirales*, family *Coronaviridae*, subfamily *Orthocoronavirinae*, genus β- Coronavirus, *subgenus Sarbecovirus*. Adapted from (Malik 2020).

Four human *α- and β-coronaviruses* (HCoV-229E, HCoV-OC43, HCoV-NL63, and HCoV-HKU1) mainly cause cold-like symptoms, especially in immunocompromised individuals and children (GREENBERG 2016; PENE et al. 2003; VABRET et al. 2003; WOO et al. 2005), whereas the other three human β-coronaviruses, MERS-CoV, SARS-CoV-1 and SARS-CoV-2 are connected to severer illnesses (CUI et al. 2018).

Members of the family *Coronaviridae,* including SARS-CoV-2, encode four structural proteins: spike (S) protein, nucleocapsid (N) protein, membrane (M) protein and the envelope (E) protein **(Figure 2)**. Furthermore, six-teen non-structural proteins (nsp 1-16) involved in different regulatory processes (e.g., formation of replicase transcriptase complex) have also been identified (KHAILANY et al. 2020).

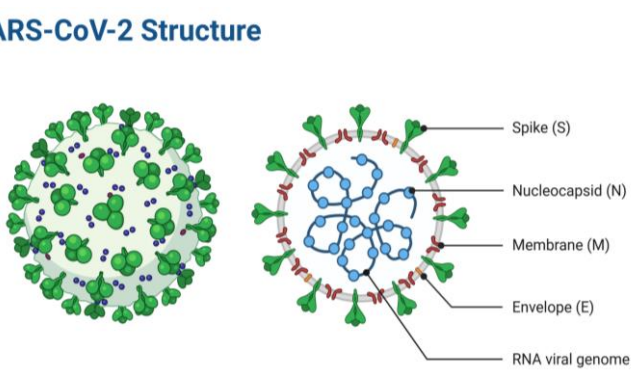

Figure 2: Structure of new SARS-CoV-2. Left: 3D structure of SARS-CoV-2. Right: SARS-CoV-2 encodes four structural proteins: spike (S) protein (green), membrane (M) protein (red), envelope (E) protein (yellow) and nucleocapsid (N) protein (light blue) capsuling the viral RNA (dark blue). Created with BioRender.com

The envelope protein is a very small, membrane integral protein with 8.4-12.0 kDa in size, (KUO et al. 2006; SCHOEMAN and FIELDING 2019) which is structured into three main parts: a small hydrophilic amino (*N*) - terminus (7-12 amino acids), a large hydrophobic transmembrane domain (25 amino acids) and a hydrophilic carboxyl (*C*) - terminus (CORSE and MACHAMER 2000; LIAO et al. 2006). The E protein is predominantly found in the endoplasmic reticulum and the Golgi complex, supporting the viral assembly and trafficking of infectious virions (CORSE and MACHAMER 2000; OPSTELTEN et al. 1995).

The nucleocapsid protein is phosphorylated and associated with the viral RNA, by capsuling the genomic material within the viral particles. The N protein contains two RNA-binding domains (*N*-terminal and *C*-terminal domain) connected with a serine/arginine rich linkage region. Due to the high amount of positively charged amino acids, it is able to bind to the viral RNA (HUANG et al. 2004; HURST et al. 2009; SAIKATENDU et al. 2007). The membrane protein with about 25-30 kDa in size has three transmembrane domains (ARMSTRONG et al. 1984), an *N*-terminal ectodomain and a C-terminal endodomain. The M protein is responsible for the shape of the virion and maintains the membrane curvature. Furthermore, the M protein is able to bind

to the nucleocapsid protein (NAL et al. 2005).

The spike glycoprotein is around 150 kDa in size and highly N-glycosylated. It is located as a trimer on the surface of the virion showing a crown-like (“corona”) appearance (BELOUZARD et al. 2012) **(Figure 3)**.

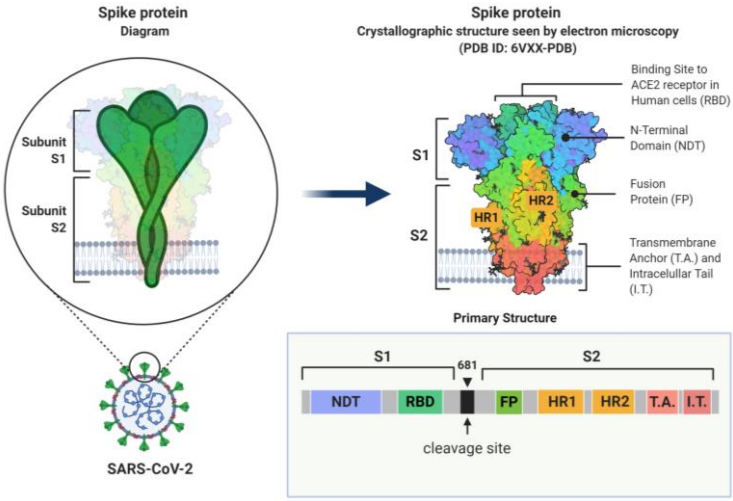

Figure 3: Structural analysis of SARS-CoV-2 spike (S) protein. The S protein consists of two subunits, S1 and S2, which are cleaved at a furine cleavage site during the entry of the host cell. The S1 subunit contains an *N*-terminal domain (NTD) and the receptor-binding domain (RBD). The S2 subunit contains the fusion protein (FP), a heptad repeat 1 (HR1), a heptad repeat 2 (HR2), a transmembrane anchor (T.A.) and an intracellular tail (I.T). Created with BioRender.com

The full-length S protein subsists in a metastable pre-fusion conformation, undergoing structural rearrangement to unite with the host cell membrane (BOSCH et al. 2003; LI 2016). Upon entry to the host cell, cleavage at a furine cleavage site is mediated by host cell proteases, splitting full-length spike protein into the S1 and S2 subunit. The S1 subunit is responsible for receptor binding, whereas the S2 subunit helps to maintain the structure of the S protein (ABRAHAM et al. 2004; LUYTJES et al. 2004; GROOT et al. 2005). Within the S1 subunit, the receptor-binding domain (RBD) is able to bind to the human angiotensin-converting enzyme 2 (ACE2) receptor with its receptor-binding

motif (RBM). The ACE2 receptor is broadly distributed in various tissue cells, including heart, testis and intestine. There, ACE2 has a regulatory function to maintain heart or kidney function or control the blood pressure (LI et al. 2005; LI et al. 2003; LUAN et al. 2020).

The entry of SARS-CoV-2 relies on an interplay between the virion and the host cell **(Figure 4)**. The viral particles interact with specific proteins that are found on the surface of the host cell. The spike protein plays an important role in this early stage of infection by facilitating receptor binding and fusion with the host cell membrane. After binding to the ACE2 receptor, the envelope protein fuses with the cell membrane, introducing the viral RNA genome into the host cell (BELOUZARD et al. 2012; SHANG et al. 2020; ZHOU et al. 2020). The RNA genome is translated into polypeptides by the host cell translation machinery and they are cleaved into non-structural proteins, including components to form the RNA-dependent RNA polymerase (RdRp) complex (HARTENIAN et al. 2021). The RdRp complex (nsp 12) generates a negative-sense genome and RNAs, which serve as templates to synthesize positive-sense progeny genomes and mRNAs (SAWICKI and SAWICKI 2005). Some of these mRNAs are translated into accessory and structural proteins which are studded on the endoplasmic reticulum - Golgi intermediate compartment (ERGIC), a mobile compartment responsible for trafficking between endoplasmic reticulum (ER) and Golgi complex (APPENZELLER-HERZOG and HAURI 2006). The positive-sense RNA is capsulated by the nucleocapsid protein and incorporated into the ERGIC. The enveloped virion is formed and released from the infected host cell by exocytosis (HARTENIAN et al. 2021).

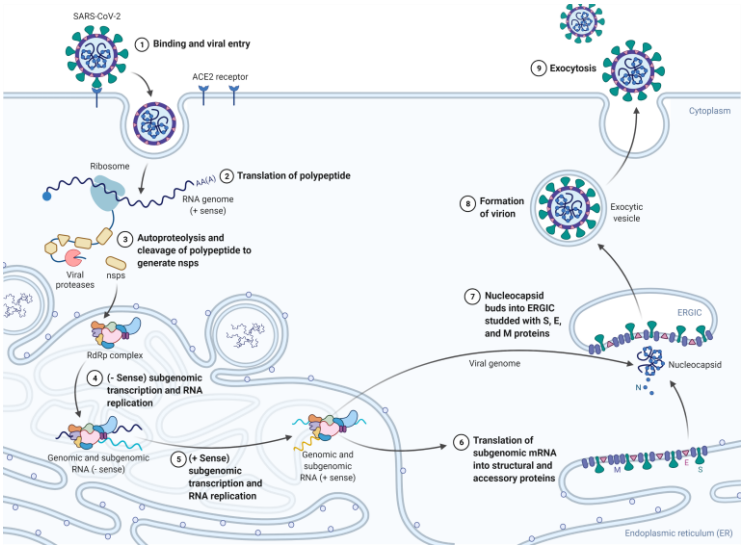

Figure 4: Replication cycle of SARS-CoV-2. Cell entry is mediated by the spike protein (1) binding to the ACE2 receptor. The RNA genome is released into the host cell (2) and translated into polypeptides. The polyproteins are cleaved into non-structural proteins (nsps) and the negative-sense RNA is transcribed (4), serving as a template to transcribe the positive-sense RNA (5). The subgenomic mRNA is translated into the structural proteins (spike protein, membrane protein and envelope protein) and other accessory proteins (6). These proteins are studded on the ERGIC, where the nucleocapsid protein (+ viral RNA) is budding (7). The virions are formed (8) and released via exocytosis (9) (HARTENIAN et al. 2021). Created with BioRender.com

1.3. Clinical manifestations

SARS-CoV-2 is mainly transmitted via droplets during the contact between infected and uninfected individuals. The main routes of transmission are coughing, sneezing, spitting or talking. Other routes were also observed, including sweat, stool, urine, and respiratory secretions (DING et al. 2004; PRAJAPAT et al. 2020; ZAYAS et al. 2012). The infection is caused by the contact of infectious droplets with the mucous membranes of eyes, nose and mouth (DU et al. 2020; WANG et al. 2020b).

COVID-19 is classified into three categories, depending on the severity of the illness: mild, severe and critical (CHEN et al. 2020b; HUANG et al. 2020; TIAN et al. 2020; WU and McGOOGAN 2020). The most common symptoms of

COVID-19 are fever, cough, shortness of breath, headache, confusion, olfactory and taste disorder. Furthermore, many patients develop severe lung disease, causing the acute respiratory distress syndrome (ARDS) and inflammatory mediator associated airway inflammation. These syndromes result in impaired alveolar oxygenation and hypoxemia (CALABRESE et al. 2020; CHEN et al. 2020a; TIAN et al. 2020). Other severe complications are metabolic acidosis, multiple organ failure or acute cardiac failure (HUANG et al. 2020). Moreover, about 26% of SARS-CoV-2 infected patients end up at the intensive care unit (ICU), and elderly or patients with pre-existing illnesses have a poor prognosis (DENG and PENG 2020). Severe events developed by patients at the ICU include pneumonia and a so-called cytokine storm, driven by an over activation of the immune system. Multiple cytokines (IL-6, IL-10, IFN-γ, TNF-α) could be detected at high amounts in the plasma of those patients (GAO et al. 2020; SPADARO et al. 2019).

Although the range of symptoms is broad, and up to now, several millions of individuals have been infected with SARS-CoV-2, most cases follow mild symptoms and patients recover within a few days or weeks. Nevertheless, cases of long-term effects (post-COVID, chronic COVID, or long-COVID) were reported in the last couple of months, affecting both asymptomatic and symptomatic patients. As SARS-CoV-2 can infiltrate every organ, various long-term effects were observed, including lung and neuronal injury (BOURGONJE et al. 2020; WANG et al. 2020a).

1.4. Treatment and prevention

Currently, no treatments are available and therefore, only supportive care is possible. There are various guidelines recommending treatments against COVID-19 such as bed rest with caloric intake, oxygen therapy via face mask, antiviral treatment (ribavirin, remdesivir, lopinavir/ritonavir, IFN-α, (hydroxy)chloroquine), plasmapheresis or immunotherapy (tocilizumab) (CHEN et al. 2020c; KLUGE et al. 2021).

Lopinavir/ritonavir are mainly used in patients with less severe syndromes during the early stage of infection. The drugs inhibit protease enzymes and were

used successfully against MERS-CoV and SARS-CoV-1 (CHUNG et al. 2020; GUL et al. 2020). Although used in the clinics, a randomized study in 2020 with 199 SARS-CoV-2 infected patients showed no significant difference between control group and treated group (CAO et al. 2020).

Remdesivir was used during the Ebola outbreaks in Africa and patients with moderate and/or severe symptoms of COVID-19 are currently treated with this drug (ANTINORI et al. 2020). The substance targets the viral replication and is approved by the Food and Drug Agency (FDA) for clinical use (CHUNG et al. 2020). A randomized study with 1,063 patients showed promising results, as the progression of COVID-19 could be stopped, and the recovery time could be shortened (BEIGEL et al. 2020).

Moreover, anti-inflammatory drugs are used as treatments for COVID-19 patients, as many patients with severe symptoms develop abnormal immune responses with high release of cytokines (e.g., IL-6, TNF-α or INF-γ) (GAO et al. 2020; SPADARO et al. 2019). Tocilizumab, a monoclonal antibody directed against the IL-6 receptor, was tested in several multicenter studies and showed an improvement of clinical syndromes (LUO et al. 2020; XU et al. 2020).

Chloroquine and hydroxychloroquine show anti-inflammatory and anti-viral efficacy in patients suffering from rheumatic diseases or Malaria (KRAFTS et al. 2012). Both drugs inhibit the entry of SARS-CoV-2 and interfere with the glycosylation of the ACE2 receptor. The FDA approved an emergency use of chloroquine and hydroxychloroquine for severe cardiac events (CHUNG et al. 2020). However, several multicenter studies were performed to test these drugs in COVID-19 patients for treatment and prophylaxis with no benefit for the patients (IBÁÑEZ et al. 2020; MÉGARBANE 2021).

Although several promising drugs and treatments are available, prevention of an infection with SARS-CoV-2 by vaccination seems to be the best option to combat the global pandemic. By end of February 2021, more than 170 vaccines are tested in pre-clinical trials with more than 65 vaccines in clinical trials (WHO 2021b). New and well-established platforms are used for the development of

vaccines against SARS-CoV-2 **(Figure 5)**: (i) whole virus vaccines (attenuated or inactivated), (ii) replicating and non-replicating viral vectors, (iii) virus-like particles, (iv) DNA or RNA-based vaccines, (v) synthetic vaccines (synthetic peptides or protein subunits), and (vi) recombinant viral or bacterial vector vaccines. Most vaccines tested in clinical trials are protein subunit vaccines (32%) followed by non-replicating viral vector vaccines (16%) (LOCHT 2020; WHO 2021b). At the end of January 2021, two messenger RNA-based (mRNA) vaccines and one replication-deficient adenovirus vaccine are authorized and recommended for prevention of COVID-19 in Europe (CDC 2021a; WHO 2021a).

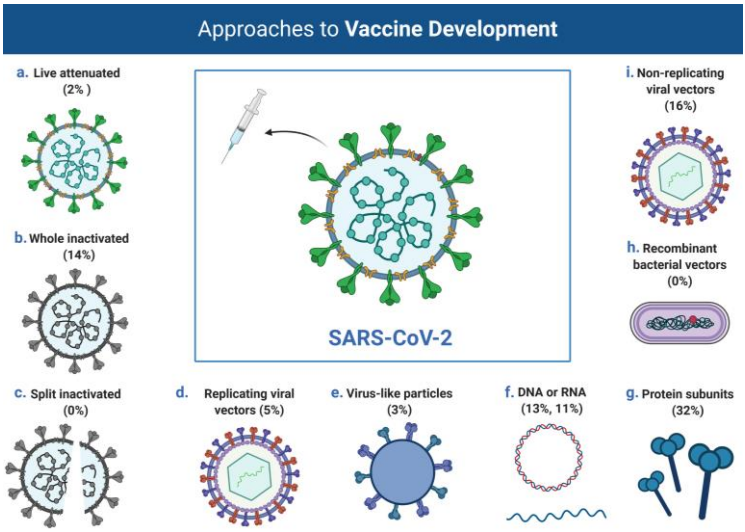

Figure 5: Approaches to vaccine development against SARS-CoV-2. Different platforms are used in the development of a vaccine. The brackets indicate the percentage of each platform tested in clinical trials. Protein subunit vaccines (32%) and non-replicating viral vector vaccines (16%) are most frequently represented in clinical trials (WHO 2021b). Created with BioRender.com

The first one, named BNT162b2, is manufactures by Pfizer, Inc., and BioNTech. Clinical trials showed an efficacy of 95.0% to prevent a SARS-CoV-2 infection. The route of application is intramuscular in the upper arm using two shots with an interval of 21 days. The vaccine is recommended for individuals older than

16 years and the most common side effects include local pain or redness at the puncture site and systemic reactions such as fever, fatigue or headache (CDC 2021c; POLACK et al. 2020; WALSH et al. 2020).

The second one, named mRNA-1273, is manufactured by ModernaTX, Inc. Clinical trials showed an efficacy of 94.1% to prevent a SARS-CoV-2 infection. The route of application is intramuscular in the upper arm using two shots with an interval of 28 days. The vaccine is recommended for individuals older than 18 years and the most common side effects include local pain or redness at the puncture site and systemic reactions such as fever, tiredness or headache (ANDERSON et al. 2020; BADEN et al. 2020; CDC 2021b).

The third one, named AZD1222 or ChAdOx1-S (recombinant), is manufactured by the University of Oxford/AstraZeneca. The route of application is intramuscular in the upper arm using two shots with an interval of 28 to 84 days. The vaccine is recommended for individuals older than 18 years. However, due to a lack of clinical data, the vaccine efficacy in individuals >65 years is uncertain. The most common side effects following vaccination include local pain at the puncture site and systemic reactions such as headache, fatigue, myalgia and nausea (EMA 2021; WHO 2021d).

The vaccines manufactured by Pfizer, Inc., BioNTech and ModernaTX, Inc. use a mRNA encoding a pre-fusion stabilized version of the full-length SARS-CoV-2 spike protein, which is delivered and translated in the cytoplasm of the host cell. In the last couple of years, mRNA became an encouraging alternative to other vaccine platforms, due to their safety, good immune response (high neutralizing and binding antibody titers, strong CD4+ and CD8+ T cell response) and the quick and low-cost manufacturing (CHUNG et al. 2020; PARDI et al. 2018; POLACK et al. 2020). Nevertheless, there is still need for improvement because of instability and inefficient delivery *in vivo* (KARIKÓ et al. 2008; KAUFFMAN et al. 2016).

In contrast, AZD1222 is based on a replication-deficient simian adenovirus expressing the codon-optimized full-length SARS-CoV-2 spike protein

intracellularly upon infection of the host cells (GILBERT and WARIMWE 2017; van DOREMALEN et al. 2020). The platform is well established and has been used to generate vaccines against several infectious pathogens including Ebola virus, Lassa virus and MERS-CoV (GILBERT and WARIMWE 2017). Preclinical and clinical studies with the new manufactured vaccine AZD1222 revealed a robust humoral and cell-mediated immune response (FOLEGATTI et al. 2020; GRAHAM et al. 2020; van DOREMALEN et al. 2020).

2. Modified Vaccinia virus Ankara (MVA) as a viral vaccine

2.1. History of MVA

The Modified Vaccinia virus Ankara (MVA) was developed by passaging the virus on chicken embryonic fibroblasts (CEF) to create a safer vaccine against smallpox. The ancestor virus of MVA is Vaccinia virus strain (VACV) Ankara, cultured and amplified in Turkey as a vaccine against smallpox. VACV has been used as a vaccine for more than 200 years, but unfortunately, its application has been associated with rare but severe side effects. These side effects range from localized reactions to even death, mainly caused by post vaccinal encephalitis (MAYR 2003). In the early 1950s, VACV was distributed to Munich, where the virus was cultivated on chorioallantois membranes (CAM) of embryonated chicken eggs, renaming the virus as Chorioallantois Vaccinia virus Ankara (CVA) (HERRLICH and MAYR 1954). During the smallpox eradication campaign, CVA was amplified to obtain a safer vaccine against smallpox (1954/55). In parallel, the University of Munich was working on the genetic stability of CVA when cultivated on different tissue cultures and in 1968, after the 516th passage on chicken embryonic fibroblasts, CVA was renamed as Modified Vaccinia virus Ankara. MVA was distributed to the Bavarian State Institute for Vaccines for further testing and to confirm suitability as a vaccine against smallpox (STICKL and HOCHSTEIN-MINTZEL 1971). First attempts to vaccinate people with a MVA vaccine preparation showed no severe side effects (STICKL 1974). In 1977, MVA was authorized as primary pre-vaccine in Germany, and until 1980, more than 120,000 humans were vaccinated with MVA with no severe adverse events even when administered to patients at high

risk such as elderly or individuals with allergies and skin affections (MAHNEL and MAYR 1994; STICKL 1974). With the eradication of smallpox in 1977, further vaccination studies with the MVA vaccine stopped (VOLZ and SUTTER 2016). Nevertheless, investigation on MVA continued and several years later, a restriction mapping of clonal isolate F6, derived from the 572nd passage on CEF cells, was performed, showing alterations compared to ancestor strain CVA (MEYER et al. 1991). Several mutations and large deletions were found, which affect genes involved in virus-host interactions. In total, around 30 kb of genetic information was lost, leading to a genome size of MVA of ~178 kb (ANTOINE et al. 1998; VOLZ and SUTTER 2016).

2.2. Taxonomy and viral life cycle

MVA belongs to the family *poxviridae*, subfamily *chordopoxvirinae*, and genus *orthopoxvirus*. Other members of genus *orthopoxvirus* include Variola virus (smallpox), monkeypox virus, cowpox virus and camelpox virus (GUBSER et al. 2004) (**Figure 6**).

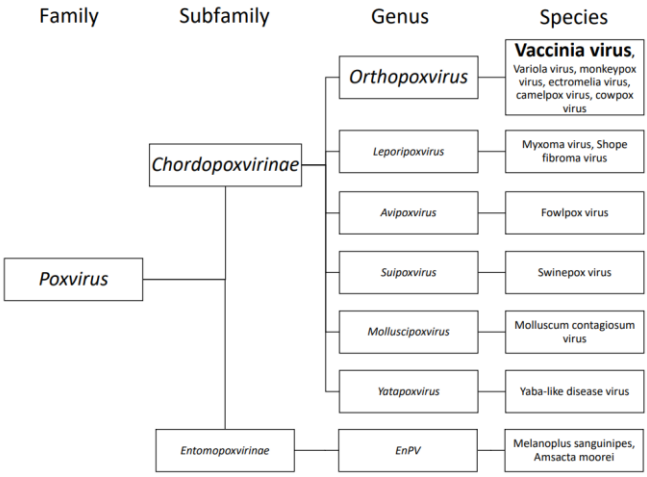

Figure 6: Classification of Modified Vaccinia virus Ankara (MVA). MVA belongs to the family *Poxvirus*, subfamily *Chordopoxvirinae,* genus *Orthopoxvirus*, species Vaccinia virus. Modified from (GUBSER et al. 2004).

Poxviruses are large and complex viruses (**Figure 7**). The envelope of extracellular virions (EV) contains two layers, an outer lipid membrane with short surface tubules visible upon electron microscope analysis and an inner lipid membrane. Inside is the core component of the virus particle with two lateral bodies that are important to deliver viral effector proteins into the host cell cytosol upon cell entry (BIDGOOD 2019; LALIBERTE et al. 2011). The core structure is formed by the core wall, which has a thick outer layer of structural proteins and a thin inner protein layer. The double-stranded DNA genome is tightly-packed as a nucleoprotein complex with the core structure. Of note, the nucleoprotein complex contains important viral enzymes that are also packaged within the virion (WESTWOOD et al. 1964).

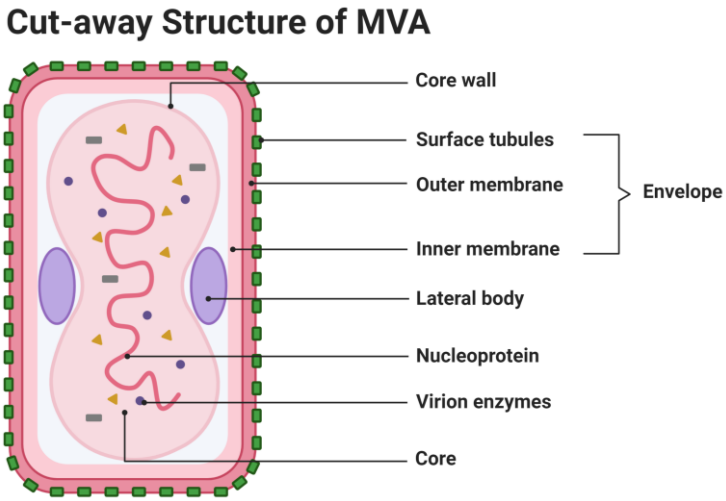

Figure 7: Schematic structure of a Modified Vaccinia virus Ankara (MVA) particle. MVA displays an envelope consisting of an outer lipid membrane (with surface tubules) and an inner lipid membrane. The inner part of the virion comprises a core structure with two lateral bodies. The core is surrounded by duplex protein layers and contains the DNA complex with viral enzymes in the inner part (WESTWOOD et al. 1964). Created with BioRender.com

Infectious viral particles are brick-shaped with a core structure containing the linear 178 kb duplex DNA. Several enzymes, including the DNA-dependent

RNA polymerase, capping and methylating enzymes are found within the virus core, enabling the virus to synthesize progeny mRNA after cell entry (**Figure 8**). Once the mature virion (MV, not shown in the graph) or extracellular virion (EV) attach to and enter the host cell, viral DNA is uncoated and early genes are transcribed. These early genes encode proteins involved in replication of viral genome and transcription of intermediate genes. Afterwards, the viral progeny DNA is used as a template to translate intermediate and late genes. The three classes of genes (early, intermediate, and late) have promoters containing distinctive sequence elements (BALDICK et al. 1992; MOSS 1996), which are recognized by viral proteins. This allows for a sequential activation of genes during the life cycle of MVA. After translation of the late structural proteins, the virion is assembled, transported to the periphery (CUDMORE et al. 1995; STOKES 1976), budded through the plasma membrane and released from the host cell (PAYNE 1980).

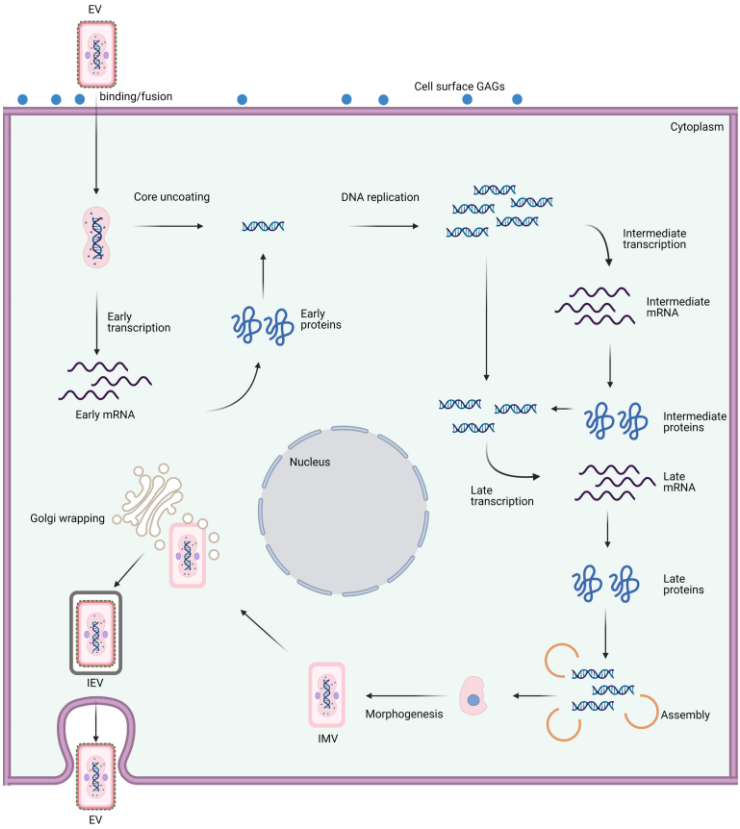

Figure 8: Viral life cycle of poxviruses. Extracellular virions (EV) bind to host cells by the interaction of virion proteins with glycosaminoglycans (GAGs) on the surface of the cell. The complete replication cycle of poxviruses occurs in the cytoplasm of infected cells and is characterized by three steps of mRNA and protein synthesis (early, intermediate and late) following assembly and morphogenesis of infectious particles. The initial intracellular mature virus (IMV) is transported to the Golgi-apparatus and wrapped with Golgi-derived membranes, renaming IMV as intracellular enveloped virus (IEV). IEV is transported to the periphery and released by the host cell. Modified from (McFADDEN 2005; SUTTER 2020). Created with BioRender.com

2.3. Virus-host interaction

Wild type VACV has a subset of viral genes (“host range” genes) encoding regulatory proteins that are important to control intracellular host defense mechanisms. Most of these proteins are expressed at the early stage of

infection, allowing VACV and other poxviruses to inhibit the host cell innate immune response (SMITH 1993). MVA lost several of these immunomodulatory genes during the attenuation process on CEF cells (ANTOINE et al. 1998; CARROLL and MOSS 1997), which might explain the highly immunogenic property despite its restricted replication capacity in mammalian cells (GÓMEZ et al. 2011). However, MVA induces a cascade-like gene expression upon infection of non-permissive cells, but the assembly of virions is blocked at the late stage of the viral replication cycle (SUTTER and MOSS 1992). Interestingly, the amount of early and late viral proteins is comparable to those produced in permissive cells (SANCHO et al. 2002). Although, MVA cannot fulfill its complete viral life cycle, the induction of an efficient immune response against viral or bacterial antigens is not affected (SUTTER et al. 1994a).

Poxviruses have developed several strategies to hamper the host cell immune response, including the inhibition of interferon pathways, the apoptotic response or production of cytokines and chemokines (SEET et al. 2003). In regard of IFN signaling pathways, VACV expresses a large panel of proteins blocking the induction of several transcription factors, such as NF-κB, IRF-3 or IRF-7 (SMITH et al. 2001). The pathways are activated by double-stranded (ds) RNAs and include the interferon-inducible protein kinase DAI (dsRNA-activated inhibitor of translation) and the 2`-5`oligoadenolyate synthase (MANCHE et al. 1992). The latter activates an endo-RNase preventing protein synthesis by the cleavage of mRNA. Upon activation, the DAI kinase phosphorylates the alpha subunit of the eukaryotic translation initiation factor 2 (eIF2α), causing an inhibition of protein synthesis at early stage. Viral proteins, such as C7, K1, K3 and E3 are able to block virus-induced phosphorylation of eIF2α. Furthermore, E3 inhibits phosphorylation of the two transcription factors IRF-3 and IRF-7 (BACKES et al. 2010; CHANG et al. 1992; SMITH et al. 2001), blocking type-I interferon release in VACV. MVA lacks several of these proteins (e.g., A52, B14, K1, C4, M2, N1), resulting in an upregulation of interferon pathways upon infection of host cells. A key feature of MVA as a viral vector vaccine is the strong induction of cytotoxic T cell responses by the activation of type-I IFNs in human antigen-presenting cells such as dendritic cells (BÜTTNER et al. 1995; DRILLIEN et al. 2004). Gene profiling analysis of MVA infected dendritic cells revealed elevated

mRNA levels of IL-12, IFN-α/β, IRF-7 and proteins activating the type-I IFN production (MDA5, RIG) (GUERRA et al. 2007). Another immune evasion mechanism of VACV connected to the interferon pathway is the expression of soluble receptors for TNF, IFN-γ, and IFN-α/β. These secreted receptors allow evading and inhibiting of the host immune system, and their high prevalence in the serum is associated with high virulence (HU et al. 1994; MOSSMAN et al. 1995; SMITH et al. 1997; SPRIGGS et al. 1992). MVA lacks genes to encode those receptors and thus, induces an innate immune response. Furthermore, MVA infection induces the production of chemokines (e.g., CCL2) and activation of the complement system, causing an increased migration of leucocytes to the source of infection (LEHMANN et al. 2009).

Besides, apoptosis of infected cells is blocked by certain VACV proteins. Programmed cell death is mediated by caspases and B-cell lymphoma (Bcl)-2 and Bcl-2-like proteins at the mitochondrion. Once apoptosis is activated, the pro-apoptotic proteins Bid, Bim and PUMA activate Bax/Bak or NOXA which assemble pores in the mitochondrial membrane (CHIPUK et al. 2010; REN et al. 2010). The pores allow the release of cytochrome c from the mitochondrial intermembrane space into the cytosol, causing the assemble of the apoptosome complex. Thereby, caspase-3 and caspase-7 are activated and the subsequent cascade leads to the death of infected cells (DANIAL and KORSMEYER 2004). Anti-apoptotic proteins such as Bcl-2, Bcl-w or Bfl-1 interfere with pro-apoptotic proteins to block Bax/Bak activation. The VACV E3 protein binds to the pro-apoptotic NOXA protein, inhibiting apoptosis in infected cells (DAVIES et al. 1992; VEYER et al. 2017).

2.4. MVA as a viral vector vaccine

Due to the replication deficiency of MVA in most cells of mammalian origin and the possibility to use the virus for high-level expression of various recombinant proteins, MVA is a promising tool to create viral vector vaccines. Moreover, recombinant Vaccinia viruses induce high levels of cytotoxic CD8+ T cells in immunized animals and humans. The intracellular expression of a target antigen allows for processing and presentation to major histocompatibility complex (MHC) class I molecules for recognition by T cells (TOWNSEND et al.

1988).

The target genes (viral or bacterial antigens) can easily be inserted into one of the deletions sites of MVA by homologous recombination. By cloning the genes into these sites, changes in genotype and phenotype can be avoided (VOLZ and SUTTER 2016). The time-point and amount of expressed antigen is controlled by the choice of an early, intermediate or late promoter. The highest amount of expressed antigen was observed with late or early/late promoters (MACKETT et al. 1984). To generate a recombinant MVA, some general rules need to be considered. A transfer plasmid is required, containing an expression cassette (poxvirus promoter and a multiple cloning site with restriction sites to insert the foreign antigen), which is flanked by poxvirus DNA sequences to direct recombination into the preferred locus (EARL et al. 1990; MACKETT et al. 1984; STAIB et al. 2004). The DNA sequence TTTTTNT functions as a stop signal for viral early gene transcription and foreign antigens should be screened for this thymidine rich regions. Furthermore, G/C-runs could lead to a frameshift in the MVA genome during DNA replication (WYATT et al. 2009). If the target antigen contains these runs of thymidines or G/Cs, the codon usage should be changed (EARL et al. 1990). The efficiency of homologous recombination is around 0.1% and screening for positive plaques can be performed either by DNA hybridization, expression of target antigen (PICCINI et al. 1987), co-integration of antibiotic selection marker (FRANKE et al. 1985) or co-expression of marker genes (WONG et al. 2011). The very first proteins that were expressed by recombinant MVAs were the *E. coli* enzymes guanine-phosphoribosyl-transferase (GPT) and β-galactosidase using gene sequences, which were inserted into deletion site III (SUTTER and MOSS 1992).

2.5. Vaccinia virus vaccines in veterinary and human vaccine trials

Various recombinant Vaccinia viruses were used in animals against viruses of veterinary importance, such as vesicular stomatitis virus (VSV) (MACKETT et al. 1985), Rinderpest virus (RPV) (YILMA et al. 1988) or rabies virus (RABV) (WIKTOR et al. 1984). Raccoonpox virus vectors were used to prevent RABV infections in raccoons (ESPOSITO et al. 1988), capripox virus vectors were

used to protect cattle against RPV (ROMERO et al. 1994), fowlpox vectors were used to protect chicken against influenza virus (WEBSTER et al. 1991) and canarypox virus were used to protect dogs against canine distemper virus (CDV) (TAYLOR et al. 1991).

Besides, several Vaccinia virus-based vaccines were used in human vaccine trials. In the beginning of the 1990s a randomized phase I clinical trial was performed in the USA to test safety and immunogenicity of a recombinant Vaccinia virus expressing the envelope protein from human immunodeficiency virus 1 (HIV-1). No severe side effects were observed and a prime-boost vaccination induced humoral and cell-mediated immune responses (COONEY et al. 1991; GRAHAM et al. 1992). A few years later, a recombinant Vaccinia virus expressing the membrane protein from Epstein-Barr virus (EBV) was administered in China to infants and young children, showing immunogenic properties. Over a period of 16 months, natural infections with EBV could be delayed or even prevented (GU et al. 1995).

The first recombinant MVA-based candidate vaccine expressing two proteins, hemagglutinin (HA) and nucleoprotein of influenza A virus, was tested in mice for immunogenicity. High levels of antibodies and cytotoxic T cells could be found. Moreover, vaccinated mice could be protected in a challenge model following infection with influenza A virus (HESSEL et al. 2014; SUTTER et al. 1994b). Over the last decades, several MVA-based vaccines were tested in various preclinical and clinical trials, including vaccines against Ebola virus (ANYWAINE et al. 2019), HIV (MUNSERI et al. 2015) and Mycobacterium tuberculosis (MANJALY THOMAS et al. 2019). Recently, an MVA-based vaccine against MERS-CoV, closely related to new SARS-CoV-2, was tested in a phase I clinical trial, showing strong humoral and cell-mediated immune response (KOCH et al. 2020; SONG et al. 2013; VOLZ et al. 2015).

3. Viral infection and host immune response

The immune system can be divided into two main parts that act in a synergetic way: adaptive and innate immunity. The latter is the first immunological barrier against pathogens, showing a rapid (within minutes or hours) and non-specific

immune response that has no immunological memory (MURPHY et al. 2014; WARRINGTON et al. 2011). The main function is to recruit certain immune cells to sites of infection and to produce cytokines causing an inflammation. Production of cytokines triggers the release of antibodies and specific glycoproteins resulting in an activation of the complement system (LING and MURALI 2019). The innate immunity is also responsible for clearance of dead cells and promotes removal of foreign substances in various organs, blood and lymph. Furthermore, the innate immunity activates the adaptive immunity by antigen presentation through phagocytes such as macrophages, neutrophils or dendritic cells (TURVEY and BROIDE 2009; WARRINGTON et al. 2011).

In contrast, the adaptive immunity acts in an antigen-dependent and antigen-specific manner and has the capacity to develop memory, allowing a rapid response after re-infection with a given pathogen (MURPHY et al. 2014; WARRINGTON et al. 2011). This branch of the immune system is activated when the innate immunity is not able to eliminate a certain pathogen and the infection is established. The main tasks are the recognition of foreign antigens, the activation of effector pathways and the development of an immunologic memory. The adaptive immunity can be further classified into cell-mediated (T cell) response and antibody-mediated (B cell) response (BONILLA and OETTGEN 2010).

T cells originate from hematopoietic stem cells in the bone marrow and mature in the thymus, expressing one unique antigen-binding receptor, known as T cell receptor (TCR). TCRs interact with antigen-presenting cells (APCs), such as macrophages or dendritic cells, to recognize a certain antigen. APCs encode cell-surface proteins, which are named major histocompatibility complex (MHC). MHC are further divided into class I, which is broadly distributed on all nucleated cells, and class II, which is found only on specific immune cells, such as macrophages and dendritic cells. Class I MHC molecules present intracellular peptides whereas class II MHC molecules display extracellular peptides. Those peptides are fragments of antigens, presented by cells after contact or infection with a pathogen (BONILLA and OETTGEN 2010; MURPHY et al. 2014). T cells bind with their TCRs to the fragmented antigens on MHC

molecules and secret cytokines which further active the immune cascade, causing a differentiation of T cells into cytotoxic T cells (CD8+ T cells) or T-helper (Th) cells (CD4+ T cells) (WARRINGTON et al. 2011). CD8+ T cells are responsible for destruction of infected cells and are activated by interaction of class I MHC bound peptides. Clonal expansion of CD8+ T cells leads to the maturation of effector cells which secrete perforin, granzyme and granulysin, thereby inducing lysis and apoptosis of infected cells. Once the infection is cleared, most effector cells die, but a small portion become memory cells which differentiate quickly into effector cells after re-infection with a known antigen (BONILLA and OETTGEN 2010; MURPHY et al. 2014; WARRINGTON et al. 2011).

The major role of CD4+ T cells is to shape the adaptive immune response by influencing the function of other immune cells. They are activated by the interplay of their TCRs with class II MHC bound molecules, releasing cytokines which active other immune cells. CD4+ T cells are divided into two types: Th1 and Th2. Once Th1 cells are activated, IFN-γ and other cytokines are released, inducing B cells to produce (neutralizing) antibodies. Th2 activation causes the release of cytokines (e.g., IL-4 and IL-13) which activate IgE-antibody producing B cells and eosinophils. Similar to cytotoxic CD8+ T cells, most Th cells die after clearance of the infection, with a small amount remaining as memory cells (BONILLA and OETTGEN 2010; MURPHY et al. 2014; NICHOLSON 2016).

B cells derive from hematopoietic stem cells in the bone marrow, expressing one unique antigen receptor after maturation. In contrast to T cells, B cells need no APCs and recognize foreign antigens directly. The main task of B cells is the production of specific antibodies against pathogens (MURPHY et al. 2014). Once B cells are activated by recognizing foreign antigens, they differentiate into antibody-secreting plasma cells or memory cells. The latter are long-living, continually expressing antigen-binding receptors and respond quickly upon re-infection with known antigens. Plasma cells are short-living, express no antigen-binding receptors and die once the infection is cleared (BONILLA and OETTGEN 2010; WARRINGTON et al. 2011). Secreted antibodies are classified into five different types: immunoglobulin (Ig) A, IgG, IgE, IgM and IgD

(MURPHY et al. 2014; SCHROEDER and CAVACINI 2010). Immunoglobulins consist of two polypeptide chains, a heavy and a light chain. Each Ig molecule has two heavy and two light chains which are connected by disulfide bonds. The structure of the B cell receptor is identical to its corresponding antibody, beside a small part at the *C*- terminus of the heavy chain. The B cell receptor has a hydrophobic part to bind to the membrane of the B cell, whereas the antibody has a hydrophilic sequence allowing secretion (MURPHY et al. 2014). The most important antibodies in terms of clearance of pathogens are IgA, IgG and IgM. The latter is expressed during early stage of infection and opsonizes the pathogen for destruction. IgA is responsible for mucosal response, either by neutralizing viral or bacterial antigens or inhibiting the binding to the mucosal surface. The main circulating immunoglobulin, IgG, is expressed at later stage of infection and opsonize the antigens for destruction and neutralizes the virus (MURPHY et al. 2014; SCHROEDER and CAVACINI 2010).

IV. MATERIAL AND METHODS

1. Materials

1.1. Organism

1.1.1. Bacterial strains

NEB 10-beta bacteria (New England Biolabs, Frankfurt, Germany) were used for heat-shock transformation and amplification of plasmid DNA.

1.1.2. Cell lines

Table 1: Overview of cell lines

Cell line	Detailed information	Experiment
A549	adenocarcinomic, alveolar basal epithelial cells (human)	protein expression, growth kinetics
CEF	chicken embryonic fibroblasts	virus amplification, protein expression
DF-1	chicken embryonic fibroblasts	virus amplification, plaque passage, growth kinetics, protein expression
HaCat	epidermal keratinocyte cells (human)	protein expression, growth kinetics
HeLa	cervical cancer cells (human)	protein expression, growth kinetics
Vero E6	kidney epithelial cells (African green monkey)	protein expression, virus neutralization assay (VNT)

1.2. Antibodies

1.2.1. Primary antibodies

Table 2: Primary antibodies used for western blot analysis (WB), immunofluorescence assay (IFA) and intracellular cytokine staining (ICS)

Antigen	Supplier	Species	WB	IFA	ICS
CD3 phycoerithrin (PE)-Cy7	Biolegend, London, United Kingdom	mouse	-	-	1:100
CD4 Brilliant Violet	Biolegend, London, United Kingdom	mouse	-	-	1:600
CD8α Alexa Fluor 488	Biolegend, London, United Kingdom	mouse	-	-	1:300
CD16/CD32	Biolegend, London, United Kingdom	mouse	-	-	1:500
HA-tag	Thermo Fisher Scientific, Planegg, Germany	mouse	1:7,000	1:1,000	-
IFN-γ	Biolegend, London, United Kingdom	mouse	-	-	1:200
spike protein	Biozol GmbH, Eching, Germany	mouse	1:1,000	1:200	-
TNF-α	Biolegend, London, United Kingdom	mouse	-	-	1:200
Vaccinia virus A27L protein	oriGene, Herford, Germany	rabbit	-	1:2,000	-

1.2.2. Secondary antibodies

Table 3: Secondary antibodies used for western blot analysis (WB) and immunofluorescence assay (IFA)

Name	Supplier	Origin	WB	IFA
Anti-mouse IgG HRP	Agilent Technologies, Waldbronn, Germany	goat	1:5,000	1:1000
Anti-rabbit IgG HRP	Cell Signaling, Frankfurt am Main, Germany	goat	1:5,000	-
Anti-rabbit IgG peroxidase conjugated	Jackson Immuno Research, Suffolk, United Kingdom	goat	-	1:5,000

1.3. Oligonucleotides

Table 4: Oligonucleotides used for control PCR

Name	Sequence (5´→ 3´)	PCR
MVA-Del 1 for	CTTCGCAGCATAAGTAGTATGTC	Deletion I
MVA-Del 1 rev	CATTACCGCTTCATTCTTATATTC	Deletion I
MVA-Del 2 for	GGGTAAAATTGTAGCATCATATACC	Deletion II
MVA-Del 2 rev	AAAGCTTTCTCTCTAGCAAAGATG	Deletion II
MVA-Del 3 for	GATGAGTGTAGATGCTGTTATTTTG	Deletion III
MVA-Del 3 rev	GCAGCTAAAAGAATAATGGAATTG	Deletion III
MVA-Del 4 for	AGATAGTGGAAGATACAACTGTTACG	Deletion IV
MVA-Del 4 rev	TCTCTATCGGTGAGATACAAATACC	Deletion IV
MVA-Del 5 for	CGTGTATAACATCTTTGATAGAATCAG	Deletion V
MVA-Del 5 rev	AACATAGCGGTGTACTAATTGATTT	Deletion V
MVA-Del 6 for	CTACAGGTTCTGGTTCTTTATCCT	Deletion VI
MVA-Del 6 rev	CACGGTCAATTAACTATAGCTCTG	Deletion VI
III-3´	GTACCGGCATCTCTAGCAGT	Deletion III
III-5´	TGACGAGGTTCCGAGTTCC	Deletion III
SARS-CoV-2 for 1	CCAGAACTCAATTACCCCCTGC	Insert
SARS-CoV-2 rev 1	CATTACAAGGTGTGCTACCGGC	Insert
SARS-CoV-2 for 2	ACAAATCGCTCCAGGGCAAAC	Insert
SARS-CoV-2 rev 2	GCCCCTATTAAACAGCCTGCAC	Insert

SARS-CoV-2 for 3	TGGCAGAGACATTGCTGACAC	Insert
SARS-CoV-2 rev 3	GCACCAAAGGTCCAACCAGAAG	Insert
SARS-CoV-2 for 4	TCAGACTAATTCTCCTCGGCGG	Insert
SARS-CoV-2 rev 4	CAGCCCTTGAGACAACTACAGC	Insert
C7L for	CATGGACTCATAATCTCTATAC	C7L
C7L rev	ATGGGTATACAGCACGAATTC	C7L

1.4. Plasmids

Table 5: Expression and shuttle plasmids

Plasmid	Supplier	Experiment
pUC57-SARS-CoV-2-S	Genewiz, Leipzig, Germany	cloning
pIIIH5red-SARS-CoV-2-S	Alina Tscherne, LMU	cloning
pIIIH5red	Gerd Sutter, LMU	cloning

1.5. Peptides

Table 6: Selected peptides with predicted class I MHC (H2d) and class II MHC (IAd and IEd) restriction

Peptide ID	Peptide	Length	Start	End	Pool #
S1	GYLQPRTFL	9	268	276	4
S2	AYSNNSIAI	9	706	714	10
S3	IYQAGSTPCNGV	12	472	483	5
S4	FTISVTTEI	9	718	726	10
S5	IYQTSNFRV	9	312	320	10
S6	IYQAGSTPC	9	472	480	5
S7	QYIKWPWYI	9	1208	1216	6
S8	CYGVSPTKL	9	379	387	11
S9	PPIKDFGGFNF	11	792	802	11
S10	VGYQPYRVVVL	11	503	513	7
S11	KYNENGTIT	9	278	286	4
S12	GYQPYRVVV	9	504	512	7
S13	QYGSFCTQL	9	755	763	8
S14	SYQTQTNSP	9	673	681	8

S15	YQPYRVVVL	9	505	513	7
S16	WPWYIWLGF	9	1212	1220	6
S17	VYAWNRKRI	9	350	358	9
S18	CGPKKSTNL	9	525	533	9
S19	KYFKNHTSP	9	1154	1162	9
S20	TRFASVYAWNRKRIS	15	345	359	1
S21	RFASVYAWNRKRISN	15	346	360	1
S22	FASVYAWNRKRISNC	15	347	361	1
S23	INITRFQTLLALHRS	15	233	247	2
S24	NYLYRLFRKSNLKPF	15	450	464	2
S25	LIRAAEIRASANLAA	15	1012	1026	3
S26	NYNYLYRLFRKSNLK	15	448	462	2
S27	ASVYAWNRKRISNCV	15	348	362	1
S28	IRAAEIRASANLAAT	15	1013	1027	3
S29	GNYNYLYRLFRKSNL	15	447	461	2
S30	AAEIRASANLAATKM	15	1015	1029	3
S31	GGNYNYLYRLFRKSN	15	446	460	2
S32	RAAEIRASANLAATK	15	1014	1028	3
S33	ATRFASVYAWNRKRI	15	344	358	1
S34	NATRFASVYAWNRKR	15	343	357	1
F2(G)	SPGAAGYDL	9	26	34	-

2. Methods

2.1. Cell culture

2.1.1. Passaging, freezing and thawing of cells

Eucaryotic cells were washed once with 1x DPBS, trypsinized with 1x TrypLE™ Select Enzym for 5-10 min at 37 °C. 7-9 ml of cell culture medium were added to stop the enzymatic reaction. One part of the cell suspension was distributed to new flasks, filled up with cell culture medium and cells were cultured at 37 °C with 5% CO_2. DF-1 cells were kept in VP-SFM medium supplemented with 2% L-glutamine and 2% heat-inactivated FBS. CEF cells were isolated from 10 to 11-day old chicken embryos and were maintained in VP-SFM medium, 10% FBS and 1% L-glutamine. Vero E6 cells were cultured in DMEM with 10% FBS

and 1% MEM non-essential amino acid solution. Human A549 cells were maintained in DMEM (+ 4500 mg/l glucose) containing 10% FBS. Human HeLa cells were maintained in MEM, 7% FBS and 1% MEM non-essential amino acid solution. Human HaCat cells were maintained in DMEM, 1% MEM non-essential amino acid solution, 10% FBS and 1% HEPES solution.

To freeze cells, the protocol for passaging cells was followed until the enzymatic reaction of trypsin was stopped. The cell suspension was centrifuged and the pellet was resuspended in freezing medium (45% FBS, 45% cell culture medium, 10% DMSO). The cells were immediately distributed to cryo tubes and frozen at -80 °C. For long term storage, cells were transferred to liquid nitrogen. To thaw the cells, cryo tubes were taken from liquid nitrogen or -80 °C, carefully thawed in a water bath (37 °C) and immediately filled up with medium to dilute the toxic DMSO. Cells were distributed to cell culture flasks and cultured at 37 °C with 5% CO_2. Medium was changed the day after to remove dead cells.

2.1.2. Generation and purification of recombinant viruses

To obtain the recombinant MVA vector virus a well-established protocol was used as described previously (ALTENBURG et al. 2014; KOCH et al. 2020; SONG et al. 2013). Briefly, clonal isolate MVA-F6sfMR was grown on CEF cells under serum-free conditions and was used as a non-recombinant backbone virus to insert the SARS-CoV-2 spike gene sequence. 6-well tissue culture plates with 90-95% confluent DF-1 or CEF cells were infected with non-recombinant MVA-F6sfMR at a multiplicity of infection (MOI) of 0.05 and transfected with 1 µg DNA of expression plasmid pIIIH5red-SARS-CoV-2-S using X-tremeGENE HP DNA Transfection Reagent according to the manual. Cells were cultured for 48 h at 37 °C and collected afterwards. Recombinant MVA viruses were clonally isolated by serial rounds of plaque purification on DF-1 or CEF cell monolayers screening for transient co-expression of the marker protein mCherry. To obtain large scale virus preparations, recombinant MVA-SARS-CoV-2-S was amplified on DF-1 cells grown in T175 tissue culture flasks. The virus was purified via ultracentrifugation through 36% sucrose and reconstituted in TBS (pH =7.4). For long term storage, recombinant viruses were frozen at -80 °C.

2.1.3. Determination of plaque-forming units (PFU)

Recombinant MVA was diluted in 10-fold dilution steps (range 1:10*4 to 1:10*9) and used to infect 6-well tissue plates with 90-95% confluent CEF cells. Each dilution was prepared in triplicates. Cells were incubated for 48 h and afterwards, fixed with ice-cold methanol: acetone (1:1) for 5 min. Plates were blocked with PBS (+ 3% FBS) for 1 h at RT or 4 °C o/n. Plates were washed 3x with PBS. Primary antibody (anti-Vaccinia virus or anti-HA) was diluted in PBS (+ 3% FBS) and plates were incubated for 1 h at RT. Subsequently, plates were washed 3x with PBS. Secondary antibody (goat anti-mouse HRP) was diluted in PBS (+ 3% FBS) and plates were incubated for 1 h at RT. Afterwards, plates were washed 3x with PBS and TrueBlue™ Peroxidase Substrate was added to each well until color change could be observed. Plaque-forming units per ml (PFU/ml) were determined by counting the plaques.

2.1.4. Growth kinetics on permissive and non-permissive cell lines

DF-1, HeLa, HaCat and A549 cells were grown on 6-well tissue plates at a confluency of 90-95% and were infected with recombinant MVA at a MOI of 0.05. After certain time points (0, 4, 8, 12, 24, 48 and 72 hpi), whole wells were collected and frozen at -20 °C. Three freeze and thaw cycles were performed before sonicating three times for 1 min. Afterwards, back titration on CEF cells was performed using the protocol descripted in chapter *2.1.3 Determination of plaque-forming units (PFU)*.

2.1.5. Low MOI passage

A monolayer of 90-95% confluent DF-1 cells was infected with recombinant MVA at a MOI of 0.05 and cultured for 48 h at 37 °C. Afterwards, the amplified virus was collected and used to re-infect confluent 6-well tissue plates with DF-1 cells at a MOI of 0.05. This procedure was repeated four times, ending up with five rounds of low MOI passaging. Genetic stability of recombinant MVA-SARS-CoV-2-S was further validated by PCR analysis and gene expression was monitored by SARS-CoV-2 spike protein specific immunostaining.

2.1.6. SARS-CoV-2 virus neutralization test (VNT) (performed at the Institute of Virology, Philipps University Marburg)

Mice were immunized according to chapter *2.4.1 vaccination experiments* and heat-inactivated serum samples were send to Prof. Dr. Stephan Becker`s lab, located at the Philipps University Marburg (Germany), to test the sera for their neutralization capacity using a protocol described previously (KREER et al. 2020). Briefly, samples were serially diluted starting with a 1:16 dilution and incubated with 100 $TCID_{50}$ SARS-CoV-2 (BavPat1/2020 isolate, European Virus Archive Global # 026V-03883) for 1 h at 37 °C. Serum/virus mixture was added to 96-well tissue culture plates with Vero E6 cells and cultured for four days. Neutralization capacity was determined as the absence of cytopathic effect compared to virus control.

2.2. Biochemistry

2.2.1. Generation of cell lysates

6-well tissue plates or 24-well tissue plates with cells at a confluency of 90- 95% were infected with recombinant MVA at a MOI of 10 and were incubated for 0, 2, 8, 12, 24 and 48 h at 37 °C. Non-infected cells and cells infected with wild-type MVA were used as controls. To generate the lysates, cells were scraped from the plates and centrifuged for 1 min at 13,000 rpm. Supernatant was removed and the pellets were washed once with pre-chilled PBS. PBS was removed and pellets were reconstituted with lysis buffer (+ proteinase inhibitor). The cells were incubated for 30-60 min on ice and centrifuged for 15 min at 13,000 rpm. The lysates were frozen at -80°C.

2.2.2. SDS-PAGE and western blot analysis

Cell lysates (description chapter *2.2.1 Generation of cell lysates*) were thawed carefully on ice and mixed with 4x reducing agent containing β-mercaptoethanol. The samples were boiled for 5 min at 95 °C and cooled down to RT. Subsequently, samples and a protein standard (Pageruler prestained protein ladder) were loaded on a pre-cast gel and proteins were separated by using 100 V for 2 h. The proteins were transferred on a nitrocellulose membrane using 100 V for 100 min. Afterwards, the membrane was blocked with blocking

buffer (1% BSA in PBST) for 1-2 h at RT. The first antibody (anti-HA) was diluted in blocking buffer and membrane was incubated for 1 h at RT before washing the membrane 3x with PBST for 10 min. The secondary antibody (goat anti-mouse HRP) was diluted in blocking buffer and the membrane was incubated for 1 h at RT. After washing 3x with PBST, the membrane was incubated with SuperSignal West Dura Extended Duration Substrate for 1 min and proteins were detected by using the ChemiDocTMMP, Imaging System.

2.2.3. Immunofluorescence

Vero E6 cells were grown on cover slips in 6-well tissue culture plates. 90-95% confluent cells were infected at a MOI of 0.05 with recombinant MVA-SARS-CoV-2-S and non-recombinant MVA. Non-infected cells served as a control. After incubation for 24 h at 37 °C, cells were fixed with 4% paraformaldehyde/PBS for 10 min on ice. Cells were washed with PBS, permeabilized with 0.1% Triton X-100/PBS and probed with an antibody against the HA-tag epitope. Non-permeabilized cells were probed with an antibody against the spike protein and fixed with 4% paraformaldehyde/PBS afterwards. A secondary goat anti-mouse antibody was used for visualization of S-specific staining by red fluorescence. DAPI (1 µg/ml) was used to stain the nuclei and cells were further analyzed by Keyence BZ-X700 microscope with a ×100 objective.

2.3. Molecular biology

2.3.1. Heat-shock transformation

Competent bacteria were carefully thawed on ice and pre-chilled plasmid DNA (100-500 ng) was added by slowly pipetting up and down. The tubes were incubated for 30 min on 4 °C and afterwards, bacteria were heat- shocked at 42 °C for 30 sec. LB-medium without antibiotics was added to the bacteria, which were then incubated for 1-3 h at 37 °C. Bacteria were plated on LB-agar plates containing antibiotics (50 µg/ml ampicillin or 50 µg/ml kanamycin) and incubated o/n at 37 °C. Colonies were selected and grown in LB-medium (+ antibiotics) for plasmid isolation.

2.3.2. Isolation of plasmid and viral DNA

To obtain small amounts of plasmid DNA, the NucleoSpin Plasmid Mini kit for plasmid DNA was used according to the manual. Briefly, bacteria were centrifuged for 1 min at 13,000 rpm. Supernatant was discarded and the pellet was resuspended with pre-chilled resuspension buffer R1 (+ RNAse inhibitor). Lysis buffer A2 was added and tubes were incubated for 5 min at RT before adding neutralization buffer A3. Tubes were centrifuged for 10 min at 13,000 rpm and the supernatant was loaded on columns. Afterwards, tubes were centrifuged for 1 min at 13,000 rpm and the flow through was discarded. Wash buffer AQ was added to the tubes and after centrifugation for 3 min at 13,000 rpm, the DNA was eluted by adding elution buffer AE.

To obtain larger amounts of plasmid DNA, the NucleoBond Xtra Midi kit was used according to the manual. Briefly, bacteria were centrifuged for 30 min at 4,500 rpm and the pellet was resuspended in pre-chilled buffer RES (+ RNAse inhibitor). Lysis Buffer LYS was added and the tubes were incubated for 5 min at RT before adding buffer NEU. The supernatant was loaded on NucleoBond Xtra Column Filter and the flow through was discarded. Buffer WASH was added and afterwards, the DNA was collected by adding buffer ELU. To precipitate the DNA, isopropanol was used and the pellet was washed once with 96% ethanol. The pellet was dried and reconstituted with ddH_2O.

To obtain viral DNA, the NucleoSpin Blood Kit was used according to the manual. Briefly, infected cells were scraped from the tissue culture plates and centrifuged for 2 min at 2,000 rpm. Supernatant was discarded, the pellet was resuspended in buffer BQ1 (+ proteinase K) and incubated at 70 °C for 15 min. Afterwards, 96% ethanol was added and the liquid was loaded on columns. The tubes were centrifuged for 1 min at 13,000 rpm, the flow through was discarded and the columns were washed twice with wash buffer BQ2. To elute the DNA, pre-heated buffer BE was added to the columns and the tubes were centrifuged for 1 min at 13,000 rpm. The DNA was stored at -20 °C until further analysis.

2.3.3. Digestion with restriction enzymes

Plasmid DNA was digested with restriction enzymes for 90 min at 37 °C.

Restriction enzymes (*NotI, PmeI, EcoRI*) were obtained from New England Biolabs, Frankfurt, Germany. The following protocol was used to digest plasmid DNA:

500-1000 ng plasmid DNA
5 µl restriction buffer (10x)
0.2 µl enzyme A
0.2 µl enzyme B
ad 50 µl ddH_2O

2.3.4. Polymerase chain reaction (PCR)

PCR was used to amply specific regions of plasmid or viral DNA using the Taq DNA polymerase according to the manual. The oligonucleotide sequences are summarized in chapter *1.3 Oligonucleotides*. The following protocol was used:

	Final concentration
0.2 µl polymerase (5 U/µl)	2.5 U/µl
2.5 µl buffer (10x)	1x
1 µl forward primer (10 µM)	0.5 µM
1 µl reverse primer (10 µM)	0.5 µM
0.75 µl MgCl2 (50 mM)	1.5 mM
0.5 µl dNTP-Mix (2.5 mM)	0.05 mM each
5 µl template	1-500 ng
14.55 µl ddH2O	-

Table 7: Temperature profile for control PCR

Step		**Temperature**	**Time**
Initial Denaturation		94 °C	5 min
Denature	30x PCR cycle	94 °C	45 sec
Anneal		Depending on primer T_m (55-70 °C)	30 sec
Extend		72 °C	90 sec/kb
Final extension		72 °C	10 min
Hold		4 °C	indefinitely

2.3.5. Quantitative real-time reverse transcription PCR (qRT-PCR) (performed at the Institute of Virology, Philipps University Marburg)

Mice were immunized as described in chapter *2.4.1 Vaccination experiments*. The immunized mice were shipped to Prof. Dr. Stephan Becker`s lab, located at the Philipps University Marburg (Germany), and challenged as descripted in chapter *2.4.2 Transduction of vaccinated mice and challenge infection with SARS-CoV-2*. Tissue samples were excised from the left lung lobes and homogenized in DMEM. Isolation of RNA was achieved using the RNeasy Mini Kit according to the manual. Briefly, cells were lysed with buffer RLT, homogenized and afterwards, ethanol was added to the mixture. The liquid was loaded on columns and centrifuged for 1 min at 13,000 rpm. The columns were washed 3x with buffer RW1 and total RNA was eluted in RNAse-free water. Total RNA was reverse transcribed and quantified by RT-PCR (OneStep RT-PCR Kit) using a protocol and primers as described before (CORMAN and DROSTEN 2020). Additionally, determination of mCherry mRNA was performed by RT-PCR for every tissue sample to confirm successful ACE2 transduction. Quantification was performed by using a standard curve based on 10-fold serial dilutions of control RNA (range: 10*2 to 10*5 copies).

2.3.6. Gel electrophoresis

Gel electrophoresis was performed to separate digested DNA or PCR products according to their sizes. Agarose (0.5-1.5%) was dissolved in 1x TAE buffer and boiled in a microwave. GelRed was added and the liquid gel was poured in a chamber. The digested DNA or PCR products were mixed with 5x DNA loading dye and loaded on the solid gel. To separate the DNA fragments, 100 V for 2 h were used. Subsequently, the DNA fragments were analyzed with UV light.

2.4. Immunology

2.4.1. Vaccination experiments

6 to 10-weeks old female BALB/c mice (Charles River, Sulzfeld, Germany) were maintained under pathogen-free conditions with free access to food and water. They were allowed to adapt to the facility for at least one week before starting

the vaccination experiments. All animal experiments were handled in compliance with the European and national regulations for animal experimentation (European Directive 2010/63/EU; Animal Welfare Acts in Germany). Immunizations were performed with recombinant MVA-SARS-CoV-2-S and non-recombinant MVA diluted in vaccination puffer (= saline, PBS). Mice vaccinated with saline served as a control. Two different concentrations (10*7 PFU and 10*8 PFU) and two different vaccination schemes (prime only, prime-boost: 21-day interval) were used by application into the quadriceps muscle of the left hind leg using the intramuscular route. Blood samples were collected on day 0, 18 and 35 post 1st immunization. To obtain serum, coagulated blood was centrifuged at 2,000 rpm for 10 min. The serum samples were stored at -20 °C.

2.4.2. Transduction of vaccinated mice and challenge infection with SARS-CoV-2 (performed at the Institute of Virology, Philipps University Marburg)

Mice were vaccinated as described in *2.4.1 Vaccination experiments* and shipped to Prof. Dr. Stephan Becker`s lab at the Philipps University Marburg (Germany) for further experiments. Mice were isolated for at least one week to adapt to the facility. Mice were kept under anesthesia (ketamine/xylazine) and inoculated with 5x 10*8 PFU Adenovirus-ACE2-mCherry (cloned at ViraQuest Inc., North Liberty, IA, USA) using the intratracheal route. Three days post transduction, mice were infected with 1.5x 10*4 $TCID_{50}$ SARS-CoV-2 (BavPat1/2020 isolate, European Virus Archive Global #026V-03883) using the intranasal route. Mice were euthanized four days post infection and serum and tissue samples were taken for further analysis.

2.4.3. Enzyme-linked immune sorbent assay (ELISA)

SARS-CoV-2-S specific IgG titers were analyzed as described previously (KALODIMOU et al. 2019). Briefly, 96-well ELISA plates were coated with recombinant COVID-19 S protein (Full Length-R683A-R685A425 HisTag, ACROBiosystems, Newark, USA) o/n at 4 °C. Plates were washed with PBS and blocked with PBS (+ 1% BSA, 0.15 M sucrose) for 1 h at 37 °C. Heat-inactivated mice sera were serially diluted three-fold in PBS (+ 1% BSA),

starting with a 1:100 dilution. ELISA plates were rinsed and mixed with the diluted mice sera and incubated for 1 h at 37 °C. Afterwards, plates were washed and probed with a goat anti-mouse IgG HRP antibody (diluted in PBS + 1% BSA) for 1 h at 37 °C. After another wash step, 3´3´,5´5´- TMB Liquid Substrate System for ELISA was added and incubated until a color change was observed. The reaction was stopped with stop reagent for TMB substrate. The absorbance of each sample was measured at 450 nm with a 620 nm reference wavelength. A positive control was used to normalize the data and the control group (PBS) was used to set the cut-off value. Therefore, the mean value of the normalized OD values from the control group plus six standard deviations was determined.

2.4.4. Prediction and generation of synthetic SARS-CoV-2-S peptides

The Immune Epitope Database and Analysis Resource (IEDB) was used for epitope predication (CD8+T cell and CD4+ T cell) on the basis of the full-length SARS-CoV-2-S sequence (NCBI ID: QHD43416.1, Uniprot ID: P0DTC2 (SPIKE_SARS2). The prediction was used only for the species “mouse” with the class I MHC alleles H2-K^d, H2-D^d and H2-L^d (CD8+ T cell) and the class II MHC alleles H2-IA^d and H2-IE^d (CD4+ T cell). To identify possible CD8+ T cell epitopes, the class I MHC Binding Prediction and class I MHC Processing Prediction tools (DHANDA et al. 2019; FLERI et al. 2017) were used, ending up with a long list of 9-11 amino acid long peptides restricted to a percentile rank cut-off of 10.0. Furthermore, all peptides with an IC_{50} score of ≤ 500 nM were selected for analysis using the class I MHC Processing Prediction tool “Proteasomal cleavage/TAP transport/MHC class I combined predictor. Peptides with a high score remained in the list of potential epitopes.

To identify probable CD4+ T cell epitopes, the class II MHC Binding Prediction tool (DHANDA et al. 2019; FLERI et al. 2017) was used ending up with a list of 15 amino acid long peptides. Peptides with a percentile rank of ≤10.0 and an IC_{50} rank of ≤1000 nM were selected for synthesis and testing. All peptides were obtained from Thermo Fisher Scientific (Planegg, Germany) as crude material. For further testing by ELISpot assay and ICS, the lyophilized peptides were

diluted in PBS or DMSO. In total, 19 potential CD8+ T cell and 15 CD4+ T cell epitopes were synthesized for further testing.

2.4.5. Enzyme-linked immunosorbent Spot assay (ELISpot assay)

ELISpot assay was performed to measure IFN-γ-producing T cells (VEIT et al. 2018). At day eight post prime or prime-boost vaccination, mice were euthanized and whole splenocytes were prepared. Cell suspensions were prepared by passing spleens through a 70 µm strainer and lysed with Red Blood Cell Lysis Buffer. Cells were centrifuged for 5 min at 1,500 rpm, washed twice and resuspended in RPMI 1640 medium (+ 10% FBS, 1% penicillin/streptomycin, 1% HEPES). ELISpot assay was performed according to the manual. Briefly, 2x 10*5 splenocytes were seeded in 96-well plates and stimulated with the peptides (2 µg/ml in RPMI medium). Non-stimulated cells and cells stimulated with PMA/ionomycin or Vaccinia virus peptide SPGAAGYD ($F2(G)_{26-34}$; H-2L^d) (TSCHARKE et al. 2005) served as controls. Cells were cultured for 48 h at 37 °C and afterwards stained according to the manual. Spots were counted for further analysis by an automated ELISpot plate reader.

2.4.6. Intracellular cytokine staining (ICS)

Intracellular cytokine staining was performed as described before (KALODIMOU et al. 2019). Briefly, splenocytes were isolated as described in chapter *2.4.5. Enzyme-linked immunosorbent Spot assay*. Cells were stimulated with 8 µg/ml $S_{269-278}$ peptide or Vaccinia virus peptide $F2_{26-34}$ to analyze SARS-CoV-2-S- or MVA-specific CD8+ T cell responses. Splenocytes stimulated with PMA/ionomycin were used as positive controls whereas splenocytes stimulated with RMPI medium were used as a negative control. After 2 h at 37 °C, brefeldin A was added and cells were cultured for 4 h at 37 °C. The stimulated cells were washed with FACS buffer (+ 2% FBS) and stained with anti-mouse CD3 phycoerithrin (PE)-Cy7, anti-mouse CD4 542 Brilliant Violet, anti-mouse CD8α Alexa Fluor 488 and CD16/CD32 for 30 min on ice. Cells were washed and fixed with fixation buffer for 20 min on RT, resuspended in FACS buffer and stored at 4 °C o/n. The next day, cells were permeabilized by using intracellular staining permeabilization wash buffer and stained with

anti-mouse IFN-γ diluted in perm wash buffer for 30 min at RT. Afterwards, cells were washed and resuspended in FACS buffer and data were acquired by MACSQuant VYB Flow Analyser. Analysis was performed by using the software FlowJo.

2.5. Statistical analysis

Data were analyzed using GraphPad Prism 5.0 (GraphPad Sodtware Inc., San Diego, CA, USA) and were expressed as mean ± standard error of the mean unless stated otherwise. Statistical analysis was performed using unpaired two-tailed t test to compare two groups. Comparison of three or more groups was analyzed by one-way ANOVA and Tukey post-hoc test. P-values less than 0.05 were considered to be statistically significant.

V. OBJECTIVES

The global pandemic caused by SARS-CoV-2 is still present, affecting the daily life of millions of people. Due to the lack of approved therapies and the need for more vaccines against SARS-CoV-2, this work describes the following milestones in the development of the new candidate vaccine MVA-SARS-CoV-2-S:

(i) Generation of recombinant MVA expressing the full-length SARS-CoV-2 spike protein (MVA-SARS-CoV-2-S).

(ii) *In vitro* characterization of recombinant MVA-SARS-CoV-2-S

a. Genome analysis and stability testing
b. Protein expression
c. Replication capacity

(iii) *In vivo* characterization of recombinant MVA-SARS-CoV-2-S in terms of adaptive immune response in BALB/c mice

a. Immunization experiments
b. Determination of SARS-CoV-2-S specific CD8+ and CD4+ T cell epitopes
c. Humoral immune response against SARS-CoV-2, including analysis of binding and neutralizing antibodies
d. Protective capacity of MVA-SARS-CoV-2-S upon challenge infection

VI. RESULTS

1. Construction and characterization of recombinant MVA-SARS-CoV-2-S

1.1. Construction of recombinant MVA-SARS-CoV-2-S

To generate the recombinant MVA-SARS-CoV-2-S (MVA-S), the encoding sequence of the spike protein from the virus isolate Wuhan HU-1 (GenBank accession no. MN908947.1) served as a template. In addition, modifications including an HA-tag and codon optimization were made. For the latter, G/C-runs and TTTTTNT regions were changed on the genomic level without affecting the amino acid sequence. Furthermore, restriction sites (*PmeI* and *NotI)* were added for cloning the SARS-CoV-2-S sequence into the MVA vector plasmid pIIIPmH5red.

The cDNA was placed under the transcriptional control of the Vaccinia virus early/late PmH5 promoter (WYATT et al. 1996) by integration of the sequence into the MVA vector plasmid pIIIPmH5red. The new plasmid, pIIIPmH5red-SARS-CoV-2-S contains a resistance gene (AmpR), flank regions (flank-1 and flank-2) of MVA genomic DNA and the reporter gene mCherry (**Figure 9**). Correct insertion and identity of the SARS-2-S sequence was confirmed by sequencing.

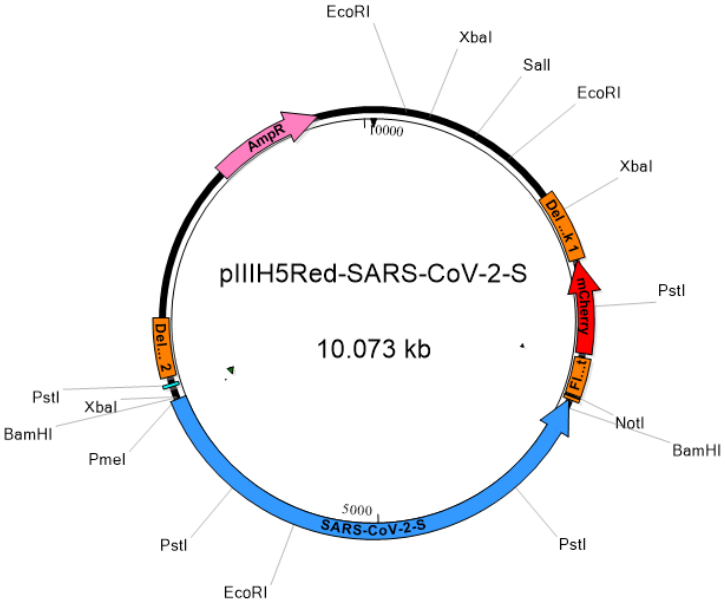

Figure 9: Vector plasmid pIIIH5red-SARS-CoV-2-S. The sequence of SARS-CoV-2-S (blue) was cloned between flanking regions (flank-1 and flank-2, orange) for homologous recombination into deletion site III of the MVA genome. The marker gene mCherry (red) was placed between two flanks (orange) for intragenomic homologous recombination during plaque purification. The resistance gene AmpR (blue) was used for selection of positive clones after integration of the SARS-CoV-2-S sequence into the plasmid.

The encoding sequence of SARS-CoV-2-S was introduced into deletion site III of MVA-F6-sfMR by homologous recombination between MVA DNA sequences adjacent to deletion site III in the MVA genome and copies cloned into plasmid pIIIPmH5red-SARS-2-S (flank-1 and flank-2). Recombinant MVA-SARS-CoV-2-S was obtained by plaque purification using the co-expressed fluorescent protein mCherry. The latter was removed by intragenomic homologous recombination during plaque purification and amplification of the recombinant virus (marker gene deletion) (**Figure 10**).

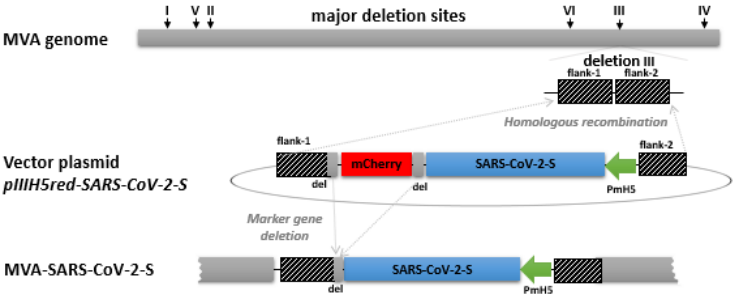

Figure 10: Construction of recombinant MVA-SARS-CoV-2-S. Schematic diagram of the MVA genome including the six major deletion sites I-VI. The encoding sequence of SARS-CoV-S was introduced into the deletion site III by homologous recombination. Deletion of the marker gene mCherry occurred by intragenomic homologous recombination.

1.2. Genetic characterization and stability of the SARS-CoV-2 spike sequence

Viral DNA was isolated and further analyzed in regard to correct insertion and genomic integrity of the SARS-CoV-2-S sequence. In addition, correct removal of the marker gene mCherry as well as the integrity of the C7L gene region were tested. The latter encodes a regulatory Vaccinia virus protein, which is important for viral gene expression in mammalian cells (BACKES et al. 2010; MEYER et al. 1991; NÁJERA et al. 2006). Therefore, different control PCRs were performed, as described previously (SONG et al. 2013; VEIT et al. 2018).

The correct length of the insert could be shown by amplifying a PCR product of about 4.8 kb **(Figure 11a**). The correct removal of mCherry could be shown by comparing the PCR product from pIIIH5red-SARS-CoV-2-S (pIII-S) with the recombinant MVA-SARS-CoV-2-S (MVA-S). A difference of ~1.0 kb in size corresponds to the size of mCherry. The absence of non-recombinant MVA could be shown by the lack of the characteristic amplicon of 0.762 kb. Specific oligonucleotides binding inside the insert region were designed, allowing an amplification of overlapping amplicons with sizes of 0.714 kb, 0.954 kb, 1.341 kb and 1.689 kb (**Figure 11b**). Next, the C7L specific PCR was performed verifying that the recombinant MVA-SARS-CoV-2-S shows no difference to non-recombinant MVA (**Figure 11c**).

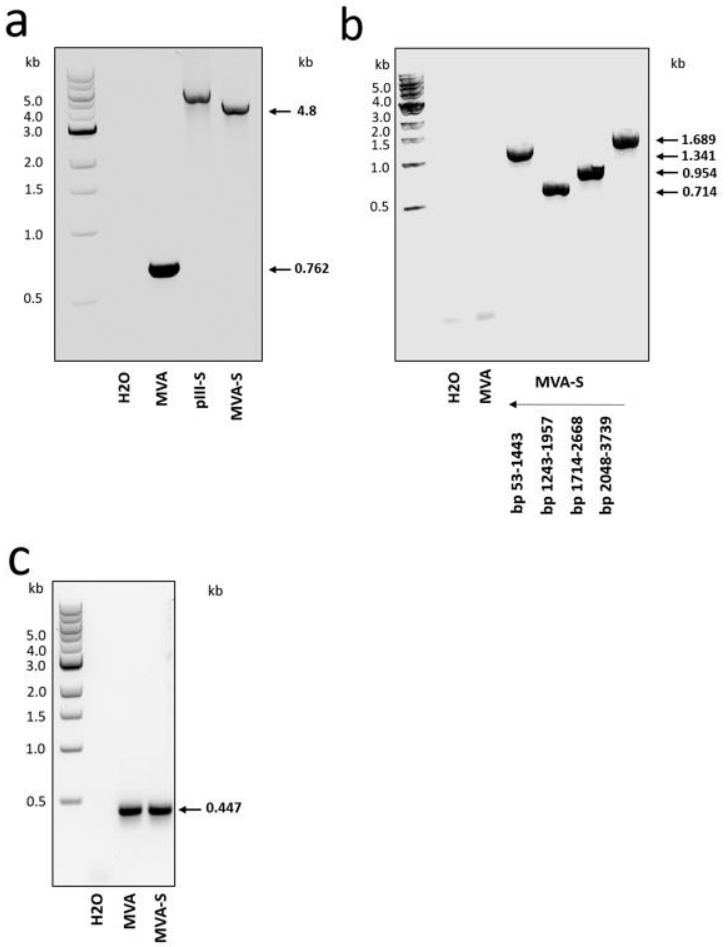

Figure 11: Genetic integrity of MVA-SARS-CoV-2-S (MVA-S). Genomic DNA was analyzed for correct insertion into (a) deletion site III, (b) correct size of the insert, and (c) genetic integrity of the C7L region. (a) line 1: H2O control. line 2: non-recombinant MVA. line 3: pIIIPmH5red-SARS-CoV-2-S (pIII-S). line 4: recombinant MVA-SARS-CoV-2-S (MVA-S). The absence of non-recombinant MVA was demonstrated by the lack of a specific DNA fragment (0.762 kb). Removal of the marker gene mCherry was shown by the reduced size (~1.0 kb) of recombinant MVA-S compared to pIII-S. (b) line 1: H_2O control. line 2: non-recombinant MVA. line 3-6: overlapping amplicons to cover full-length S protein. (c) line 1: H_2O control. line 2: non-recombinant MVA. line 3: MVA-SARS-CoV-2-S (MVA-S).

To confirm genetic integrity, recombinant MVA-SARS-CoV-2-S was passaged five times on DF-1 cells at a MOI of 0.05 (“low MOI passage”). Afterwards, genomic analysis and stable protein expression were further validated. In regard of genomic analysis, the six deletion PCRs of passage 1 and passage 5 were performed by using oligonucleotides that bind to the flank regions of the six major MVA deletions sites I-VI. No difference could be observed between passage 1 and passage 5 in terms of stability of the SARS-CoV-2-S sequence (**Figure 12**).

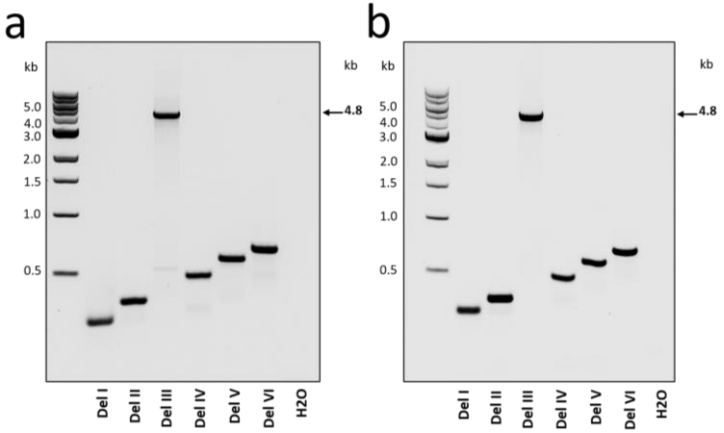

Figure 12: Genetic stability of the six major deletion sites of MVA-SARS-CoV-2-S (MVA-S) following serial passages on DF-1 cells. Viral DNA was isolated and tested for stability of the six major deletion sites after serially passaging MVA-S on DF-1 cells for (a) one time or (b) five times. (a, b) line 1: deletion site I. line 2: deletion site II. line 3: deletion site III. line 4: deletion site IV. line 5: deletion site V. line 6: deletion site VI. line 7: H_2O control.

To screen for stable protein expression following low MOI passage, immunostaining was conducted (**Figure 13**). A total of 60 clonal MVA-S isolates were collected after the fifth passage on DF-1 cells and used to infect DF-1 cells grown on 24-well tissue culture plates. Cells infected with non-recombinant MVA were used as control. Cells were incubated for 48 h and stained with anti-Vaccinia and anti-HA antibodies. Plaques were counted and 60/60 MVA-S isolates were tested positive for unimpaired expression of the recombinant SARS-CoV-2-S protein.

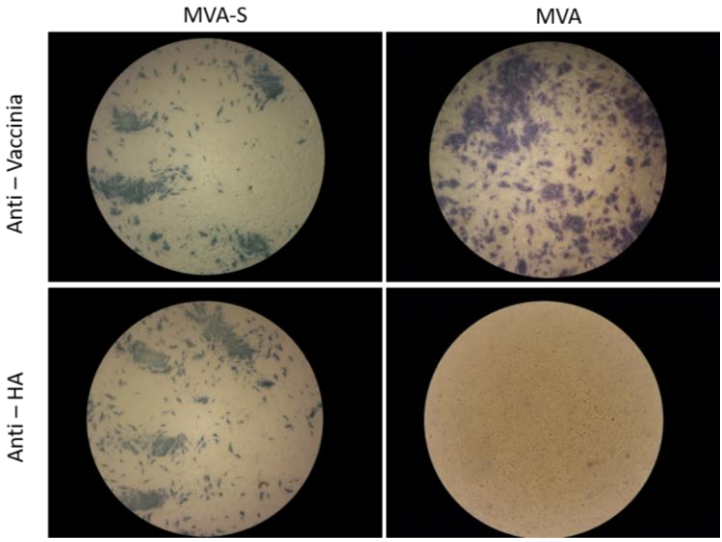

Figure 13: Low MOI passage of recombinant MVA-SARS-CoV-2-S (MVA-S). Recombinant MVA-S was serially passaged on DF-1 cells and unimpaired recombinant gene expression was screened by immunostaining using an antibody directed against the HA-tag.

1.3. Protein expression of full-length SARS-CoV-2 spike protein

To evaluate the expression pattern of the recombinant spike protein, Vero E6 cells were infected with recombinant MVA-SARS-CoV-2-S (MVA-S) and stained with antibodies directed against the HA-tag or the spike protein and were further analyzed using fluorescence microscopy. The antibody directed against the HA-tag at the *C*-terminal part of the recombinant spike protein showed specific staining in permeabilized cells, which corresponds to the expected intercellular localization of the *C*-terminus of the SARS-CoV-2-S protein. The SARS-CoV-1/SARS-CoV-2 specific antibody recognizes a region in the external domain of the spike protein and allows staining in non-permeabilized cells, which indicates a translocation of the SARS-CoV-2-S protein to the cytoplasm membrane (**Figure 14**).

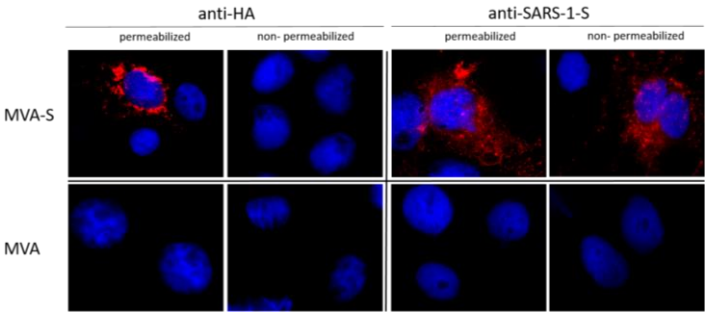

Figure 14: Immunostaining of SARS-CoV-2 spike protein in MVA-SARS-CoV-2-S (MVA-S) infected Vero E6 cells. Cells were infected at a MOI of 0.5 with recombinant MVA-S or non-recombinant MVA (control) and fixed with paraformaldehyde. Permeabilized and non-permeabilized cells were probed with antibodies directed against the HA-tag or the spike protein and further stained with a secondary antibody to perform S-specific fluorescent staining (red). Cell nuclei were counterstained using DAPI (blue).

In addition, the recombinant spike protein was examined in more detail by using Western Blot analysis. Vero E6 cells were infected with recombinant MVA-SARS-CoV-2-S and non-recombinant MVA (control) and lysates were prepared after certain time-points to screen for protein expression over time. The proteins were separated by SDS-PAGE according to their sizes and stained with a specific antibody directed against the HA-tag. Two prominent bands at 190 kDa and 90-100 kDa could be observed (**Figure 15**). The higher band might refer to the full-length spike protein whereas the lower band might refer to the S2 cleavage product as the HA-tag is located at the *C*-terminal part of the spike protein. Due to the early transcription of SARS-CoV-2-S by the MVA PmH5 promoter, high protein amounts were already detectable two hours post infection, continuously increasing until 24 hours post infection. The expected size of SARS-CoV-2-S is around 145 kDa which leads to the hypothesis that the spike protein might be glycosylated. Indeed, NetNGlyc 1.0 server analysis indicated at least 17 N-glycosylation sites for co- and post-translational modifications. The treatment of cell lysates with PNGase F, which removes all N-linked oligosaccharide chains, reduced the molecular masses of the recombinant SARS-CoV-2-S protein bands from 190 kDa to 145 kDa and from 90-100 kDa to 65 kDa, perfectly matching the expected sizes of unmodified full-length SARS-CoV-2-S and the S2 cleavage product (**Figure 15**).

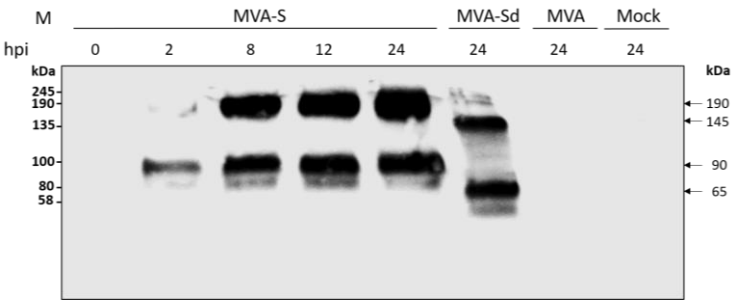

Figure 15: Synthesis of full-length spike protein in MVA-SARS-CoV-2-S (MVA-S) infected Vero E6 cells. Cells were infected at a MOI of 10 and collected after the indicated time points. Furthermore, deglycosylation of the S protein was performed using PNGase F (MVA-Sd). Polypeptides were separated by SDS-PAGE and analyzed with an antibody directed against the HA-tag. Lysates from non-infected (Mock) or non-recombinant MVA infected (MVA) cells were used as controls.

1.4. Growth kinetics on permissive and non-permissive cell lines

Beside genomic stability and stable expression of SARS-CoV-2-S, another important feature of (recombinant) MVA is the replication deficiency in mammalian cell lines. To confirm the replication deficiency, a multiple-step growth analysis on various mammalian cell lines was performed. Three cell lines of human origin (HaCat, HeLa, and A549 cells) were infected with recombinant MVA-SARS-CoV-2-S (MVA-S) and non-recombinant MVA (control) and collected after the indicated time points. Furthermore, the avian cell line DF-1, which was used to amplify the recombinant MVA-S, served as a control cell line permissive for MVA growth. No virus replication could be observed in human cell lines up to 72 hours post infection. In DF-1 cells, however, recombinant MVA-S productively amplified to levels comparable with non-recombinant MVA (**Figure 16**).

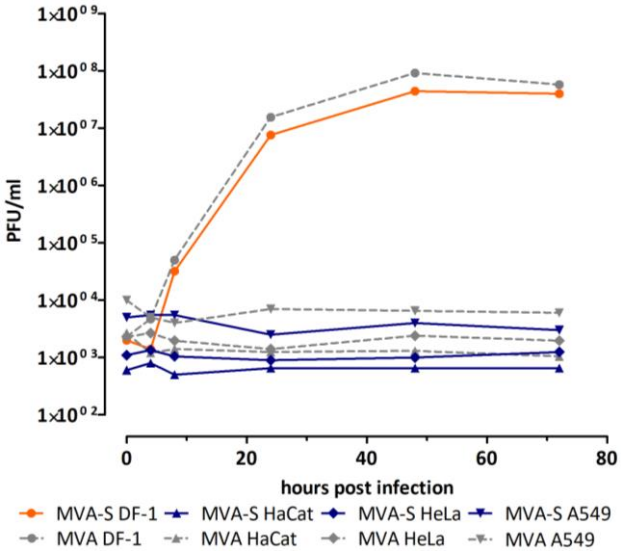

Figure 16: Multiple-step growth analysis of recombinant MVA-SARS-CoV-2-S (MVA-S) and non-recombinant MVA (MVA). Cells were infected at a MOI of 0.05 with MVA-S or MVA and collected at the indicated time points. Titration was performed on CEF cells and plaque-forming units (PFU) were determined. MVA-S and MVA could be amplified on DF-1 cells but failed to replicate on all tested cells of human origin (HaCat, HeLa, and A549 cells).

2. Immune response

2.1. Determination of a potential CD8+ T cell epitope

Information about antigen specificities of SARS-CoV-2-S specific T cells is limited. Due to that, the IEDB was used for selection of putative S-specific peptide epitopes for activation of CD8+ T cell and CD4+ T cell response. The predicted peptides were divided into pools of three to six peptides. BALB/c mice were vaccinated with 10*8 PFU and euthanized eight days post prime immunization. Splenocytes were further processed to test the activation capacity of different peptide pools. Several peptide pools showed responses above the background signal **(Figure 17a)** and, after testing single peptides, the immunodominant SARS-CoV-2 S H2-K^d epitope $S_{269-278}$ (GYLQPRTFL; S1 N-terminal) could be identified (**Figure 17b**).

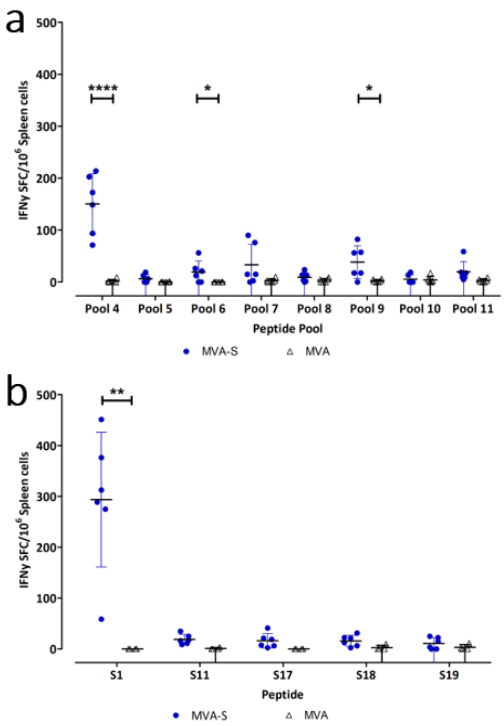

Figure 17: Identification of H2-d restricted T cell epitopes of the SARS-CoV-2-S protein. BALB/c mice (n= 4-6) were immunized once with 10*8 PFU MVA-SARS-CoV-2-S (MVA-S) or non-recombinant MVA (MVA) via the i.m. route. Splenocytes were collected and further processed eight days post immunization and stimulated with pools of peptides (9-12 mer) or single peptides from positive pools and were analyzed by IFN-γ ELISPOT assay. (a) IFN-γ spot forming-cells (SFC) measured by ELISpot assay after stimulation with peptide pools. (b) IFN-γ SFC measured by ELISpot assay after stimulation of single peptides from the two most promising pools P4 and P9. Statistical differences between MVA-S and MVA groups were analyzed by unpaired two-tailed t tests. Asterisks represent statistically significant differences between the groups. * $p < 0.05$, ** $p < 0.01$, **** $p < 0.0001$

The predicted CD4+ T cell epitopes were not tested in the prime only schedule, but were included as pools of three to six peptides to test CD4+ T cell response upon prime-boost vaccination (chapter *2.2.1. Spike specific CD8+ and CD4+ T cell response*)

2.2. T cell response

To assess the S-antigen specific T cell response (CD8+ and CD4+) upon vaccination with MVA-SARS-CoV-2-S, two different vaccination schedules (prime only, prime-boost) with two different doses (low dose: 10*7 PFU and high dose: 10*8 PFU) were performed (**Figure 18**).

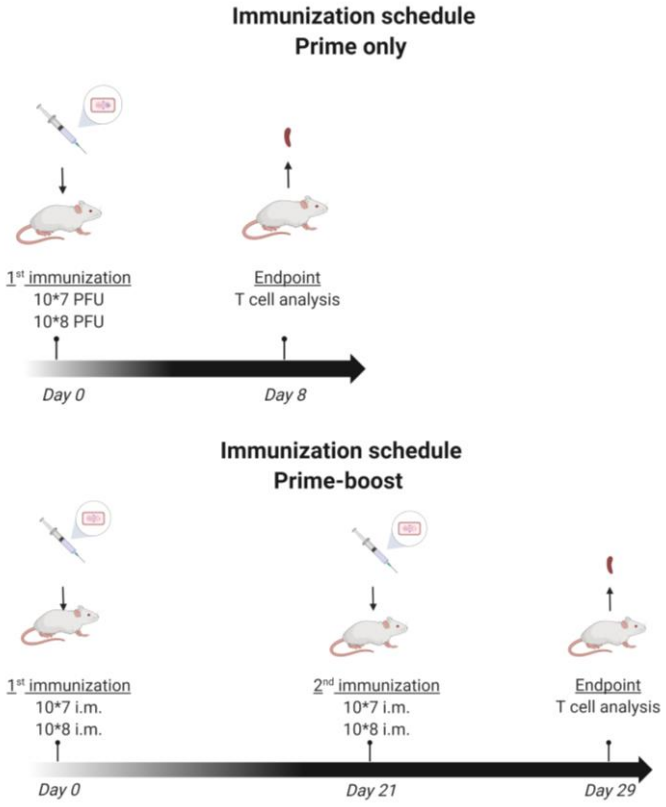

Figure 18: Schematic diagram of two immunization schedules (prime only and prime-boost) with MVA-SARS-CoV-2-S (MVA-S) to test T cell responses. Groups of BALB/c mice (n=4-6) were vaccinated with 10*7 PFU (low dose) or 10*8 PFU (high dose) of MVA-S via the i.m. route using a prime only or prime-boost schedule. T cell responses were examined at day eight post 1st immunization (prime only) or 2nd immunization (prime-boost). Created with BioRender.com

2.2.1. Spike specific CD8+ and CD4+ T cell response

S-antigen specific CD8+ T cell response was determined by IFN-γ ELISpot assay and intracellular cytokine staining (ICS). Splenocytes of mice vaccinated according to the prime only or prime-boost schedule were isolated at day eight post last immunization and stimulated with the immunodominant SARS-CoV-2-S H2-K^d epitope $S_{269-278.}$ A single application of MVA-SARS-CoV-2-S (MVA-S) induced detectible levels of $S_{269-278}$ epitope-specific induced CD8+ T cells with mean numbers of 342 IFN-γ spot-forming-cells (SFC) in splenocytes for the low dose and 275 SFC for the high dose. Mice vaccinated with non-recombinant MVA showed no detectible SFC (**Figure 19a**).

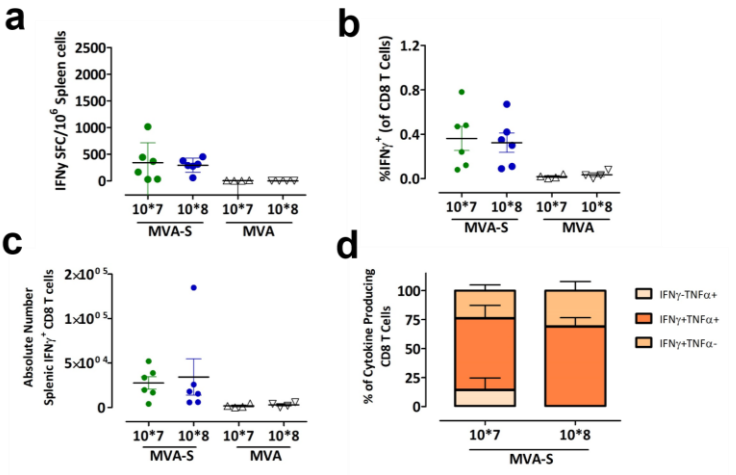

Figure 19: Activation of SARS-CoV-2-S specific CD8+ T cell response after prime only immunization with MVA-SARS-CoV-2-S (MVA-S). Groups of BALB/c mice (n= 4-6) were immunized once with 10*7 or 10*8 PFU MVA-S using the i.m. route. Mice vaccinated with non-recombinant MVA were used as controls. Splenocytes were collected and isolated at day eight post immunization and stimulated with the H2^d restricted peptide of the SARS-CoV-2-S protein $S_{268-276}$ and measured by (a) IFN-γ ELISpot assay and (b-d) IFN-γ and TNF-α ICS plus FACS analysis. (b, c) IFN-γ produced by CD8+ T cells measured by FACS analysis. Graphs show (b) frequency and (c) absolute number of IFN-γ producing CD8+ T cells. (d) cytokine profile of $S_{268-276}$ specific CD8+ T cells. Graphs show the mean frequency of IFN-γ-TNF-α+, IFN-γ+ TNF-α+ and IFN-γ+ TNF-α- cells within the positive CD8+ T cell population.

Intracellular cytokine staining (ICS) for IFN-γ was performed to complement the ELISpot results, showing mean values of 0.32% (high dose) and 0.36% (low dose) IFN-γ positive splenic CD8+ T cells (**Figure 19b**). The absolute numbers of IFN-γ positive CD8+ T cells were 27,487 (low dose) and 34,294 (high dose). Mice vaccinated with non-recombinant MVA showed no detectible number of IFN-γ positive CD8+ T cells (**Figure 19c**). Substantial numbers of IFN-γ positive CD8+ T cells showed co-expression of TNF-α, with mean values of 61.7% (low dose) and 68.7% (high dose) from total IFN-γ expressing cells (**Figure 19d**). No significant difference between the two doses could be observed for the prime only schedule in terms of the CD8+ T cell response.

The second immunization at day 21 with 10*7 PFU (low dose) or 10*8 PFU (high dose) of MVA-SARS-CoV-2-S increased the number of S-specific CD8+ T cells. At day eight post second immunization, splenocytes were isolated and stimulated with the immunodominant SARS-CoV-2 S H2-K^d epitope $S_{269-278}$. ELISpot analysis revealed mean numbers of 1,020 IFN-γ SFC (low dose) and 1,159 IFN-γ SFC (high dose) in vaccinated animals. Mice vaccinated with saline (PBS) showed no SFC (**Figure 20a**).

Intracellular cytokine staining revealed mean values of 0.62 % (high dose) and 0.60% (low dose) IFN-γ positive splenic CD8+ T cells (**Figure 20b**) and total numbers of 40,873 (low dose) and 49,553 IFN-γ positive CD8+ T cells (**Figure 20c**). As already seen for the prime only immunization, a high proportion of IFN-γ positive CD8+ T cells co-expressed TNF-α (~70% for low and high dose) (**Figure 20d**).

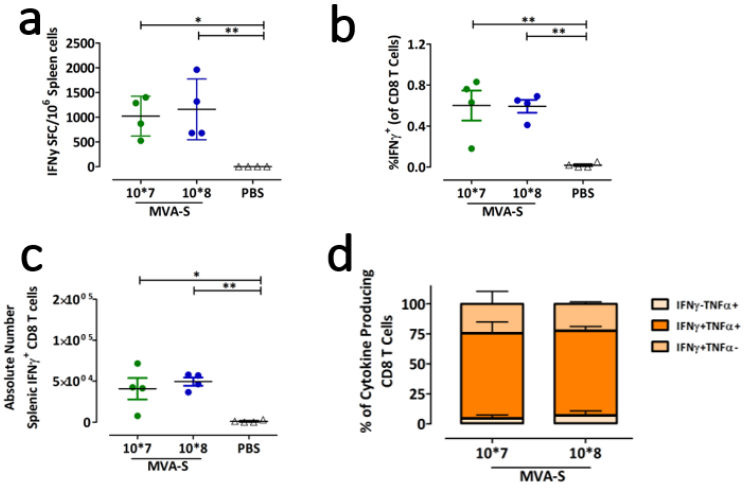

Figure 20: Activation of SARS-CoV-2-S specific CD8+ T cell response after prime- boost immunization with MVA-SARS-CoV-2-S (MVA-S). Groups of BALB/c mice (n=4) were immunized twice with 10*7 or 10*8 PFU of MVA-S over a 21-day interval using the i.m. route. Mice vaccinated with saline (PBS) served as controls. Splenocytes were collected and isolated at day eight post boost immunization and stimulated with the $H2^d$ restricted peptide of the SARS-2-S protein $S_{268-276}$ and measured by (a) IFN-γ ELISpot assay and (b-d) IFN-γ and TNF-α ICS plus FACS analysis. (b, c) IFN-γ produced by CD8+ T cells measured by FACS analysis. Graphs show (b) frequency and (c) absolute number of IFN-γ producing CD8+ T cells. (d) cytokine profile of $S_{268-276}$ specific CD8+ T cells. Graphs show the mean frequency of IFN-γ-TNF-α+, IFN-γ+ TNF-α+ and IFN-γ+ TNF-α- cells within the positive CD8+ T cell population. Differences between the groups were analyzed by one-way ANOVA and Tukey post-hoc test. Asterisks represent statistically significant differences between the groups. * $p < 0.05$, ** $p < 0.01$

Moreover, activation of S-specific CD4+ T cells was analyzed. The predicted epitopes for MHC II binding were tested after a prime-boost immunization with low dose (10*7 PFU) or high dose (10*8 PFU) of MVA-SARS-CoV-2-S. Splenocytes were collected at day eight post 2nd immunization and stimulated with three pools containing three to six peptides (15 mer). The presence of small amounts of S-specific CD4+ T cells could be demonstrated with mean values of 10-20 SFC (low dose) and 16-25 SFC (high dose) (**Figure 21**).

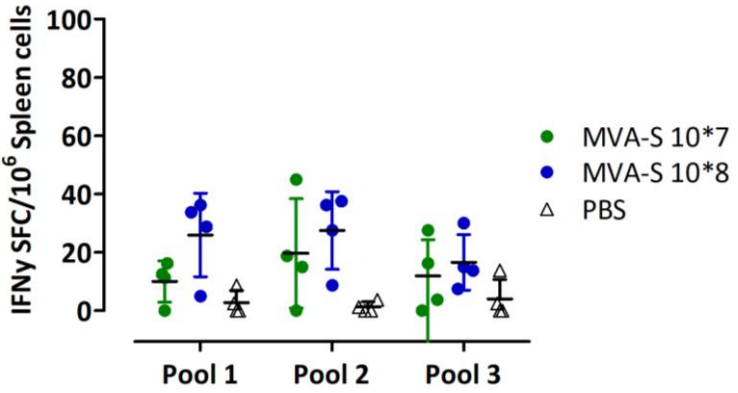

Figure 21: Analysis of predicted peptides to activate CD4+ T cell response upon prime-boost vaccination with MVA-SARS-CoV-2-S (MVA-S). Groups of BALB/c mice (n= 4-6) were immunized twice over a 21-day interval with 10*7 PFU or 10*8 PFU MVA-S using the i.m. route. Mice vaccinated with saline (PBS) served as controls. Splenocytes were collected and isolated at day eight post 2nd immunization and stimulated with three different pools (three to six peptides/pool) containing 15 mer peptides. IFN-γ spot-forming cells (SFU) were measured by ELISpot assay.

2.2.2. MVA-specific CD8+ T cell response

The MVA-specific immunodominant CD8+ T cell epitope $F2(G)_{26-34}$ served as a control for detection and analysis of MVA vector-specific CD8+ T cell response in BALB/c mice. A single application of MVA-SARS-CoV-2-S (MVA-S) induced substantial levels of $F2(G)_{26-34}$ epitope-specific CD8+ T cells with mean values of 337 IFN-γ SFC (low dose) and 496 IFN-γ SFC (high dose). Mice vaccinated with non-recombinant MVA showed mean values of 477 IFN-γ SFC (low dose) and 481 IFN-γ SFC (high dose) (**Figure 22a**). Intracellular cytokine staining revealed values of 0.39% (low dose) and 0.26% (high dose) IFN-γ positive CD8+ T cells in the spleen (**Figure 20b**) and total numbers of 33,310 (low dose) and 16,624 (high dose) IFN-γ positive CD8+ T cells (**Figure 22c**). Mice vaccinated with non-recombinant MVA showed mean values of 0.37% (low dose) and 0.22% (high dose) IFN-γ positive splenic CD8+ T cells (**Figure 22b**) and total numbers of 32,777 (low dose) and 16,672 (high dose) IFN-γ positive CD8+ T cells (**Figure 22c**). A high proportion of IFN-γ positive CD8+ T cells also co-expressed TNF-α (68.5% for low dose and 37.7% for high dose) in mice vaccinated with MVA-S. In the control group mean values of 77.4% (low dose)

and 47.6% (high dose) of IFN-γ+ TNF-α+ CD8+ T cells were observed.

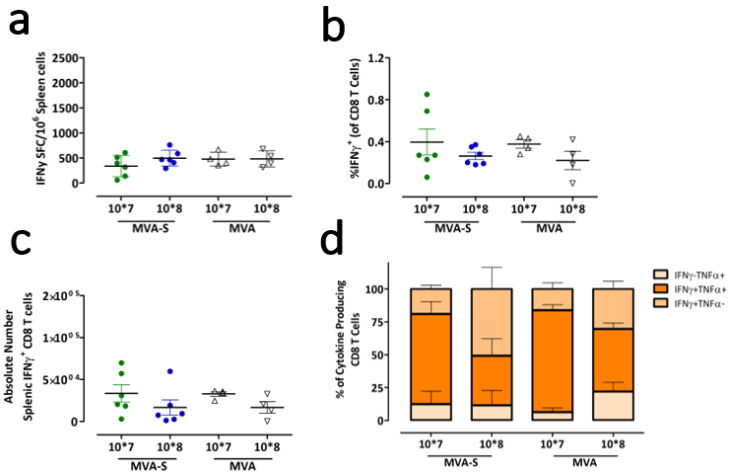

Figure 22: Induction of MVA-specific CD8+ T cell response upon prime immunization with MVA-SARS-CoV-2-S (MVA-S). Groups of BALB/c mice (n=4-6) were vaccinated once with 10*7 PFU (low dose) or 10*8 PFU (high dose) MVA-S. Mice vaccinated with non-recombinant MVA were used as controls. Splenocytes were collected at day eight post immunization and stimulated with the $H2^d$ restricted MVA-specific peptide $F2(G)_{26-34}$. Measurement of IFN-γ was performed by IFN-γ ELISpot assay and IFN-γ and TNF-α ICS plus FACS analysis. (a) IFN-γ spot-forming-cells (SFC) for splenocytes analysis by ELISpot assay. (b) percentage of CD8+ T cells producing IFN-γ. (c) absolute number of CD8+ T cells producing IFN-γ. (d) cytokine profile of CD8+ T cells stimulated by MVA-specific $F2(G)_{26-34}$ peptide. Graph shows mean frequency of IFN-γ- TNF-α+, IFN-γ+ TNF-α+ and IFN-γ+ TNF-α- cells within the positive CD8+ T cell population.

The second immunization at day 21 with 10*7 PFU (low dose) or 10*8 PFU (high dose) MVA-S increased the number of MVA-specific CD8+ T cells. At day eight post 2nd immunization, splenocytes were collected and stimulated with the MVA-specific $F2(G)_{26-34}$ peptide. ELISpot analysis revealed mean numbers of 1,054 IFN-γ SFC (low dose) and 1,230 IFN-γ SFC (high dose) in vaccinated animals. Mice vaccinated with saline (PBS) showed no SFC (**Figures 23a**). Intracellular cytokine staining revealed mean values of 0.70% (high dose) and 0.64% (low dose) IFN-γ positive splenic CD8+ T cells (**Figure 23b**) and total numbers of 48,733 (low dose) and 61,620 IFN-γ positive CD8+ T cells (**Figure 23c**). As already seen for the prime only immunization, a high proportion of IFN-

γ positive CD8+ T cells co-expressed TNF-α (~70% for low and high dose) (**Figure 23d**).

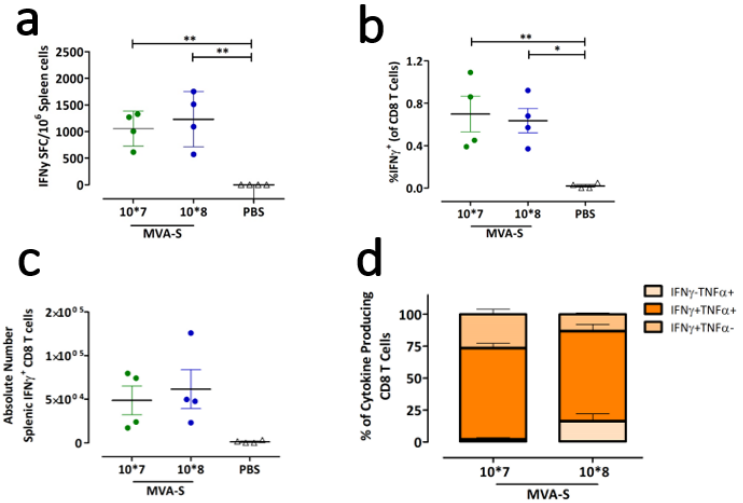

Figure 23: Induction of MVA-specific CD8+ T cell response upon prime-boost vaccination (21-day interval) with MVA-SARS-CoV-2-S (MVA-S). Groups of BALB/c mice (n=4) were immunized twice with 10*7 PFU (low dose) or 10*8 PFU (high dose) MVA-S over a 21-day interval. Mice vaccinated with saline (PBS) were used as controls. Splenocytes were collected at day eight post 2nd immunization and stimulated with the $H2^d$ restricted MVA-specific peptide $F2(G)_{26-34}$. Measurement of IFN-γ was performed by IFN-γ ELISpot assay and IFN-γ and TNF-α ICS plus FACS analysis. **(a)** IFN-γ spot-forming- cells (SFC) for splenocytes analysis by ELISpot assay. **(b)** percentage of CD8+ T cells producing IFN-γ. **(c)** absolute number of CD8+ T cells producing IFN-γ. **(d)** cytokine profile of CD8+ T cells stimulated by MVA-specific $F2(G)_{26-34}$ peptide. Graph shows mean frequency of IFN-γ- TNF-α+, IFN-γ+ TNF-α+ and IFN-γ+ TNF-α- cells within the positive CD8+ T cell population. Differences between the groups were evaluated by one-way ANOVA and Tukey post-hoc test. Asterisks represent statistically significant differences between the groups. * $p < 0.05$, ** $p < 0.01$.

2.3. Spike specific humoral immune response

To evaluate the S-antigen specific humoral immune response upon vaccination with MVA-SARS-CoV-2-S (MVA-S), BALB/c mice were vaccinated twice with 10*7 PFU (low dose) or 10*8 PFU (high dose) MVA-S over a 21-day interval. Serum samples were collected at day 18 post 1st immunization and at day 14 post 2nd immunization (**Figure 24**).

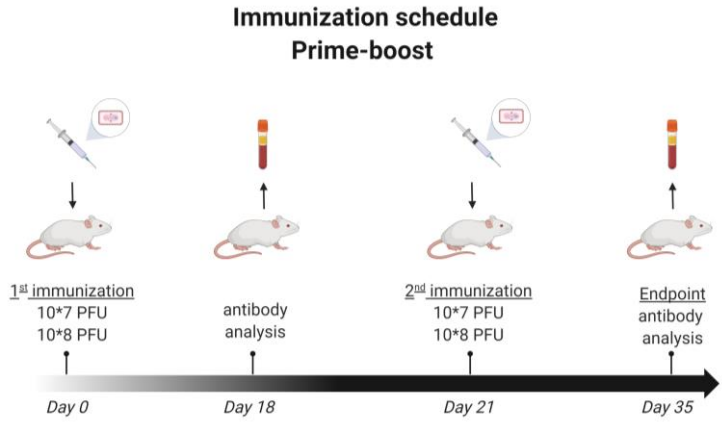

Figure 24: Schematic diagram of prime-boost immunization schedule with MVA-SARS-CoV-2-S (MVA-S) to test humoral immune response. Groups of BALB/c mice (n=7-12) were vaccinated twice with 10*7 PFU (low dose) or 10*8 PFU (high dose) MVA-S via the i.m route. Serum samples were collected at day 18 post 1st immunization and at day 14 post 2nd immunization and tested for S-antigen specific B cell response. Created with BioRender.com

Serum samples from immunized mice were tested for serum IgG antibodies by ELISA using full-length SARS-CoV-2 spike protein as the antigen. A single application led to seroconversion in 3/8 low dose vaccinated and 4/6 high dose vaccinated mice. A second immunization led to seroconversion in all vaccinated mice, showing mean titers of 1:900 (low dose) and 1:1,257 (high dose). No S-specific antibodies could be detected in mice vaccinated with saline (PBS) (**Figure 25a**).

In addition, the neutralizing capacity was further validated by using a virus neutralizing assay (VNT_{100}). Following a single application of MVA-S, no neutralizing activity could be found in low dose or high dose vaccinated mice with a VNT_{100} assay. A second immunization led to neutralizing activity in 79% of all sera from vaccinated mice (low dose and high dose) with average reciprocal VNT_{100} titers of 19.8 (low dose) and 105.8 (high dose). Mice vaccinated with saline (PBS) showed no detectible levels of neutralizing antibodies (**Figure 25b**).

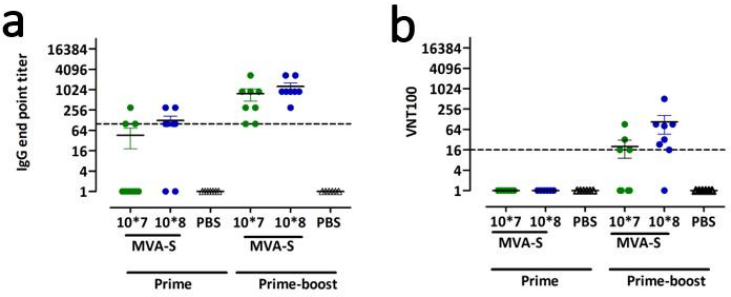

Figure 25: S-antigen specific humoral immune response induced upon vaccination with MVA-SARS-CoV-2-S (MVA-S). Groups of BALB/c mice (n= 7-12) were vaccinated twice with 10*7 PFU (low dose) or 10*8 (high dose) MVA-S over a 21-day interval using the i.m. route. Mice vaccinated with saline (PBS) were used as a control. Serum samples were collected at day 18 post 1st immunization and at day 14 post 2nd immunization and tested for (a) SARS-CoV-2-S specific IgG titers by ELISA and SARS-CoV-2 neutralizing antibodies by (b) virus neutralization (VNT_{100}). VNT_{100} assay was performed by Prof. Dr. Stephan Becker`s lab.

2.4. Protective capacity upon challenge infection

To determine the protective capacity of the MVA-SARS-CoV-2-S (MVA-S) vaccine, an adenoviral transduction-based model was used, as described before (SUN et al. 2020a; WONG et al. 2020). Immunized BALB/c mice (MVA-S or PBS as control) were intratracheally transduced with 5x10*8 PFU of an adenoviral vector two weeks after the second immunization. The adenoviral vector expresses the human ACE2 receptor and the reporter protein mCherry (ViraQuest Inc., North Liberty, IA, USA). Three days later, mice were challenged by infection with 1.5x10*4 $TCID_{50}$ SARS-CoV-2 (isolate BavPat1/2020 isolate, European Virus Archive Global # 026V-03883). Four days later, mice were euthanized and the viral load was measured in blood samples and lung tissue samples (**Figure 26**).

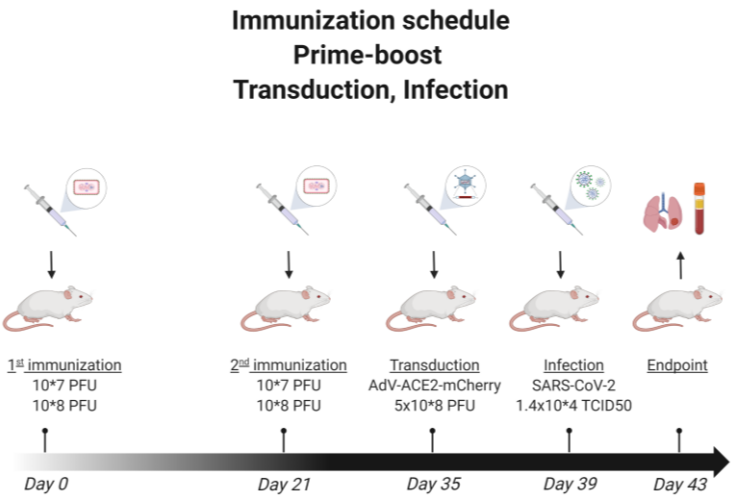

Figure 26: Vaccination schedule prime-boost, following transduction with AdV-ACE2-mCherry and challenge infection with SARS-CoV-2. BALB/c mice were vaccinated with MVA-SARS-CoV-2-S (10*7 or 10*8 PFU) over a 21-day interval. At day 35, mice were inoculated with 5x 10*8 PFU AdV-ACE2-mCherry. Three days later, mice were infected with 1.4x 10*4 $TCID_{50}$ SARS-CoV-2 using the intranasal route. At day 43, four days after the infection, mice were euthanized and serum samples and tissue samples were collected. Created with BioRender.com

The control group showed elevated amounts of viral RNA (>1000 SARS-CoV-2 genome equivalents/ng of total RNA), whereas the lung tissue samples of mice vaccinated with low or high dose MVA-SARS-CoV-2-S showed no detectible amount of viral RNA (<100 genome equivalents/ng of total RNA) (**Figure 27a**). To confirm adenoviral vector transduction took place, real-time RT-PCR analysis of co-expressed mCherry was performed, showing comparable levels of mCherry in all three groups (**Figure 27b**). Moreover, high levels of SARS-CoV-2 (>1000 $TCID_{50}$/ml) could be detected in lung tissue samples of the control group, whereas no replicative SARS-CoV-2 could be detected in mice vaccinated with low dose or high dose of MVA-SARS-CoV-2 (**Figure 27c**). Furthermore, using a VNT_{100} assay, neutralizing antibodies could be detected in the sera of the vaccinated groups (10/11) but not in the control group (0/4) (**Figure 27d**).

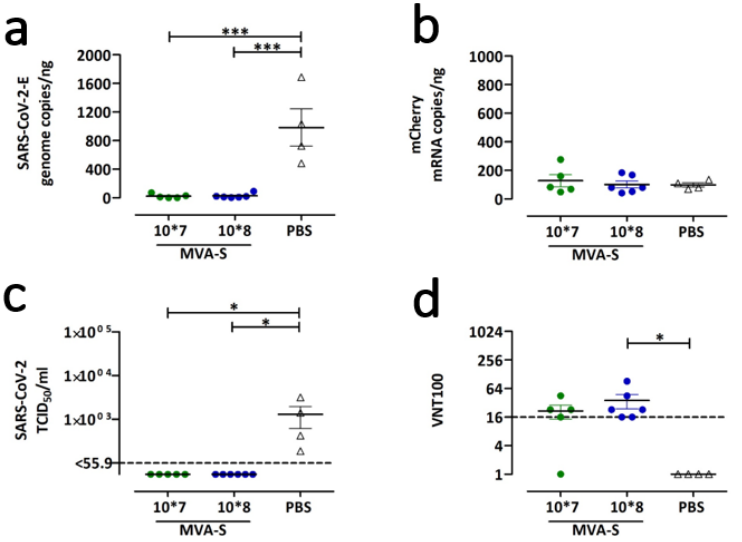

Figure 27: Protective capacity of MVA-SARS-CoV-2-S (MVA-S) immunization. Groups of BALB/c mice (n=4-6) were immunized twice with MVA-S (10*7 or 10*8 PFU) over a 21-day interval. Mice immunized with PBS served as a control. At day 43, mice were euthanized and lung tissue samples were tested for (a) viral load (genome copies/ng of total RNA), (b) the expression level of reporter gene mCherry (mRNA copies/ng of total RNA) and (c) the amount of replicative SARS-CoV-2 (TCID50/ml). Serum samples were analyzed for neutralizing antibodies (VNT100) (d). Statistical analysis was performed by one-way ANOVA and Tukey post-hoc test and the statistical significance of differences between vaccinated groups and control group is indicated as follows *, $p < 0.05$, ***, $p < 0.001$. Experiments were performed by Prof. Dr. Stephan Becker`s lab.

VII. DISCUSSION

Since COVID-19 became a global pandemic in 2020, tremendous efforts have been undertaken by researchers worldwide to develop suitable treatments and efficient vaccines against severe acute respiratory syndrome coronavirus 2 (SARS-CoV-2). Prophylactic immunization of people with high risk for infections, including healthcare personal, elderly or people with pre-existing illnesses, should be performed to combat the global spread of SARS-CoV-2. SARS-CoV-2 spike (S) protein has been chosen as an antigen for vaccine development by many researchers, as published data from other coronaviruses indicated potential cytotoxic T cell and B cell response, including neutralizing antibodies (BISHT et al. 2004; SONG et al. 2013; VEIT et al. 2018; YANG et al. 2004). With beginning of 2021, several spike protein-based vaccines are in preclinical or clinical trials. Two mRNA vaccines and one replication-deficient simian adenovirus expressing the full-length S protein are already licensed and used as a prevention of COVID-19 in Europe. However, little is known about long-living immunity and with the spread of new virus variants (ECDC 2020; WHO 2020), suitable and broad-reactive vaccines are urgently needed.

Modified Vaccinia virus Ankara (MVA), an attenuated vaccinia virus strain (VACV), lacking virulence factors and immune evasion proteins, is broadly used as a vector platform to develop vaccines against various viral and bacterial infections. In this study, a recombinant MVA expressing the full-length SARS-CoV-2 spike (S) protein was generated to investigate S-specific humoral and cell-mediated immune responses in BALB/c mice. Thereby, the activation of CD4+ and CD8+ T cells as well as circulating antibodies upon vaccination with two doses of recombinant MVA-SARS-CoV-2-S (MVA-S) was demonstrated. Protective capacity tested with an adenoviral transduction model revealed first promising data for protection from a SARS-CoV-2 infection. In addition, the compatibility with clinical use and a potential industrial large-scale production could be confirmed. Therefore, replication efficiency on DF-1 cells, an optimized cell line for manufacturing process, was confirmed. Moreover, stable expression of the full-length spike protein upon serial passages of MVA-SARS-CoV-2-S at

low MOI was demonstrated. Taken together, these data demonstrate that recombinant MVA-S might be a promising candidate vaccine against SARS-CoV-2.

Vaccine-induced immunity vs. viral infection

Vaccination remains the most efficient way to prevent infectious diseases, as seen by the remarkable success of vaccines against diphtheria, tetanus, polio and smallpox (PLOTKIN 2008). The global burden of infectious diseases could be reduced, and in the case of smallpox, completely eradicated by vaccination (BREMAN and ARITA 2011). However, vaccine development is still a challenging area of research since by now, no licensed vaccines are available for several life-threatening infectious pathogens such as HIV (JOHNSTON and FAUCI 2007; McMICHAEL et al. 2009) and *Plasmodium falciparum* (HILL 2006). The protective capacity of vaccines is based on the induction of immunological memory responses, which combat an infection or re-infection with a certain pathogen (SALLUSTO et al. 2010). The protective capacity of most of the licensed vaccines is related to a strong humoral immunity, determined by high levels of neutralizing antibodies on the mucosal surfaces or in serum of vaccinated individuals (PLOTKIN 2008). Strong humoral immunity is one strategy against viruses that infect via the mucosal route, including influenza virus and coronaviruses (BELSHE et al. 2000; PULENDRAN and AHMED 2011). Vaccine-induced antibodies are the first line of defense on the mucosal surface and in the blood, with the purpose to control specific pathogens before infecting cells and spreading of the virus (PLOTKIN 2008). Moreover, T cell response plays an important role in eradicating pathogens which are antigenically highly variable (PULENDRAN and AHMED 2011; SALLUSTO et al. 2010). Besides, CD4+ T cells support proliferation and expansion of B cells to control an ongoing infection (PLOTKIN 2008). The importance of cell-mediated and humoral immunity was e.g., demonstrated by a phase I clinical trial using a recombinant MVA candidate vaccine against MERS-CoV in 2018. Koch and colleagues immunized healthy individuals twice over a 28-day interval with recombinant MVA expressing MERS-CoV spike protein (MVA-MERS-S). Administration of the vaccine was performed with two different doses by using the i.m. route. All individuals immunized with the higher dose showed a

seroconversion after the booster immunization and more than 90% showed a specific T cell response (KOCH et al. 2020). These data are highly notable, as the new SARS-CoV-2 is closely related to MERS-CoV and the results of this study might help to better understand the immunological pathways of a SARS-CoV-2 infection.

It is known that a synergetic interaction between B cell and T cell responses is needed for protective capacity against poxviruses. In the course of the smallpox eradication program, individuals were tested for long-term humoral immunity upon vaccination. The amounts of circulating VACV-specific antibodies decreased within the first years, but remained stable for several decades (AMANNA et al. 2006; el-AD et al. 1990). Moreover, long-living cell-mediated immunity could be observed even decades after immunization with stable levels of VACV-specific CD4+ T cells and CD8+ T cells (AMARA et al. 2004; HAMMARLUND et al. 2003). These findings suggest that a successful vaccine should induce a balanced humoral and cell-mediated immunity to protect against infectious diseases.

MVA vector platform for construction of a candidate vaccine against SARS-CoV-2

Several new vaccine platforms, including (non)-replicating adenoviral vector vaccines or mRNA-based vaccines are currently being tested in preclinical and clinical trials against the new SARS-CoV-2. Strong cell-mediated and humoral immunity was induced in immunized individuals, but little is known about tolerability and long-term immunity of those vaccines (BADEN et al. 2020; CDC 2021a; CHUNG et al. 2020; LOCHT 2020).

In contrast, the MVA vector platform had been used for decades to develop vaccines against various bacterial and viral infections. The replication deficiency of MVA in mammalian cells, the capacity to insert long DNA sequences into the MVA genome, the gene expression at the cytosolic site and the stability of freeze-dried vaccines (GÓMEZ et al. 2011) are some of the great advantages of this vector platform. In comparison to MVA, replicative competent viruses can be related with severe side effects in elderly or

immunocompromised individuals, which raises concerns regarding the usage of those vector vaccine platforms. MVA has no survivability in infected host cells of mammalian origin, and therefore, a complete clearance of recombinant virus and the expressed target antigen can be assumed to occur within days after the vaccination (ALTENBURG et al. 2014). Evidence of strong induction of cell-mediated and humoral immunity had been shown *in vitro*, *in vivo* and in several clinical trials for MVA-based vaccines (COONEY et al. 1991; GU et al. 1995; KOCH et al. 2020; SONG et al. 2013). Humoral immunity is strongly induced by expressing the target antigen in its native form (VRIES and RIMMELZWAAN 2016).

The main advantage of MVA as a vector platform is the ability of living virus to infect mainly antigen-presenting cells, thus leading to intracellular expression of target antigens (DRAPER and HEENEY 2010). As a result, antigens are processed by the infected cells and presented on class I or class II MHC molecules, causing strong activation of the CD8+ and the CD4+ T cell responses (ALTENBURG et al. 2014; MURPHY et al. 2014). This immunogenic capacity of MVA is related to the fact that MVA, in contrast to wild type VACV, lacks several immunomodulatory proteins. Multiple intracellular host cell detection mechanisms are activated upon infection, resulting in the release of various interferons, chemokines and inflammatory cytokines (ALTENBURG et al. 2014; DELALOYE et al. 2009). MVA lacks IFN-α/β receptors, causing a type-I interferon response upon infection. Several *in vitro* studies with antigen presenting cells, such as dendritic cells, revealed high levels of TNF-α, IFN-β and IFN-α upon infection with MVA (BLANCHARD et al. 1998; DAI et al. 2014; WAIBLER et al. 2007). Besides, MVA lacks a functional receptor for IFN-γ, which represents an advantage for using MVA as a vaccine, since IFN-γ is a crucial factor for activating cytotoxic T cells (BLANCHARD et al. 1998). Moreover, cytotoxic T cells are not the only immune cells that a recruited to the infection site. Studies revealed the immigration of other immune cell subpopulations such as monocytes, CD4+ T cells and neutrophils (LEHMANN et al. 2009). All these findings confirm the favorable immunogenic properties of MVA, with the recruitment of a high number of various immune cells to the site of administration and the release of high amounts of proinflammatory cytokines

(BLANCHARD et al. 1998; WAIBLER et al. 2007).

Challenges for the development of a vaccine against SARS-CoV-2

Published data from vaccine candidates against SARS-CoV-1 and MERS-CoV accelerated the development of vaccines against SARS-CoV-2 (XU et al. 2019). Preclinical studies and animal models indicate the following: (i) the spike protein is most likely to induce neutralizing antibodies (COLEMAN et al. 2014), (ii) most antibodies are directed against the receptor-binding domain (RBD) (DU et al. 2013), (iii) induced neutralizing antibodies show protective capacity in various animal models (rabbits, non-human primates) (MUNSTER et al. 2017), (iv) clinical trials with three different vaccines against MERS, a DNA-based vaccine (YOON and KIM 2019), a replication-deficient chimpanzee adenovirus (JIA et al. 2019) and a MVA-based vaccine (KOCH et al. 2020; SONG et al. 2013), all expressing the S protein, induced robust humoral immunity, (v) many vaccine candidates induced cell-mediated immunity too, which plays a crucial role in viral clearance (ZHAO et al. 2014; ZHAO et al. 2009). Although, the available data about vaccine candidates against SARS and MERS show promising results, especially when using the spike protein as target antigen, there are several obstacles to circumvent.

One important issue to be discussed is the antibody-dependent enhancement (ADE) that had been verified for SARS and MERS during *in vitro* and *in vivo* studies. ADE increases the severity of several infections occurring when antibodies at sub-neutralizing levels bind to the viral antigen without inhibiting or clearing the infection (LEE et al. 2020). In terms of respiratory infections, ADE can lead to an enhanced respiratory infection (ERD). ERD includes antibody mediated mechanisms but also non-antibody-based mechanisms such as cytokine cascades or cell-mediated immunopathology (GRAHAM 2016; KIM et al. 1969; LEE et al. 2020). Antibodies directed against the spike protein have been found to mediate ADE in MERS and SARS infected individuals (WANG et al. 2014), causing viral infection of normally unaffected macrophages or B cells (YIP et al. 2014). Until now, the extent to which ADE might contribute to COVID-19 immunopathology is still unclear and further evaluations in terms of safety are needed when using spike protein-based vaccines (DANDEKAR and

PERLMAN 2005; POLAND et al. 2020). Besides, several animal studies of candidate vaccines against SARS-CoV-1 and MERS-CoV indicated lung pathology upon live virus challenge. Infiltration of eosinophils, elevated Th2 responses, and augmented infectivity was observed for whole-virus vaccines and S protein-based vaccines (BOLLES et al. 2011; DANDEKAR and PERLMAN 2005).

Moreover, a known obstacle and acute problem for several RNA viruses is their high genomic mutation rate. RNA viruses show a mutation rate of 10*-6 to 10*-4 substitutions per nucleotide site per cell infection. In contrast, DNA viruses show a lower mutation rate with 10*-8 to 10*-6 substitutions per nucleotide site per cell infection (PECK and LAURING 2018; VIGNUZZI and ANDINO 2012). One explanation for the higher mutation rate found in RNA viruses is the expression of their own replication machinery, including the RNA-dependent RNA polymerase (RdRp), whereas DNA viruses use the host cell polymerases (DUFFY 2018). The RdRp lacks a proofreading activity and thus, mistakes during replication are not corrected. Members of the *Nidovirales* family, including SARS-CoV-2, show fewer mutation rates, because of their RdRp-independent proofreading activity (GORBALENYA et al. 2006; PECK and LAURING 2018). The ability to quickly change the genome allows the virus to emerge into novel hosts and to escape vaccine-based immunity (VIGNUZZI et al. 2005), thus hampering the development of suitable candidate vaccines. As mentioned above, many neutralizing antibodies are directed against the RBD. Indeed, several mutations within the RBD have been observed for MERS-CoV (TAI et al. 2016; TANG et al. 2014), raising concerns about the mutation rate of SARS-CoV-2 and the efficacy of S protein-based vaccines. As expected, several mutants of SARS-CoV-2 have already been documented to globally accumulate in less than 12 months after the outbreak of the pandemic. Three of these new variants are notable, as they are associated with more severe outcome of COVID-19 and increased infectivity of SARS-CoV-2 (CDC 2021a; WHO 2020). The first variant, B.1.1.7, which was first detected in the United Stated of America and is predominantly prevalent in the United Kingdom, carries a large number of different mutations and recent studies indicate higher risk of death compared to other variants upon infection (PUBLIC HEALTH

ENGLAND 2021). The second variant, B.1.351, shares mutations with variant B.1.1.7 and is broadly distributed in South Africa (WHO 2020). The third variant, P1, was first described in Brazil (TOOVEY et al. 2021), and is characterized by 17 unique mutations. Three of these mutations are found within the RBD (K417T, E484K, N501Y) and non-peer reviewed publication preprints indicate that this variant decreases the ability of antibodies to recognize and neutralize SARS-CoV-2 (PUBLIC HEALTH ENGLAND 2021). Two specific mutations, N501Y and D614G (VOLZ et al. 2020), are shared by all three variants with the latter causing an increased infectivity of the virus (KORBER et al. 2020; YURKOVETSKIY et al. 2020). The prevalence of new variants raises the concern about the efficacy of SARS-CoV-2 vaccines currently being tested in preclinical and clinical trials. Hence, the vaccine targeting the full-length spike protein as used in the three licensed vaccines and our MVA-SARS-CoV-2-S vaccine, might be more effective than RBD-based vaccines.

Future prospective

New SARS-CoV-2 is still present and only a suitable vaccine will combat the global pandemic. With the prevalence of new and more infectious variants of the virus, mainly focusing on the S protein as target antigen used for vaccine development may need to be reconsidered. Nevertheless, several vaccine candidates based on different platforms are currently being tested in preclinical and clinical trials and show promising data for induction of cell-mediated and humoral immunity. The here descripted recombinant MVA expressing the full-length SARS-CoV-2 spike protein shows convincing data in terms of genetic stability, safety and tolerability upon vaccination and strong induction of CD8+ T cell responses as well as high antibody responses. Future work would include a more detailed analysis of the immunogenetic capacity of MVA-SARS-CoV-2-S in preclinical and clinical trials.

VIII. SUMMARY

The severe acute respiratory syndrome coronavirus 2 (SARS-CoV-2) is the causative agent of COVID-19 and led to a global pandemic in 2020. Globally, millions of people are infected with several thousands of individuals dying every day because of COVID-19. Up to now, no treatments are available and the most promising option to eradicate SARS-CoV-2 is a successful vaccine. Many researchers worldwide are working on different vaccines against SARS-CoV-2, with three different vaccines already licensed for immunization in Europe. Nevertheless, little is known about long-living immunity, tolerability or protective capacity of these new platform vaccines. This fact as well as the observed prevalence of new and more infectious virus variants strengthens the necessity of developing immunogenic and broad-reactive candidate vaccines of different origin.

In this work, the construction and preclinical characterization of recombinant MVA expressing the full-length SARS-CoV-2 spike protein is described. *In vitro* characterization including high genetic stability, replicative deficiency in mammalian cells, combined with a stable and robust expression of the spike antigen, revealed first promising data for further *in vivo* testing. BALB/c mice developed a robust S antigen specific CD8+ T cell response even after one immunization, that could be increased after a second immunization. Vaccinated mice using a prime-boost schedule over a 21-day interval showed elevated levels of serum antibodies against the spike protein. In addition, those serum antibodies can neutralize SARS-CoV-2 in the respective assay. Prime-boost vaccination with MVA-SARS-CoV-2-S could protect mice transduced with a human ACE2-expressing adenovirus from an infection with SARS-CoV-2.

IX. ZUSAMMENFASSUNG

Das *severe acute respiratory syndrome coronavirus 2* (SARS-CoV-2) führte im Jahr 2020 zur globalen Pandemie COVID-19. Weltweit infizierten sich bereits mehrere Millionen Menschen mit dem Virus und Tausende Infizierte sterben täglich mit oder an COVID-19. Da es bis jetzt keine wirksamen Behandlungsmöglichkeiten gibt, scheint eine Impfung die einzige Möglichkeit zu sein, die globale Pandemie einzudämmen. Unzählige Wissenschaftler arbeiten unter Hochdruck an der Entwicklung neuer Impfstoffe gegen das SARS-CoV-2 und mit Ende Februar 2021 gibt es in Europa bereits drei zugelassene Impfstoffe. Jedoch ist wenig bekannt über Langzeit-Immunogenität, Verträglichkeit oder Schutzwirkung dieser neuen Impfstoffe und das Auftreten neuer, noch infektiöserer Virus Varianten verdeutlichen die Notwendigkeit mehrerer wirksamer Impfstoffe.

In dieser Arbeit wurde die Konstruktion und präklinische Charakterisierung eines rekombinanten MVA, das das native SARS-CoV-2 Spike Protein exprimiert, beschrieben. Eine *in-vitro* Charakterisierung in Bezug auf genetische Stabilität, der Unfähigkeit von MVA sich auf Säugerzellen zu replizieren, sowie eine stabile Expression des Spike Proteins zeigten erste, vielversprechende Ergebnisse zur weiteren Testung *in vivo*. BALB/c Mäuse zeigten eine robuste S Antigen spezifische CD8+ T Zellantwort bereits nach einer Immunisierung, die nach einer zweiten Immunisierung erhöht werden konnte. BALB/c Mäuse, die in einem 21- Tage Intervall immunisiert wurden, wiesen erhöhte Serumantikörper gegen das Spike Protein auf und darüber hinaus konnte mit einem entsprechenden Assay eine neutralisierende Wirkung gegen das SARS-CoV-2 demonstriert werden. Immunisierte BALB/c Mäuse, die mit einem humanen ACE2-exprimierenden Adenovirus transduziert wurden, konnten vor einer Infektion mit SARS-CoV-2 geschützt werden.

X. REFERENCES

Abraham, Sushma; Kienzle, Thomas E.; Lapps, William; Brian, David A. (2004): Deduced sequence of the bovine coronavirus spike protein and identification of the internal proteolytic cleavage site. In *Virology* 176 (1), pp. 296–301. DOI: 10.1016/0042-6822(90)90257-R.

Altenburg, Arwen F.; Kreijtz, Joost H. C. M.; Vries, Rory D. de; Song, Fei; Fux, Robert; Rimmelzwaan, Guus F. et al. (2014): Modified Vaccinia Virus Ankara (MVA) as Production Platform for Vaccines against Influenza and Other Viral Respiratory Diseases. In *Viruses* 6 (7), pp. 2735–2761. DOI: 10.3390/v6072735.

Amanna, Ian J.; Slifka, Mark K.; Crotty, Shane (2006): Immunity and immunological memory following smallpox vaccination. In *Immunological reviews* 211, pp. 320–337. DOI: 10.1111/j.0105-2896.2006.00392.x.

Amara, Rama Rao; Nigam, Pragati; Sharma, Sunita; Liu, Jinyan; Bostik, Vanda (2004): Long-Lived Poxvirus Immunity, Robust CD4 Help, and Better Persistence of CD4 than CD8 T Cells. In *Journal of Virology* 78 (8), pp. 3811–3816. DOI: 10.1128/JVI.78.8.3811-3816.2004.

Anderson, Evan J.; Rouphael, Nadine G.; Widge, Alicia T.; Jackson, Lisa A.; Roberts, Paul C.; Makhene, Mamodikoe et al. (2020): Safety and Immunogenicity of SARS-CoV-2 mRNA-1273 Vaccine in Older Adults. In *The New England journal of medicine*. DOI: 10.1056/NEJMoa2028436.

Antinori, Spinello; Cossu, Maria Vittoria; Ridolfo, Anna Lisa; Rech, Roberto; Bonazzetti, Cecilia; Pagani, Gabriele et al. (2020): Compassionate remdesivir treatment of severe Covid-19 pneumonia in intensive care unit (ICU) and Non-ICU patients: Clinical outcome and differences in post-treatment hospitalisation status. In *Pharmacological Research* 158, p. 104899. DOI: 10.1016/j.phrs.2020.104899.

Antoine, G.; Scheiflinger, F.; Dorner, F.; Falkner, F. G. (1998): The complete genomic sequence of the modified vaccinia Ankara strain: comparison with other orthopoxviruses. In *Virology* 244 (2), pp. 365–396. DOI: 10.1006/viro.1998.9123.

Anywaine, Zacchaeus; Whitworth, Hilary; Kaleebu, Pontiano; Praygod, George; Shukarev, Georgi; Manno, Daniela et al. (2019): Safety and Immunogenicity of a 2-Dose Heterologous Vaccination Regimen With Ad26.ZEBOV and MVA-BN-Filo Ebola Vaccines: 12-Month Data From a Phase 1 Randomized Clinical Trial in Uganda and Tanzania. In *The Journal of Infectious Diseases* 220 (1), pp. 46–56. DOI: 10.1093/infdis/jiz070.

Appenzeller-Herzog, Christian; Hauri, Hans-Peter (2006): The ER-Golgi intermediate compartment (ERGIC): in search of its identity and function. In *Journal of cell science* 119 (Pt 11), pp. 2173–2183. DOI: 10.1242/jcs.03019.

Armstrong, John; Niemann, Heiner; Smeekens, Sjef; Rottier, Peter; Warren, Graham (1984): Sequence and topology of a model intracellular membrane protein, E1 glycoprotein, from a coronavirus. In *Nature* 308 (5961), pp. 751–752. DOI: 10.1038/308751a0.

Backes, Simone; Sperling, Karin M.; Zwilling, Joachim; Gasteiger, Georg; Ludwig, Holger; Kremmer, Elisabeth et al. (2010): Viral host-range factor C7 or K1 is essential for modified vaccinia virus Ankara late gene expression in human and murine cells, irrespective of their capacity to inhibit protein kinase R-

mediated phosphorylation of eukaryotic translation initiation factor 2alpha. In *The Journal of general virology* 91 (Pt 2), pp. 470–482. DOI: 10.1099/vir.0.015347-0.

Baden, Lindsey R.; El Sahly, Hana M.; Essink, Brandon; Kotloff, Karen; Frey, Sharon; Novak, Rick et al. (2020): Efficacy and Safety of the mRNA-1273 SARS-CoV-2 Vaccine. In *The New England journal of medicine*. DOI: 10.1056/NEJMoa2035389.

Baldick, C. J.; Keck, J. G.; Moss, B. (1992): Mutational analysis of the core, spacer, and initiator regions of vaccinia virus intermediate-class promoters. In *Journal of Virology* 66 (8), pp. 4710–4719.

Beigel, John H.; Tomashek, Kay M.; Dodd, Lori E.; Mehta, Aneesh K.; Zingman, Barry S.; Kalil, Andre C. et al. (2020): Remdesivir for the Treatment of Covid-19 — Final Report. In *The New England journal of medicine*. DOI: 10.1056/NEJMoa2007764.

Belouzard, Sandrine; Millet, Jean K.; Licitra, Beth N.; Whittaker, Gary R. (2012): Mechanisms of Coronavirus Cell Entry Mediated by the Viral Spike Protein. In *Viruses* 4 (6), pp. 1011–1033. DOI: 10.3390/v4061011.

Belshe, R. B.; Gruber, W. C.; Mendelman, P. M.; Mehta, H. B.; Mahmood, K.; Reisinger, K. et al. (2000): Correlates of immune protection induced by live, attenuated, cold-adapted, trivalent, intranasal influenza virus vaccine. In *The Journal of Infectious Diseases* 181 (3), pp. 1133–1137. DOI: 10.1086/315323.

Bidgood, Susanna R. (2019): Continued poxvirus research: From foe to friend. In *PLoS Biology* 17 (1). DOI: 10.1371/journal.pbio.3000124.

Bisht, Himani; Roberts, Anjeanette; Vogel, Leatrice; Bukreyev, Alexander; Collins, Peter L.; Murphy, Brian R. et al. (2004): Severe acute respiratory syndrome coronavirus spike protein expressed by attenuated vaccinia virus protectively immunizes mice. In *Proceedings of the National Academy of Sciences of the United States of America* 101 (17), pp. 6641–6646. DOI: 10.1073/pnas.0401939101.

Blanchard, T. J.; Alcami, A.; Andrea, P.; Smith, G. L. (1998): Modified vaccinia virus Ankara undergoes limited replication in human cells and lacks several immunomodulatory proteins: implications for use as a human vaccine. In *The Journal of general virology* 79 (Pt 5), pp. 1159–1167. DOI: 10.1099/0022-1317-79-5-1159.

Bolles, Meagan; Deming, Damon; Long, Kristin; Agnihothram, Sudhakar; Whitmore, Alan; Ferris, Martin et al. (2011): A Double-Inactivated Severe Acute Respiratory Syndrome Coronavirus Vaccine Provides Incomplete Protection in Mice and Induces Increased Eosinophilic Proinflammatory Pulmonary Response upon Challenge ▿ . In *Journal of Virology* 85 (23), pp. 12201–12215. DOI: 10.1128/JVI.06048-11.

Bonilla, Francisco A.; Oettgen, Hans C. (2010): Adaptive immunity. In *The Journal of allergy and clinical immunology* 125 (2 Suppl 2), S33-40. DOI: 10.1016/j.jaci.2009.09.017.

Bosch, Berend Jan; van der Zee, Ruurd; Haan, Cornelis A. M. de; Rottier, Peter J. M. (2003): The Coronavirus Spike Protein Is a Class I Virus Fusion Protein: Structural and Functional Characterization of the Fusion Core Complex. In *Journal of Virology* 77 (16), pp. 8801–8811. DOI: 10.1128/JVI.77.16.8801-8811.2003.

Bourgonje, Arno R.; Abdulle, Amaal Eman; Timens, Wim; Hillebrands, Jan-Luuk; Navis, Gerjan J.; Gordijn, Sanne J. et al. (2020): Angiotensin-converting enzyme-2 (ACE2), SARS-CoV-2 and

pathophysiology of coronavirus disease 2019 (COVID-19). In *The Journal of Pathology*. DOI: 10.1002/path.5471.

Breman, Joel G.; Arita, Isao (2011): The certification of smallpox eradication and implications for guinea worm, poliomyelitis, and other diseases: confirming and maintaining a negative. In *Vaccine* 29 Suppl 4, D41-8. DOI: 10.1016/j.vaccine.2011.06.018.

Büttner, M.; Czerny, C. P.; Lehner, K. H.; Wertz, K. (1995): Interferon induction in peripheral blood mononuclear leukocytes of man and farm animals by poxvirus vector candidates and some poxvirus constructs. In *Veterinary immunology and immunopathology* 46 (3-4), pp. 237–250. DOI: 10.1016/0165-2427(94)05357-x.

Calabrese, Fiorella; Pezzuto, Federica; Fortarezza, Francesco; Hofman, Paul; Kern, Izidor; Panizo, Angel et al. (2020): Pulmonary pathology and COVID-19: lessons from autopsy. The experience of European Pulmonary Pathologists. In *Virchows Archiv*, pp. 1–14. DOI: 10.1007/s00428-020-02886-6.

Cao, Bin; Wang, Yeming; Wen, Danning; Liu, Wen; Wang, Jingli; Fan, Guohui et al. (2020): A Trial of Lopinavir–Ritonavir in Adults Hospitalized with Severe Covid-19. In *The New England journal of medicine*. DOI: 10.1056/NEJMoa2001282.

Carroll, M. W.; Moss, B. (1997): Poxviruses as expression vectors. In *Current opinion in biotechnology* 8 (5), pp. 573–577. DOI: 10.1016/s0958-1669(97)80031-6.

CDC (2021a): Different COVID-19 Vaccines. Available online at https://www.cdc.gov/coronavirus/2019-ncov/vaccines/different-vaccines.html, checked on 1/30/2021.

CDC (2021b): Information about the Moderna COVID-19 Vaccine. Available online at https://www.cdc.gov/coronavirus/2019-ncov/vaccines/different-vaccines/Moderna.html, updated on 1/25/2021, checked on 1/30/2021.

CDC (2021c): Information about the Pfizer-BioNTech COVID-19 Vaccine. Available online at https://www.cdc.gov/coronavirus/2019-ncov/vaccines/different-vaccines/Pfizer-BioNTech.html, updated on 1/25/2021, checked on 1/30/2021.

Chang, H. W.; Watson, J. C.; Jacobs, B. L. (1992): The E3L gene of vaccinia virus encodes an inhibitor of the interferon-induced, double-stranded RNA-dependent protein kinase. In *Proceedings of the National Academy of Sciences of the United States of America* 89 (11), pp. 4825–4829.

Chen, Nanshan; Zhou, Min; Dong, Xuan; Qu, Jieming; Gong, Fengyun; Han, Yang et al. (2020a): Epidemiological and clinical characteristics of 99 cases of 2019 novel coronavirus pneumonia in Wuhan, China: a descriptive study. In *Lancet (London, England)* 395 (10223), pp. 507–513. DOI: 10.1016/S0140-6736(20)30211-7.

Chen, Tao; Di Wu; Chen, Huilong; Yan, Weiming; Yang, Danlei; Chen, Guang et al. (2020b): Clinical characteristics of 113 deceased patients with coronavirus disease 2019: retrospective study. In *The BMJ* 368. DOI: 10.1136/bmj.m1091.

Chen, Zhi-Min; Fu, Jun-Fen; Shu, Qiang; Chen, Ying-Hu; Hua, Chun-Zhen; Li, Fu-Bang et al. (2020c): Diagnosis and treatment recommendations for pediatric respiratory infection caused by the 2019 novel coronavirus. In *World Journal of Pediatrics*, pp. 1–7. DOI: 10.1007/s12519-020-00345-5.

Chipuk, Jerry E.; Moldoveanu, Tudor; Llambi, Fabien; Parsons, Melissa J.; Green, Douglas R. (2010): The BCL-2 Family Reunion. In *Molecular cell* 37 (3), pp. 299–310. DOI: 10.1016/j.molcel.2010.01.025.

Chung, Jee Young; Thone, Melissa N.; Kwon, Young Jik (2020): COVID-19 vaccines: The status and perspectives in delivery points of view. In *Advanced Drug Delivery Reviews* 170, pp. 1–25. DOI: 10.1016/j.addr.2020.12.011.

Coleman, Christopher M.; Liu, Ye V.; Mu, Haiyan; Taylor, Justin K.; Massare, Michael; Flyer, David C. et al. (2014): Purified coronavirus spike protein nanoparticles induce coronavirus neutralizing antibodies in mice. In *Vaccine* 32 (26), pp. 3169–3174. DOI: 10.1016/j.vaccine.2014.04.016.

Cooney, E. L.; Collier, A. C.; Greenberg, P. D.; Coombs, R. W.; Zarling, J.; Arditti, D. E. et al. (1991): Safety of and immunological response to a recombinant vaccinia virus vaccine expressing HIV envelope glycoprotein. In *Lancet (London, England)* 337 (8741), pp. 567–572. DOI: 10.1016/0140-6736(91)91636-9.

Corman, Victor M.; Drosten, Christian (2020): Authors' response: SARS-CoV-2 detection by real-time RT-PCR. In *Eurosurveillance* 25 (21). DOI: 10.2807/1560-7917.ES.2020.25.21.2001035.

Coronaviridae Study Group of the International Committee on Taxonomy of Viruses. (2020): The species Severe acute respiratory syndrome-related coronavirus: classifying 2019-nCoV and naming it SARS-CoV-2. In *Nature Microbiology*, pp. 1–9. DOI: 10.1038/s41564-020-0695-z.

Corse, Emily; Machamer, Carolyn E. (2000): Infectious Bronchitis Virus E Protein Is Targeted to the Golgi Complex and Directs Release of Virus-Like Particles. In *Journal of Virology* 74 (9), pp. 4319–4326.

Cudmore, S.; Cossart, P.; Griffiths, G.; Way, M. (1995): Actin-based motility of vaccinia virus. In *Nature* 378 (6557), pp. 636–638. DOI: 10.1038/378636a0.

Cui, Jie; Li, Fang; Shi, Zheng-Li (2018): Origin and evolution of pathogenic coronaviruses. In *Nature Reviews. Microbiology* 17 (3), pp. 181–192. DOI: 10.1038/s41579-018-0118-9.

Dai, Peihong; Wang, Weiyi; Cao, Hua; Avogadri, Francesca; Dai, Lianpan; Drexler, Ingo et al. (2014): Modified Vaccinia Virus Ankara Triggers Type I IFN Production in Murine Conventional Dendritic Cells via a cGAS/STING-Mediated Cytosolic DNA-Sensing Pathway. In *PLoS Pathogens* 10 (4). DOI: 10.1371/journal.ppat.1003989.

Dandekar, Ajai A.; Perlman, Stanley (2005): Immunopathogenesis of coronavirus infections: implications for SARS. In *Nature Reviews. Immunology* 5 (12), pp. 917–927. DOI: 10.1038/nri1732.

Danial, Nika N.; Korsmeyer, Stanley J. (2004): Cell death: critical control points. In *Cell* 116 (2), pp. 205–219. DOI: 10.1016/s0092-8674(04)00046-7.

Davies, M. V.; Elroy-Stein, O.; Jagus, R.; Moss, B.; Kaufman, R. J. (1992): The vaccinia virus K3L gene product potentiates translation by inhibiting double-stranded-RNA-activated protein kinase and phosphorylation of the alpha subunit of eukaryotic initiation factor 2. In *Journal of Virology* 66 (4), pp. 1943–1950.

Delaloye, Julie; Roger, Thierry; Steiner-Tardivel, Quynh-Giao; Le Roy, Didier; Knaup Reymond, Marlies; Akira, Shizuo et al. (2009): Innate Immune Sensing of Modified Vaccinia Virus Ankara (MVA) Is Mediated by TLR2-TLR6, MDA-5 and the NALP3 Inflammasome. In *PLoS Pathogens* 5 (6). DOI:

10.1371/journal.ppat.1000480.

Deng, Sheng-Qun; Peng, Hong-Juan (2020): Characteristics of and Public Health Responses to the Coronavirus Disease 2019 Outbreak in China. In *Journal of Clinical Medicine* 9 (2). DOI: 10.3390/jcm9020575.

Dhanda, Sandeep Kumar; Mahajan, Swapnil; Paul, Sinu; Yan, Zhen; Kim, Haeuk; Jespersen, Martin Closter et al. (2019): IEDB-AR: immune epitope database—analysis resource in 2019. In *Nucleic Acids Research* 47 (W1), W502-6. DOI: 10.1093/nar/gkz452.

Ding, Yanqing; He, Li; Zhang, Qingling; Huang, Zhongxi; Che, Xiaoyan; Hou, Jinlin et al. (2004): Organ distribution of severe acute respiratory syndrome (SARS) associated coronavirus (SARS-CoV) in SARS patients: implications for pathogenesis and virus transmission pathways. In *The Journal of Pathology* 203 (2), pp. 622–630. DOI: 10.1002/path.1560.

Draper, Simon J.; Heeney, Jonathan L. (2010): Viruses as vaccine vectors for infectious diseases and cancer. In *Nature Reviews. Microbiology* 8 (1), pp. 62–73. DOI: 10.1038/nrmicro2240.

Drillien, Robert; Spehner, Danièle; Hanau, Daniel (2004): Modified vaccinia virus Ankara induces moderate activation of human dendritic cells. In *The Journal of general virology* 85 (Pt 8), pp. 2167–2175. DOI: 10.1099/vir.0.79998-0.

Drosten, Christian; Günther, Stephan; Preiser, Wolfgang; van der Werf, Sylvie; Brodt, Hans-Reinhard; Becker, Stephan et al. (2003): Identification of a novel coronavirus in patients with severe acute respiratory syndrome. In *The New England journal of medicine* 348 (20), pp. 1967–1976. DOI: 10.1056/NEJMoa030747.

Du, Lanying; Kou, Zhihua; Ma, Cuiqing; Tao, Xinrong; Wang, Lili; Zhao, Guangyu et al. (2013): A Truncated Receptor-Binding Domain of MERS-CoV Spike Protein Potently Inhibits MERS-CoV Infection and Induces Strong Neutralizing Antibody Responses: Implication for Developing Therapeutics and Vaccines. In *PLoS ONE* 8 (12). DOI: 10.1371/journal.pone.0081587.

Du, Rong-Hui; Liang, Li-Rong; Yang, Cheng-Qing; Wang, Wen; Cao, Tan-Ze; Li, Ming et al. (2020): Predictors of mortality for patients with COVID-19 pneumonia caused by SARS-CoV-2: a prospective cohort study. In *The European Respiratory Journal* 55 (5). DOI: 10.1183/13993003.00524-2020.

Duffy, Siobain (2018): Why are RNA virus mutation rates so damn high? In *PLoS Biology* 16 (8). DOI: 10.1371/journal.pbio.3000003.

Earl, P. L.; Hügin, A. W.; Moss, B. (1990): Removal of cryptic poxvirus transcription termination signals from the human immunodeficiency virus type 1 envelope gene enhances expression and immunogenicity of a recombinant vaccinia virus. In *Journal of Virology* 64 (5), pp. 2448–2451.

ECDC (2020): Rapid increase of a SARS-CoV-2 variant with multiple spike protein mutations observed in the United Kingdom. Available online at https://www.ecdc.europa.eu/sites/default/files/documents/SARS-CoV-2-variant-multiple-spike-protein-mutations-United-Kingdom.pdf, updated on December 2020, checked on 2/13/2021.

el-Ad, B.; Roth, Y.; Winder, A.; Tochner, Z.; Lublin-Tennenbaum, T.; Katz, E.; Schwartz, T. (1990): The persistence of neutralizing antibodies after revaccination against smallpox. In *The Journal of Infectious Diseases* 161 (3), pp. 446–448. DOI: 10.1093/infdis/161.3.446.

EMA (2021): COVID-19 Vaccine AstraZeneca. 2021. Available online at https://www.ema.europa.eu/en/documents/product-information/covid-19-vaccine-astrazeneca-product-information-approved-chmp-29-january-2021-pending-endorsement_en.pdf, updated on 2021, checked on 2/13/2021.

Esposito, J. J.; Knight, J. C.; Shaddock, J. H.; Novembre, F. J.; Baer, G. M. (1988): Successful oral rabies vaccination of raccoons with raccoon poxvirus recombinants expressing rabies virus glycoprotein. In *Virology* 165 (1), pp. 313–316. DOI: 10.1016/0042-6822(88)90692-7.

Fleri, Ward; Paul, Sinu; Dhanda, Sandeep Kumar; Mahajan, Swapnil; Xu, Xiaojun; Peters, Bjoern; Sette, Alessandro (2017): The Immune Epitope Database and Analysis Resource in Epitope Discovery and Synthetic Vaccine Design. In *Frontiers in Immunology* 8. DOI: 10.3389/fimmu.2017.00278.

Folegatti, Pedro M.; Ewer, Katie J.; Aley, Parvinder K.; Angus, Brian; Becker, Stephan; Belij-Rammerstorfer, Sandra et al. (2020): Safety and immunogenicity of the ChAdOx1 nCoV-19 vaccine against SARS-CoV-2: a preliminary report of a phase ½, single-blind, randomised controlled trial. In *Lancet (London, England)* 396 (10249), pp. 467–478. DOI: 10.1016/S0140-6736(20)31604-4.

Franke, C. A.; Rice, C. M.; Strauss, J. H.; Hruby, D. E. (1985): Neomycin resistance as a dominant selectable marker for selection and isolation of vaccinia virus recombinants. In *Molecular and Cellular Biology* 5 (8), pp. 1918–1924.

Gao, Yong; Li, Tuantuan; Han, Mingfeng; Li, Xiuyong; Wu, Dong; Xu, Yuanhong et al. (2020): Diagnostic utility of clinical laboratory data determinations for patients with the severe COVID-19. In *Journal of Medical Virology*. DOI: 10.1002/jmv.25770.

Gilbert, Sarah C.; Warimwe, George M. (2017): Rapid development of vaccines against emerging pathogens: The replication-deficient simian adenovirus platform technology. In *Vaccine* 35 (35), pp. 4461–4464. DOI: 10.1016/j.vaccine.2017.04.085.

Gómez, Carmen E.; Nájera, José L.; Krupa, Magdalena; Perdiguero, Beatriz; Esteban, Mariano (2011): MVA and NYVAC as vaccines against emergent infectious diseases and cancer. In *Current gene therapy* 11 (3), pp. 189–217. DOI: 10.2174/156652311795684731.

Gorbalenya, Alexander E.; Enjuanes, Luis; Ziebuhr, John; Snijder, Eric J. (2006): Nidovirales: Evolving the largest RNA virus genome. In *Virus Research* 117 (1), pp. 17–37. DOI: 10.1016/j.virusres.2006.01.017.

Graham, B. S.; Belshe, R. B.; Clements, M. L.; Dolin, R.; Corey, L.; Wright, P. F. et al. (1992): Vaccination of vaccinia-naive adults with human immunodeficiency virus type 1 gp160 recombinant vaccinia virus in a blinded, controlled, randomized clinical trial. The AIDS Vaccine Clinical Trials Network. In *The Journal of Infectious Diseases* 166 (2), pp. 244–252. DOI: 10.1093/infdis/166.2.244.

Graham, Barney S. (2016): Vaccines Against Respiratory Syncytial Virus: The Time Has Finally Come. In *Vaccine* 34 (30), pp. 3535–3541. DOI: 10.1016/j.vaccine.2016.04.083.

Graham, Simon P.; McLean, Rebecca K.; Spencer, Alexandra J.; Belij-Rammerstorfer, Sandra; Wright, Daniel; Ulaszewska, Marta et al. (2020): Evaluation of the immunogenicity of prime-boost vaccination with the replication-deficient viral vectored COVID-19 vaccine candidate ChAdOx1 nCoV-19. In *NPJ Vaccines* 5. DOI: 10.1038/s41541-020-00221-3.

Greenberg, Stephen B. (2016): Update on Human Rhinovirus and Coronavirus Infections. In *Seminars in Respiratory and Critical Care Medicine* 37 (4), pp. 555–571. DOI: 10.1055/s-0036-1584797.

Groot, R. J. de; Luytjes, W.; Horzinek, M. C.; van der Zeijst, B.A.M.; Spaan, W.J.M.; Lenstra, J. A. (2005): Evidence for a coiled-coil structure in the spike proteins of coronaviruses☆. In *Journal of Molecular Biology* 196 (4), pp. 963–966. DOI: 10.1016/0022-2836(87)90422-0.

Gu, S. Y.; Huang, T. M.; Ruan, L.; Miao, Y. H.; Lu, H.; Chu, C. M. et al. (1995): First EBV vaccine trial in humans using recombinant vaccinia virus expressing the major membrane antigen. In *Developments in biological standardization* 84, pp. 171–177.

Gubser, Caroline; Hué, Stéphane; Kellam, Paul; Smith, Geoffrey L. (2004): Poxvirus genomes: a phylogenetic analysis. In *The Journal of general virology* 85 (Pt 1), pp. 105–117. DOI: 10.1099/vir.0.19565-0.

Guerra, Susana; Nájera, José Luis; González, José Manuel; López-Fernández, Luis A.; Climent, Nuria; Gatell, José M. et al. (2007): Distinct Gene Expression Profiling after Infection of Immature Human Monocyte-Derived Dendritic Cells by the Attenuated Poxvirus Vectors MVA and NYVAC ▿ †. In *Journal of Virology* 81 (16), pp. 8707–8721. DOI: 10.1128/JVI.00444-07.

Gul, Muhammad Hamdan; Htun, Zin Mar; Shaukat, Nauman; Imran, Muhammad; Khan, Ahmad (2020): Potential specific therapies in COVID-19. In *Therapeutic Advances in Respiratory Disease* 14. DOI: 10.1177/1753466620926853.

Guy, James S.; Breslin, Jamie J.; Breuhaus, Babetta; Vivrette, Sally; Smith, Lynda G. (2000): Characterization of a Coronavirus Isolated from a Diarrheic Foal. In *Journal of Clinical Microbiology* 38 (12), pp. 4523–4526.

Hammarlund, Erika; Lewis, Matthew W.; Hansen, Scott G.; Strelow, Lisa I.; Nelson, Jay A.; Sexton, Gary J. et al. (2003): Duration of antiviral immunity after smallpox vaccination. In *Nature medicine* 9 (9), pp. 1131–1137. DOI: 10.1038/nm917.

Hartenian, Ella; Nandakumar, Divya; Lari, Azra; Ly, Michael; Tucker, Jessica M.; Glaunsinger, Britt A. (2021): The molecular virology of coronaviruses. In *The Journal of Biological Chemistry* 295 (37), pp. 12910–12934. DOI: 10.1074/jbc.REV120.013930.

HERRLICH, A.; MAYR, A. (1954): Vergleichende experimentelle Arbeiten über die Vaccine-Kuhpocken-Viren. In *Archiv fur Hygiene und Bakteriologie* 138 (7), pp. 479–504.

Hessel, Annett; Savidis-Dacho, Helga; Coulibaly, Sogue; Portsmouth, Daniel; Kreil, Thomas R.; Crowe, Brian A. et al. (2014): MVA Vectors Expressing Conserved Influenza Proteins Protect Mice against Lethal Challenge with H5N1, H9N2 and H7N1 Viruses. In *PLoS ONE* 9 (2). DOI: 10.1371/journal.pone.0088340.

Hill, Adrian V. S. (2006): Pre-erythrocytic malaria vaccines: towards greater efficacy. In *Nature Reviews. Immunology* 6 (1), pp. 21–32. DOI: 10.1038/nri1746.

Hu, Ben; Guo, Hua; Zhou, Peng; Shi, Zheng-Li (2020): Characteristics of SARS-CoV-2 and COVID-19. In *Nature Reviews. Microbiology*, pp. 1–14. DOI: 10.1038/s41579-020-00459-7.

Hu, F. Q.; Smith, C. A.; Pickup, D. J. (1994): Cowpox virus contains two copies of an early gene

encoding a soluble secreted form of the type II TNF receptor. In *Virology* 204 (1), pp. 343–356. DOI: 10.1006/viro.1994.1539.

Huang, Chaolin; Wang, Yeming; Li, Xingwang; Ren, Lili; Zhao, Jianping; Hu, Yi et al. (2020): Clinical features of patients infected with 2019 novel coronavirus in Wuhan, China. In *Lancet (London, England)* 395 (10223), pp. 497–506. DOI: 10.1016/S0140-6736(20)30183-5.

Huang, Qiulong; Yu, Liping; Petros, Andrew M.; Gunasekera, Angelo; Liu, Zhihong; Xu, Nan et al. (2004): Structure of the N-terminal RNA-binding domain of the SARS CoV nucleocapsid protein. In *Biochemistry* 43 (20), pp. 6059–6063. DOI: 10.1021/bi036155b.

Hurst, Kelley R.; Koetzner, Cheri A.; Masters, Paul S. (2009): Identification of In Vivo-Interacting Domains of the Murine Coronavirus Nucleocapsid Protein ▿. In *Journal of Virology* 83 (14), pp. 7221–7234. DOI: 10.1128/JVI.00440-09.

Ibáñez, Sebastián; Martínez, Oriela; Valenzuela, Francisca; Silva, Francisco; Valenzuela, Omar (2020): Hydroxychloroquine and chloroquine in COVID-19: should they be used as standard therapy? In *Clinical Rheumatology*, pp. 1–5. DOI: 10.1007/s10067-020-05202-4.

JHU (2021): COVID-19 Dashboard by the Center for Systems Science and Engineering (CSSE) at Johns Hopkins University. Available online at https://coronavirus.jhu.edu/map.html, updated on February 2021.

Jia, Wenxu; Channappanavar, Rudragouda; Zhang, Chao; Li, Mingxi; Zhou, Haixia; Zhang, Shuyuan et al. (2019): Single intranasal immunization with chimpanzee adenovirus-based vaccine induces sustained and protective immunity against MERS-CoV infection. In *Emerging Microbes & Infections* 8 (1), pp. 760–772. DOI: 10.1080/22221751.2019.1620083.

Johnston, Margaret I.; Fauci, Anthony S. (2007): An HIV vaccine—evolving concepts. In *The New England journal of medicine* 356 (20), pp. 2073–2081. DOI: 10.1056/NEJMra066267.

Kalodimou, Georgia; Veit, Svenja; Jany, Sylvia; Kalinke, Ulrich; Broder, Christopher C.; Sutter, Gerd; Volz, Asisa (2019): A Soluble Version of Nipah Virus Glycoprotein G Delivered by Vaccinia Virus MVA Activates Specific CD8 and CD4 T Cells in Mice. In *Viruses* 12 (1). DOI: 10.3390/v12010026.

Karikó, Katalin; Muramatsu, Hiromi; Welsh, Frank A.; Ludwig, János; Kato, Hiroki; Akira, Shizuo; Weissman, Drew (2008): Incorporation of Pseudouridine Into mRNA Yields Superior Nonimmunogenic Vector With Increased Translational Capacity and Biological Stability. In *Molecular therapy : the journal of the American Society of Gene Therapy* 16 (11), pp. 1833–1840. DOI: 10.1038/mt.2008.200.

Kauffman, Kevin J.; Webber, Matthew J.; Anderson, Daniel G. (2016): Materials for non-viral intracellular delivery of messenger RNA therapeutics. In *Journal of controlled release : official journal of the Controlled Release Society* 240, pp. 227–234. DOI: 10.1016/j.jconrel.2015.12.032.

Khailany, Rozhgar A.; Safdar, Muhamad; Ozaslan, Mehmet (2020): Genomic characterization of a novel SARS-CoV-2. In *Gene Reports* 19, p. 100682. DOI: 10.1016/j.genrep.2020.100682.

Kim, H. W.; Canchola, J. G.; Brandt, C. D.; Pyles, G.; Chanock, R. M.; Jensen, K.; Parrott, R. H. (1969): Respiratory syncytial virus disease in infants despite prior administration of antigenic inactivated vaccine. In *American journal of epidemiology* 89 (4), pp. 422–434. DOI: 10.1093/oxfordjournals.aje.a120955.

Kluge, S.; Janssens, U.; Welte, T.; Weber-Carstens, S.; Schälte, G.; Spinner, C. D. et al. (2021): S2k-Leitlinie – Empfehlungen zur stationären Therapie von Patienten mit COVID-19. In *Pneumologie (Stuttgart, Germany)* 75 (2), pp. 88–112. DOI: 10.1055/a-1334-1925.

Koch, Till; Dahlke, Christine; Fathi, Anahita; Kupke, Alexandra; Krähling, Verena; Okba, Nisreen M. A. et al. (2020): Safety and immunogenicity of a modified vaccinia virus Ankara vector vaccine candidate for Middle East respiratory syndrome: an open-label, phase 1 trial. In *The Lancet. Infectious diseases* 20 (7), pp. 827–838. DOI: 10.1016/S1473-3099(20)30248-6.

Korber, Bette; Fischer, Will M.; Gnanakaran, Sandrasegaram; Yoon, Hyejin; Theiler, James; Abfalterer, Werner et al. (2020): Tracking Changes in SARS-CoV-2 Spike: Evidence that D614G Increases Infectivity of the COVID-19 Virus. In *Cell* 182 (4), 812-827.e19. DOI: 10.1016/j.cell.2020.06.043.

Krafts, Kristine; Hempelmann, Ernst; Skórska-Stania, Agnieszka (2012): From methylene blue to chloroquine: a brief review of the development of an antimalarial therapy. In *Parasitology research* 111 (1), pp. 1–6. DOI: 10.1007/s00436-012-2886-x.

Kreer, Christoph; Zehner, Matthias; Weber, Timm; Ercanoglu, Meryem S.; Gieselmann, Lutz; Rohde, Cornelius et al. (2020): Longitudinal Isolation of Potent Near-Germline SARS-CoV-2-Neutralizing Antibodies from COVID-19 Patients. In *Cell* 182 (4), 843-854.e12. DOI: 10.1016/j.cell.2020.06.044.

Ksiazek, Thomas G.; Erdman, Dean; Goldsmith, Cynthia S.; Zaki, Sherif R.; Peret, Teresa; Emery, Shannon et al. (2003): A novel coronavirus associated with severe acute respiratory syndrome. In *The New England journal of medicine* 348 (20), pp. 1953–1966. DOI: 10.1056/NEJMoa030781.

Kuo, Lili; Hurst, Kelley R.; Masters, Paul S. (2006): Exceptional Flexibility in the Sequence Requirements for Coronavirus Small Envelope Protein Function ▿. In *Journal of Virology* 81 (5), pp. 2249–2262. DOI: 10.1128/JVI.01577-06.

Lai, Chih-Cheng; Shih, Tzu-Ping; Ko, Wen-Chien; Tang, Hung-Jen; Hsueh, Po-Ren (2020): Severe acute respiratory syndrome coronavirus 2 (SARS-CoV-2) and coronavirus disease-2019 (COVID-19): The epidemic and the challenges. In *International journal of antimicrobial agents* 55 (3), p. 105924. DOI: 10.1016/j.ijantimicag.2020.105924.

Laliberte, Jason P.; Weisberg, Andrea S.; Moss, Bernard (2011): The Membrane Fusion Step of Vaccinia Virus Entry Is Cooperatively Mediated by Multiple Viral Proteins and Host Cell Components. In *PLoS Pathogens* 7 (12). DOI: 10.1371/journal.ppat.1002446.

Lee, Wen Shi; Wheatley, Adam K.; Kent, Stephen J.; DeKosky, Brandon J. (2020): Antibody-dependent enhancement and SARS-CoV-2 vaccines and therapies. In *Nature Microbiology* 5 (10), pp. 1185–1191. DOI: 10.1038/s41564-020-00789-5.

Lehmann, Michael H.; Kastenmuller, Wolfgang; Kandemir, Judith D.; Brandt, Florian; Suezer, Yasemin; Sutter, Gerd (2009): Modified Vaccinia Virus Ankara Triggers Chemotaxis of Monocytes and Early Respiratory Immigration of Leukocytes by Induction of CCL2 Expression ▿. In *Journal of Virology* 83 (6), pp. 2540–2552. DOI: 10.1128/JVI.01884-08.

Li, Fang (2016): Structure, Function, and Evolution of Coronavirus Spike Proteins. In *Annual review of virology* 3 (1), pp. 237–261. DOI: 10.1146/annurev-virology-110615-042301.

Li, Fang; Li, Wenhui; Farzan, Michael; Harrison, Stephen C. (2005): Structure of SARS coronavirus

spike receptor-binding domain complexed with receptor. In *Science (New York, N.Y.)* 309 (5742), pp. 1864–1868. DOI: 10.1126/science.1116480.

Li, Qun; Guan, Xuhua; Wu, Peng; Wang, Xiaoye; Zhou, Lei; Tong, Yeqing et al. (2020): Early Transmission Dynamics in Wuhan, China, of Novel Coronavirus-Infected Pneumonia. In *The New England journal of medicine* 382 (13), pp. 1199–1207. DOI: 10.1056/NEJMoa2001316.

Li, Wenhui; Moore, Michael J.; Vasilieva, Natalya; Sui, Jianhua; Wong, Swee Kee; Berne, Michael A. et al. (2003): Angiotensin-converting enzyme 2 is a functional receptor for the SARS coronavirus. In *Nature* 426 (6965), pp. 450–454. DOI: 10.1038/nature02145.

Liao, Y.; Yuan, Q.; Torres, J.; Tam, J. P.; Liu, D. X. (2006): Biochemical and functional characterization of the membrane association and membrane permeabilizing activity of the severe acute respiratory syndrome coronavirus envelope protein. In *Virology* 349 (2), pp. 264–275. DOI: 10.1016/j.virol.2006.01.028.

Ling, Morris; Murali, Mandakolathur (2019): Analysis of the Complement System in the Clinical Immunology Laboratory. In *Clinics in laboratory medicine* 39 (4), pp. 579–590. DOI: 10.1016/j.cll.2019.07.006.

Locht, Camille (2020): Vaccines against COVID-19. In *Anaesthesia, Critical Care & Pain Medicine* 39 (6), pp. 703–705. DOI: 10.1016/j.accpm.2020.10.006.

Lu, Roujian; Zhao, Xiang; Li, Juan; Niu, Peihua; Yang, Bo; Wu, Honglong et al. (2020): Genomic characterisation and epidemiology of 2019 novel coronavirus: implications for virus origins and receptor binding. In *Lancet (London, England)* 395 (10224), pp. 565–574. DOI: 10.1016/S0140-6736(20)30251-8.

Luan, Junwen; Lu, Yue; Jin, Xiaolu; Zhang, Leiliang (2020): Spike protein recognition of mammalian ACE2 predicts the host range and an optimized ACE2 for SARS-CoV-2 infection. In *Biochemical and Biophysical Research Communications* 526 (1), pp. 165–169. DOI: 10.1016/j.bbrc.2020.03.047.

Luo, Pan; Liu, Yi; Qiu, Lin; Liu, Xiulan; Liu, Dong; Li, Juan (2020): Tocilizumab treatment in COVID-19: A single center experience. In *Journal of Medical Virology*. DOI: 10.1002/jmv.25801.

Luytjes, Willem; Sturman, Lawrence S.; Bredenbee, Peter J.; Charite, Jeroen; van der Zeijst, Bernard A.M.; Horzinek, Marian C.; Spaan, Willy J.M. (2004): Primary structure of the glycoprotein E2 of coronavirus MHV-A59 and identification of the trypsin cleavage site. In *Virology* 161 (2), pp. 479–487. DOI: 10.1016/0042-6822(87)90142-5.

Mackett, M.; Smith, G. L.; Moss, B. (1984): General method for production and selection of infectious vaccinia virus recombinants expressing foreign genes. In *Journal of Virology* 49 (3), pp. 857–864.

Mackett, M.; Yilma, T.; Rose, J. K.; Moss, B. (1985): Vaccinia virus recombinants: expression of VSV genes and protective immunization of mice and cattle. In *Science (New York, N.Y.)* 227 (4685), pp. 433–435. DOI: 10.1126/science.2981435.

Mahnel, H.; MAYR, A. (1994): Erfahrungen bei der Schutzimpfung gegen Orthopocken von Mensch und Tier mit dem Impfstamm MVA. In *Berliner und Munchener tierarztliche Wochenschrift* 107 (8), pp. 253–256.

Malik, Y. A. (2020): Properties of Coronavirus and SARS-CoV-2. In *The Malaysian journal of pathology*

42 (1), pp. 3–11.

Manche, L.; Green, S. R.; Schmedt, C.; Mathews, M. B. (1992): Interactions between double-stranded RNA regulators and the protein kinase DAI. In *Molecular and Cellular Biology* 12 (11), pp. 5238–5248.

Manjaly Thomas, Zita-Rose; Satti, Iman; Marshall, Julia L.; Harris, Stephanie A.; Lopez Ramon, Raquel; Hamidi, Ali et al. (2019): Alternate aerosol and systemic immunisation with a recombinant viral vector for tuberculosis, MVA85A: A phase I randomised controlled trial. In *PLoS Medicine* 16 (4). DOI: 10.1371/journal.pmed.1002790.

Mayr, Anton (2003): Smallpox vaccination and bioterrorism with pox viruses. In *Comparative immunology, microbiology and infectious diseases* 26 (5-6), pp. 423–430. DOI: 10.1016/S0147-9571(03)00025-0.

McFadden, Grant (2005): Poxvirus tropism. In *Nature Reviews. Microbiology* 3 (3), pp. 201–213. DOI: 10.1038/nrmicro1099.

McMichael, Andrew J.; Borrow, Persephone; Tomaras, Georgia D.; Goonetilleke, Nilu; Haynes, Barton F. (2009): The immune response during acute HIV-1 infection: clues for vaccine development. In *Nature Reviews. Immunology* 10 (1), pp. 11–23. DOI: 10.1038/nri2674.

Mégarbane, Bruno (2021): Chloroquine and hydroxychloroquine to treat COVID-19: between hope and caution. In *Clinical toxicology (Philadelphia, Pa.)* 59 (1), pp. 70–71. DOI: 10.1080/15563650.2020.1748194.

Meyer, H.; Sutter, G.; MAYR, A. (1991): Mapping of deletions in the genome of the highly attenuated vaccinia virus MVA and their influence on virulence. In *The Journal of general virology* 72 (Pt 5), pp. 1031–1038. DOI: 10.1099/0022-1317-72-5-1031.

Moss, B. (1996): Genetically engineered poxviruses for recombinant gene expression, vaccination, and safety. In *Proceedings of the National Academy of Sciences of the United States of America* 93 (21), pp. 11341–11348.

Mossman, K.; Upton, C.; Buller, R. M.; McFadden, G. (1995): Species specificity of ectromelia virus and vaccinia virus interferon-gamma binding proteins. In *Virology* 208 (2), pp. 762–769. DOI: 10.1006/viro.1995.1208.

Munseri, Patricia. J.; Kroidl, Arne; Nilsson, Charlotta; Joachim, Agricola; Geldmacher, Christof; Mann, Philipp et al. (2015): Priming with a Simplified Intradermal HIV-1 DNA Vaccine Regimen followed by Boosting with Recombinant HIV-1 MVA Vaccine Is Safe and Immunogenic: A Phase IIa Randomized Clinical Trial. In *PLoS ONE* 10 (4). DOI: 10.1371/journal.pone.0119629.

Munster, Vincent J.; Wells, Daniel; Lambe, Teresa; Wright, Daniel; Fischer, Robert J.; Bushmaker, Trenton et al. (2017): Protective efficacy of a novel simian adenovirus vaccine against lethal MERS-CoV challenge in a transgenic human DPP4 mouse model. In *NPJ Vaccines* 2. DOI: 10.1038/s41541-017-0029-1.

Murphy, Kenneth M.; Travers, Paul; Walport, Mark (2014): Janeway Immunologie. With assistance of Michael Ehrenstein, Claudia Mauri, Allan Mowat, Andrey Shaw. 7., Auflage, korrigierter Nachdruck 2014. Berlin, Heidelberg: Springer Spektrum.

Nájera, José Luis; Gómez, Carmen Elena; Domingo-Gil, Elena; Gherardi, María Magdalena; Esteban, Mariano (2006): Cellular and Biochemical Differences between Two Attenuated Poxvirus Vaccine Candidates (MVA and NYVAC) and Role of the C7L Gene. In *Journal of Virology* 80 (12), pp. 6033–6047. DOI: 10.1128/JVI.02108-05.

Nal, Béatrice; Chan, Cheman; Kien, Francois; Siu, Lewis; Tse, Jane; Chu, Kid et al. (2005): Differential maturation and subcellular localization of severe acute respiratory syndrome coronavirus surface proteins S, M and E. In *The Journal of general virology* 86 (Pt 5), pp. 1423–1434. DOI: 10.1099/vir.0.80671-0.

Nicholson, Lindsay B. (2016): The immune system. In *Essays in Biochemistry* 60 (3), pp. 275–301. DOI: 10.1042/EBC20160017.

Okba, Nisreen M.A.; Müller, Marcel A.; Li, Wentao; Wang, Chunyan; GeurtsvanKessel, Corine H.; Corman, Victor M. et al. (2020): Severe Acute Respiratory Syndrome Coronavirus 2−Specific Antibody Responses in Coronavirus Disease Patients. In *Emerging Infectious Diseases* 26 (7), pp. 1478–1488. DOI: 10.3201/eid2607.200841.

Opstelten, D. J.; Raamsman, M. J.; Wolfs, K.; Horzinek, M. C.; Rottier, P. J. (1995): Envelope glycoprotein interactions in coronavirus assembly. In *The Journal of Cell Biology* 131 (2), pp. 339–349. DOI: 10.1083/jcb.131.2.339.

Pardi, Norbert; Hogan, Michael J.; Porter, Frederick W.; Weissman, Drew (2018): mRNA vaccines — a new era in vaccinology. In *Nature reviews. Drug discovery* 17 (4), pp. 261–279. DOI: 10.1038/nrd.2017.243.

Payne, L. G. (1980): Significance of extracellular enveloped virus in the in vitro and in vivo dissemination of vaccinia. In *The Journal of general virology* 50 (1), pp. 89–100. DOI: 10.1099/0022-1317-50-1-89.

Peck, Kayla M.; Lauring, Adam S. (2018): Complexities of Viral Mutation Rates. In *Journal of Virology* 92 (14). DOI: 10.1128/JVI.01031-17.

Pene, Frédéric; Merlat, Annabelle; Vabret, Astrid; Rozenberg, Flore; Buzyn, Agnès; Dreyfus, François et al. (2003): Coronavirus 229E-Related Pneumonia in Immunocompromised Patients. In *Clinical Infectious Diseases: An Official Publication of the Infectious Diseases Society of America* 37 (7), pp. 929–932. DOI: 10.1086/377612.

Piccini, A.; Perkus, M. E.; Paoletti, E. (1987): Vaccinia virus as an expression vector. In *Methods in enzymology* 153, pp. 545–563. DOI: 10.1016/0076-6879(87)53077-4.

Plotkin, Stanley A. (2008): Vaccines: correlates of vaccine-induced immunity. In *Clinical Infectious Diseases: An Official Publication of the Infectious Diseases Society of America* 47 (3), pp. 401–409. DOI: 10.1086/589862.

Polack, Fernando P.; Thomas, Stephen J.; Kitchin, Nicholas; Absalon, Judith; Gurtman, Alejandra; Lockhart, Stephen et al. (2020): Safety and Efficacy of the BNT162b2 mRNA Covid-19 Vaccine. In *The New England journal of medicine*. DOI: 10.1056/NEJMoa2034577.

Poland, Gregory A.; Ovsyannikova, Inna G.; Crooke, Stephen N.; Kennedy, Richard B. (2020): SARS-CoV-2 Vaccine Development: Current Status. In *Mayo Clinic Proceedings* 95 (10), pp. 2172–2188. DOI: 10.1016/j.mayocp.2020.07.021.

Prajapat, Manisha; Sarma, Phulen; Shekhar, Nishant; Avti, Pramod; Sinha, Shweta; Kaur, Hardeep et al. (2020): Drug targets for corona virus: A systematic review. In *Indian journal of pharmacology* 52 (1), pp. 56–65. DOI: 10.4103/ijp.IJP_115_20.

Public Health England (2021): Investigation of novel SARS-CoV-2 variant: Variant of Concern 202012/01. Available online at https://assets.publishing.service.gov.uk/government/uploads/system/uploads/attachment_data/file/959426/Variant_of_Concern_VOC_202012_01_Technical_Briefing_5.pdf, updated on 2/1/2021, checked on 2/9/2021.

Pulendran, Bali; Ahmed, Rafi (2011): Immunological mechanisms of vaccination. In *Nature Immunology* 12 (6), pp. 509–517.

Ren, Decheng; Tu, Ho-Chou; Kim, Hyungjin; Wang, Gary X.; Bean, Gregory R.; Takeuchi, Osamu et al. (2010): BID, BIM, and PUMA Are Essential for Activation of the BAX- and BAK-Dependent Cell Death Program. In *Science (New York, N.Y.)* 330 (6009), pp. 1390–1393. DOI: 10.1126/science.1190217.

Romero, C. H.; Barrett, T.; Chamberlain, R. W.; Kitching, R. P.; Fleming, M.; Black, D. N. (1994): Recombinant capripoxvirus expressing the hemagglutinin protein gene of rinderpest virus: protection of cattle against rinderpest and lumpy skin disease viruses. In *Virology* 204 (1), pp. 425–429. DOI: 10.1006/viro.1994.1548.

Saikatendu, Kumar Singh; Joseph, Jeremiah S.; Subramanian, Vanitha; Neuman, Benjamin W.; Buchmeier, Michael J.; Stevens, Raymond C.; Kuhn, Peter (2007): Ribonucleocapsid Formation of Severe Acute Respiratory Syndrome Coronavirus through Molecular Action of the N-Terminal Domain of N Protein ▿ . In *Journal of Virology* 81 (8), pp. 3913–3921. DOI: 10.1128/JVI.02236-06.

Sallusto, Federica; Lanzavecchia, Antonio; Araki, Koichi; Ahmed, Rafi (2010): From Vaccines to Memory and Back. In *Immunity* 33 (4), pp. 451–463. DOI: 10.1016/j.immuni.2010.10.008.

Sancho, M. Carmen; Schleich, Sibylle; Griffiths, Gareth; Krijnse-Locker, Jacomine (2002): The Block in Assembly of Modified Vaccinia Virus Ankara in HeLa Cells Reveals New Insights into Vaccinia Virus Morphogenesis. In *Journal of Virology* 76 (16), pp. 8318–8334. DOI: 10.1128/JVI.76.16.8318-8334.2002.

Sawicki, S. G.; Sawicki, D. L. (2005): Coronavirus Transcription: A Perspective. In *Coronavirus Replication and Reverse Genetics* 287, pp. 31–55. DOI: 10.1007/3-540-26765-4_2.

Schoeman, Dewald; Fielding, Burtram C. (2019): Coronavirus envelope protein: current knowledge. In *Virology Journal* 16. DOI: 10.1186/s12985-019-1182-0.

Schroeder, Harry W.; Cavacini, Lisa (2010): Structure and Function of Immunoglobulins. In *The Journal of allergy and clinical immunology* 125 (2 0 2), S41-52. DOI: 10.1016/j.jaci.2009.09.046.

Seet, Bruce T.; Johnston, J. B.; Brunetti, Craig R.; Barrett, John W.; Everett, Helen; Cameron, Cheryl et al. (2003): Poxviruses and immune evasion. In *Annual review of immunology* 21, pp. 377–423. DOI: 10.1146/annurev.immunol.21.120601.141049.

Shang, Jian; Wan, Yushun; Luo, Chuming; Ye, Gang; Geng, Qibin; Auerbach, Ashley; Li, Fang (2020): Cell entry mechanisms of SARS-CoV-2. In *Proceedings of the National Academy of Sciences of the United States of America* 117 (21), pp. 11727–11734. DOI: 10.1073/pnas.2003138117.

Siddell, S. G.; Anderson, R.; Cavanagh, D.; Fujiwara, K.; Klenk, H. D.; Macnaughton, M. R. et al. (2008): Coronaviridae1. In *Intervirology* 20 (4), pp. 181–189. DOI: 10.1159/000149390.

Smith, E. J.; Marié, I.; Prakash, A.; García-Sastre, A.; Levy, D. E. (2001): IRF3 and IRF7 phosphorylation in virus-infected cells does not require double-stranded RNA-dependent protein kinase R or Ikappa B kinase but is blocked by Vaccinia virus E3L protein. In *The Journal of Biological Chemistry* 276 (12), pp. 8951–8957. DOI: 10.1074/jbc.M008717200.

Smith, G. L. (1993): Vaccinia virus glycoproteins and immune evasion. The sixteenth Fleming Lecture. In *The Journal of general virology* 74 (Pt 9), pp. 1725–1740. DOI: 10.1099/0022-1317-74-9-1725.

Smith, G. L.; Symons, J. A.; Khanna, A.; Vanderplasschen, A.; Alcamí, A. (1997): Vaccinia virus immune evasion. In *Immunological reviews* 159, pp. 137–154. DOI: 10.1111/j.1600-065x.1997.tb01012.x.

Song, Fei; Fux, Robert; Provacia, Lisette B.; Volz, Asisa; Eickmann, Markus; Becker, Stephan et al. (2013): Middle East Respiratory Syndrome Coronavirus Spike Protein Delivered by Modified Vaccinia Virus Ankara Efficiently Induces Virus-Neutralizing Antibodies. In *Journal of Virology* 87 (21), pp. 11950–11954. DOI: 10.1128/JVI.01672-13.

Song, Yang; Zhang, Min; Yin, Ling; Wang, Kunkun; Zhou, Yiyi; Zhou, Mi; Lu, Yun (2020): COVID-19 treatment: close to a cure? A rapid review of pharmacotherapies for the novel coronavirus (SARS-CoV-2). In *International journal of antimicrobial agents* 56 (2), p. 106080. DOI: 10.1016/j.ijantimicag.2020.106080.

Spadaro, Savino; Park, Mirae; Turrini, Cecilia; Tunstall, Tanushree; Thwaites, Ryan; Mauri, Tommaso et al. (2019): Biomarkers for Acute Respiratory Distress syndrome and prospects for personalised medicine. In *Journal of Inflammation (London, England)* 16. DOI: 10.1186/s12950-018-0202-y.

Spriggs, D. R.; Deutsch, S.; Kufe, D. W. (1992): Genomic structure, induction, and production of TNF-alpha. In *Immunology series* 56, pp. 3–34.

Staib, Caroline; Drexler, Ingo; Sutter, Gerd (2004): Construction and isolation of recombinant MVA. In *Methods in molecular biology (Clifton, N.J.)* 269, pp. 77–100. DOI: 10.1385/1-59259-789-0:077.

Stickl, H.; Hochstein-Mintzel, V. (1971): Die intrakutane Pockenimpfung mit einem schwach virulenten Vakzinia-Virus („MVA-Virus“. In *Munchener medizinische Wochenschrift (1950)* 113 (35), pp. 1149–1153.

Stickl, H. A. (1974): Smallpox vaccination and its consequences: first experiences with the highly attenuated smallpox vaccine “MVA”. In *Preventive medicine* 3 (1), pp. 97–101. DOI: 10.1016/0091-7435(74)90066-8.

Stokes, G. V. (1976): High-voltage electron microscope study of the release of vaccinia virus from whole cells. In *Journal of Virology* 18 (2), pp. 636–643.

Sun, Jing; Zhuang, Zhen; Zheng, Jian; Li, Kun; Wong, Roy Lok-Yin; Liu, Donglan et al. (2020a): Generation of a Broadly Useful Model for COVID-19 Pathogenesis, Vaccination, and Treatment. In *Cell* 182 (3), 734-743.e5. DOI: 10.1016/j.cell.2020.06.010.

Sun, Pengfei; Lu, Xiaosheng; Xu, Chao; Sun, Wenjuan; Pan, Bo (2020b): Understanding of COVID-19 based on current evidence. In *Journal of Medical Virology*. DOI: 10.1002/jmv.25722.

Sutter, G.; Moss, B. (1992): Nonreplicating vaccinia vector efficiently expresses recombinant genes. In *Proceedings of the National Academy of Sciences of the United States of America* 89 (22), pp. 10847–10851.

Sutter, G.; Ramsey-Ewing, A.; Rosales, R.; Moss, B. (1994a): Stable expression of the vaccinia virus K1L gene in rabbit cells complements the host range defect of a vaccinia virus mutant. In *Journal of Virology* 68 (7), pp. 4109–4116.

Sutter, G.; Wyatt, L. S.; Foley, P. L.; Bennink, J. R.; Moss, B. (1994b): A recombinant vector derived from the host range-restricted and highly attenuated MVA strain of vaccinia virus stimulates protective immunity in mice to influenza virus. In *Vaccine* 12 (11), pp. 1032–1040. DOI: 10.1016/0264-410x(94)90341-7.

Sutter, Gerd (2020): A vital gene for modified vaccinia virus Ankara replication in human cells. In *Proceedings of the National Academy of Sciences of the United States of America* 117 (12), pp. 6289–6291. DOI: 10.1073/pnas.2001335117.

Tai, Wanbo; Wang, Yufei; Fett, Craig A.; Zhao, Guangyu; Li, Fang; Perlman, Stanley et al. (2016): Recombinant Receptor-Binding Domains of Multiple Middle East Respiratory Syndrome Coronaviruses (MERS-CoVs) Induce Cross-Neutralizing Antibodies against Divergent Human and Camel MERS-CoVs and Antibody Escape Mutants. In *Journal of Virology* 91 (1). DOI: 10.1128/JVI.01651-16.

Tang, Xian-Chun; Agnihothram, Sudhakar S.; Jiao, Yongjun; Stanhope, Jeremy; Graham, Rachel L.; Peterson, Eric C. et al. (2014): Identification of human neutralizing antibodies against MERS-CoV and their role in virus adaptive evolution. In *Proceedings of the National Academy of Sciences of the United States of America* 111 (19), E2018-26. DOI: 10.1073/pnas.1402074111.

Taylor, J.; Trimarchi, C.; Weinberg, R.; Languet, B.; Guillemin, F.; Desmettre, P.; Paoletti, E. (1991): Efficacy studies on a canarypox-rabies recombinant virus. In *Vaccine* 9 (3), pp. 190–193. DOI: 10.1016/0264-410x(91)90152-v.

Tian, Sijia; Hu, Nan; Lou, Jing; Chen, Kun; Kang, Xuqin; Xiang, Zhenjun et al. (2020): Characteristics of COVID-19 infection in Beijing. In *The Journal of Infection* 80 (4), pp. 401–406. DOI: 10.1016/j.jinf.2020.02.018.

Toovey, Oliver T.R.; Harvey, Kirsty N.; Bird, Paul W.; Tang, Julian Wei-Tze Wei-Tze (2021): Introduction of Brazilian SARS-CoV-2 484K.V2 related variants into the UK. In *The Journal of Infection*. DOI: 10.1016/j.jinf.2021.01.025.

Townsend, A.; Bastin, J.; Gould, K.; Brownlee, G.; Andrew, M.; Coupar, B. et al. (1988): Defective presentation to class I-restricted cytotoxic T lymphocytes in vaccinia-infected cells is overcome by enhanced degradation of antigen. In *The Journal of Experimental Medicine* 168 (4), pp. 1211–1224. DOI: 10.1084/jem.168.4.1211.

Tscharke, David C.; Karupiah, Gunasegaran; Zhou, Jie; Palmore, Tara; Irvine, Kari R.; Haeryfar, S. MansourM. et al. (2005): Identification of poxvirus CD8+ T cell determinants to enable rational design and characterization of smallpox vaccines. In *The Journal of Experimental Medicine* 201 (1), pp. 95–104. DOI: 10.1084/jem.20041912.

Turvey, Stuart E.; Broide, David H. (2009): Chapter 2: Innate Immunity. In *The Journal of allergy and*

clinical immunology 125 (2 Suppl 2), S24-32. DOI: 10.1016/j.jaci.2009.07.016.

Vabret, Astrid; Mourez, Thomas; Gouarin, Stéphanie; Petitjean, Joëlle; Freymuth, François (2003): An Outbreak of Coronavirus OC43 Respiratory Infection in Normandy, France. In *Clinical Infectious Diseases: An Official Publication of the Infectious Diseases Society of America* 36 (8), pp. 985–989. DOI: 10.1086/374222.

van Doremalen, Neeltje; Lambe, Teresa; Spencer, Alexandra; Belij-Rammerstorfer, Sandra; Purushotham, Jyothi N.; Port, Julia R. et al. (2020): ChAdOx1 nCoV-19 vaccine prevents SARS-CoV-2 pneumonia in rhesus macaques. In *Nature* 586 (7830), pp. 578–582. DOI: 10.1038/s41586-020-2608-y.

Veit, Svenja; Jany, Sylvia; Fux, Robert; Sutter, Gerd; Volz, Asisa (2018): CD8+ T Cells Responding to the Middle East Respiratory Syndrome Coronavirus Nucleocapsid Protein Delivered by Vaccinia Virus MVA in Mice. In *Viruses* 10 (12). DOI: 10.3390/v10120718.

Veyer, David L.; Carrara, Guia; Maluquer de Motes, Carlos; Smith, Geoffrey L. (2017): Vaccinia virus evasion of regulated cell death. In *Immunology letters* 186, pp. 68–80. DOI: 10.1016/j.imlet.2017.03.015.

Vignuzzi, Marco; Andino, Raul (2012): Closing the gap: the challenges in converging theoretical, computational, experimental and real-life studies in virus evolution. In *Current Opinion in Virology* 2 (5), pp. 515–518. DOI: 10.1016/j.coviro.2012.09.008.

Vignuzzi, Marco; Stone, Jeffrey K.; Arnold, Jamie J.; Cameron, Craig E.; Andino, Raul (2005): Quasispecies diversity determines pathogenesis through cooperative interactions within a viral population. In *Nature* 439 (7074), pp. 344–348. DOI: 10.1038/nature04388.

Volz, A.; Sutter, G. (2016): Modified Vaccinia Virus Ankara: History, Value in Basic Research, and Current Perspectives for Vaccine Development. In *Advances in Virus Research* 97, pp. 187–243. DOI: 10.1016/bs.aivir.2016.07.001.

Volz, Asisa; Kupke, Alexandra; Song, Fei; Jany, Sylvia; Fux, Robert; Shams-Eldin, Hosam et al. (2015): Protective Efficacy of Recombinant Modified Vaccinia Virus Ankara Delivering Middle East Respiratory Syndrome Coronavirus Spike Glycoprotein. In *Journal of Virology* 89 (16), pp. 8651–8656. DOI: 10.1128/JVI.00614-15.

Volz, Erik; Hill, Verity; McCrone, John T.; Price, Anna; Jorgensen, David; O'Toole, Áine et al. (2020): Evaluating the Effects of SARS-CoV-2 Spike Mutation D614G on Transmissibility and Pathogenicity. In *Cell* 184 (1), 64-75.e11. DOI: 10.1016/j.cell.2020.11.020.

Vries, Rory D. de; Rimmelzwaan, Guus F. (2016): Viral vector-based influenza vaccines. In *Human Vaccines & Immunotherapeutics* 12 (11), pp. 2881–2901. DOI: 10.1080/21645515.2016.1210729.

Waibler, Zoe; Anzaghe, Martina; Ludwig, Holger; Akira, Shizuo; Weiss, Siegfried; Sutter, Gerd; Kalinke, Ulrich (2007): Modified Vaccinia Virus Ankara Induces Toll-Like Receptor-Independent Type I Interferon Responses ▿ . In *Journal of Virology* 81 (22), pp. 12102–12110. DOI: 10.1128/JVI.01190-07.

Walsh, Edward E.; Frenck, Robert W.; Falsey, Ann R.; Kitchin, Nicholas; Absalon, Judith; Gurtman, Alejandra et al. (2020): Safety and Immunogenicity of Two RNA-Based Covid-19 Vaccine Candidates. In *The New England journal of medicine*. DOI: 10.1056/NEJMoa2027906.

Wang, Fuzhou; Kream, Richard M.; Stefano, George B. (2020a): Long-Term Respiratory and

Neurological Sequelae of COVID-19. In *Medical Science Monitor : International Medical Journal of Experimental and Clinical Research* 26, e928996-1-e928996-10. DOI: 10.12659/MSM.928996.

Wang, Mei-Yue; Zhao, Rong; Gao, Li-Juan; Gao, Xue-Fei; Wang, De-Ping; Cao, Ji-Min (2020b): SARS-CoV-2: Structure, Biology, and Structure-Based Therapeutics Development. In *Frontiers in Cellular and Infection Microbiology* 10. DOI: 10.3389/fcimb.2020.587269.

Wang, Sheng-Fan; Tseng, Sung-Pin; Yen, Chia-Hung; Yang, Jyh-Yuan; Tsao, Ching-Han; Shen, Chun-Wei et al. (2014): Antibody-dependent SARS coronavirus infection is mediated by antibodies against spike proteins. In *Biochemical and Biophysical Research Communications* 451 (2), pp. 208–214. DOI: 10.1016/j.bbrc.2014.07.090.

Warrington, Richard; Watson, Wade; Kim, Harold L.; Antonetti, Francesca Romana (2011): An introduction to immunology and immunopathology. In *Allergy, Asthma, and Clinical Immunology : Official Journal of the Canadian Society of Allergy and Clinical Immunology* 7 (Suppl 1), S1. DOI: 10.1186/1710-1492-7-S1-S1.

Webster, R. G.; Kawaoka, Y.; Taylor, J.; Weinberg, R.; Paoletti, E. (1991): Efficacy of nucleoprotein and haemagglutinin antigens expressed in fowlpox virus as vaccine for influenza in chickens. In *Vaccine* 9 (5), pp. 303–308. DOI: 10.1016/0264-410x(91)90055-b.

Westwood, J. C.; Harris, W. J.; Zwartouw, H. T.; Titmuss, D. H.; Appleyard, G. (1964): Studies on the Structure of Vaccinia Virus. In *Journal of general microbiology* 34, pp. 67–78. DOI: 10.1099/00221287-34-1-67.

WHO (2019): Middle East respiratory syndrome coronavirus (MERS-CoV). Available online at https://www.who.int/en/news-room/fact-sheets/detail/middle-east-respiratory-syndrome-coronavirus-(mers-cov), checked on 2/10/2021.

WHO (2020): SARS-CoV-2 Variants. Available online at https://www.who.int/csr/don/31-december-2020-sars-cov2-variants/en/, updated on 12/31/2020, checked on 2/9/2021.

WHO (2021a): AZD1222 vaccine against COVID-19 developed by Oxford University and Astra Zeneca: Background paper. Available online at file:///C:/Users/ru63fax/AppData/Local/Temp/WHO-2019-nCoV-vaccines-SAGE-recommendation-AZD1222-background-2021.1-eng.pdf, updated on 2/10/2021, checked on 2/13/2021.

WHO (2021b): Draft landscape and tracker of COVID-19 candidate vaccines. Available online at https://www.who.int/publications/m/item/draft-landscape-of-covid-19-candidate-vaccines, checked on 1/30/2021.

WHO (2021c): Severe Acute Respiratory Syndrome (SARS). Available online at https://www.who.int/health-topics/severe-acute-respiratory-syndrome#tab=tab_3, checked on 2/10/2021.

WHO (2021d): Interim recommendations for use of the AZD1222 (ChAdOx1-S [recombinant]) vaccine against COVID-19 developed by Oxford University and AstraZeneca. Available online at file:///C:/Users/ru63fax/AppData/Local/Temp/WHO-2019-nCoV-vaccines-SAGE-recommendation-AZD1222-2021.1-eng.pdf, updated on 2/10/2021, checked on 2/13/2021.

Wiktor, T. J.; Macfarlan, R. I.; Reagan, K. J.; Dietzschold, B.; Curtis, P. J.; Wunner, W. H. et al. (1984): Protection from rabies by a vaccinia virus recombinant containing the rabies virus glycoprotein gene. In

Proceedings of the National Academy of Sciences of the United States of America 81 (22), pp. 7194–7198.

Wong, Lok-Yin Roy; Li, Kun; Sun, Jing; Zhuang, Zhen; Zhao, Jincun; McCray, Paul B.; Perlman, Stanley (2020): Sensitization of Non-permissive Laboratory Mice to SARS-CoV-2 with a Replication-Deficient Adenovirus Expressing Human ACE2. In *STAR Protocols* 1 (3), p. 100169. DOI: 10.1016/j.xpro.2020.100169.

Wong, Yik Chun; Lin, Leon C. W.; Melo-Silva, Carolina R.; Smith, Stewart A.; Tscharke, David C. (2011): Engineering recombinant poxviruses using a compact GFP-blasticidin resistance fusion gene for selection. In *Journal of virological methods* 171 (1), pp. 295–298. DOI: 10.1016/j.jviromet.2010.11.003.

Woo, Patrick C. Y.; Lau, Susanna K. P.; Lam, Carol S. F.; Lau, Candy C. Y.; Tsang, Alan K. L.; Lau, John H. N. et al. (2012): Discovery of Seven Novel Mammalian and Avian Coronaviruses in the Genus Deltacoronavirus Supports Bat Coronaviruses as the Gene Source of Alphacoronavirus and Betacoronavirus and Avian Coronaviruses as the Gene Source of Gammacoronavirus and Deltacoronavirus. In *Journal of Virology* 86 (7), pp. 3995–4008. DOI: 10.1128/JVI.06540-11.

Woo, Patrick C. Y.; Lau, Susanna K. P.; Tsoi, Hoi-wah; Huang, Yi; Poon, Rosana W. S.; Chu, Chung-ming et al. (2005): Clinical and Molecular Epidemiological Features of Coronavirus HKU1–Associated Community-Acquired Pneumonia. In *The Journal of Infectious Diseases* 192 (11), pp. 1898–1907. DOI: 10.1086/497151.

Wu, Zunyou; McGoogan, Jennifer M. (2020): Characteristics of and Important Lessons From the Coronavirus Disease 2019 (COVID-19) Outbreak in China: Summary of a Report of 72 314 Cases From the Chinese Center for Disease Control and Prevention. In *JAMA* 323 (13), pp. 1239–1242. DOI: 10.1001/jama.2020.2648.

Wyatt, L. S.; Shors, S. T.; Murphy, B. R.; Moss, B. (1996): Development of a replication-deficient recombinant vaccinia virus vaccine effective against parainfluenza virus 3 infection in an animal model. In *Vaccine* 14 (15), pp. 1451–1458. DOI: 10.1016/s0264-410x(96)00072-2.

Wyatt, Linda S.; Earl, Patricia L.; Xiao, Wei; Americo, Jeffrey L.; Cotter, Catherine A.; Vogt, Jennifer; Moss, Bernard (2009): Elucidating and Minimizing the Loss by Recombinant Vaccinia Virus of Human Immunodeficiency Virus Gene Expression Resulting from Spontaneous Mutations and Positive Selection ▿. In *Journal of Virology* 83 (14), pp. 7176–7184. DOI: 10.1128/JVI.00687-09.

Xu, Jiuyang; Jia, Wenxu; Wang, Pengfei; Zhang, Senyan; Shi, Xuanling; Wang, Xinquan; Zhang, Linqi (2019): Antibodies and vaccines against Middle East respiratory syndrome coronavirus. In *Emerging Microbes & Infections* 8 (1), pp. 841–856. DOI: 10.1080/22221751.2019.1624482.

Xu, Xiaoling; Han, Mingfeng; Li, Tiantian; Sun, Wei; Wang, Dongsheng; Fu, Binqing et al. (2020): Effective treatment of severe COVID-19 patients with tocilizumab. In *Proceedings of the National Academy of Sciences of the United States of America* 117 (20), pp. 10970–10975. DOI: 10.1073/pnas.2005615117.

Yang, Zhi-yong; Kong, Wing-pui; Huang, Yue; Roberts, Anjeanette; Murphy, Brian R.; Subbarao, Kanta; Nabel, Gary J. (2004): A DNA vaccine induces SARS coronavirus neutralization and protective immunity in mice. In *Nature* 428 (6982), pp. 561–564. DOI: 10.1038/nature02463.

Yilma, T.; Owens, S.; Adams, D. S. (1988): High levels of interferon in synovial fluid of retrovirus-infected goats. In *Journal of interferon research* 8 (1), pp. 45–50. DOI: 10.1089/jir.1988.8.45.

Yip, Ming Shum; Leung, Nancy Hiu Lan; Cheung, Chung Yan; Li, Ping Hung; Lee, Horace Hok Yeung; Daëron, Marc et al. (2014): Antibody-dependent infection of human macrophages by severe acute respiratory syndrome coronavirus. In *Virology Journal* 11. DOI: 10.1186/1743-422X-11-82.

Yoon, In-Kyu; Kim, Jerome H. (2019): First clinical trial of a MERS coronavirus DNA vaccine. In *The Lancet. Infectious diseases* 19 (9), pp. 924–925. DOI: 10.1016/S1473-3099(19)30397-4.

Yurkovetskiy, Leonid; Wang, Xue; Pascal, Kristen E.; Tomkins-Tinch, Christopher; Nyalile, Thomas P.; Wang, Yetao et al. (2020): Structural and Functional Analysis of the D614G SARS-CoV-2 Spike Protein Variant. In *Cell* 183 (3), 739-751.e8. DOI: 10.1016/j.cell.2020.09.032.

Zaki, Ali M.; van Boheemen, Sander; Bestebroer, Theo M.; Osterhaus, Albert D. M. E.; Fouchier, Ron A. M. (2012): Isolation of a novel coronavirus from a man with pneumonia in Saudi Arabia. In *The New England journal of medicine* 367 (19), pp. 1814–1820. DOI: 10.1056/NEJMoa1211721.

Zayas, Gustavo; Chiang, Ming C.; Wong, Eric; MacDonald, Fred; Lange, Carlos F.; Senthilselvan, Ambikaipakan; King, Malcolm (2012): Cough aerosol in healthy participants: fundamental knowledge to optimize droplet-spread infectious respiratory disease management. In *BMC Pulmonary Medicine* 12. DOI: 10.1186/1471-2466-12-11.

Zhao, Jincun; Li, Kun; Wohlford-Lenane, Christine; Agnihothram, Sudhakar S.; Fett, Craig; Zhao, Jingxian et al. (2014): Rapid generation of a mouse model for Middle East respiratory syndrome. In *Proceedings of the National Academy of Sciences of the United States of America* 111 (13), pp. 4970–4975. DOI: 10.1073/pnas.1323279111.

Zhao, Jincun; Zhao, Jingxian; van Rooijen, Nico; Perlman, Stanley (2009): Evasion by Stealth: Inefficient Immune Activation Underlies Poor T Cell Response and Severe Disease in SARS-CoV-Infected Mice. In *PLoS Pathogens* 5 (10). DOI: 10.1371/journal.ppat.1000636.

Zhong, N. S.; Zheng, B. J.; Li, Y. M.; Poon, L. L.M.; Xie, Z. H.; Chan, K. H. et al. (2003): Epidemiology and cause of severe acute respiratory syndrome (SARS) in Guangdong, People's Republic of China, in February, 2003. In *Lancet (London, England)* 362 (9393), pp. 1353–1358. DOI: 10.1016/S0140-6736(03)14630-2.

Zhou, Peng; Yang, Xing-Lou; Wang, Xian-Guang; Hu, Ben; Zhang, Lei; Zhang, Wei et al. (2020): A pneumonia outbreak associated with a new coronavirus of probable bat origin. In *Nature* 579 (7798), pp. 270–273. DOI: 10.1038/s41586-020-2012-7.

Zhu, Na; Zhang, Dingyu; Wang, Wenling; Li, Xingwang; Yang, Bo; Song, Jingdong et al. (2020): A Novel Coronavirus from Patients with Pneumonia in China, 2019. In *The New England journal of medicine* 382 (8), pp. 727–733. DOI: 10.1056/NEJMoa2001017.

XI. APPENDIX

1.1. Chemicals

Chemical	Supplier
2-Propanol ≥ 99.8%	Carl Roth, Karlsruhe, Germany
Acetone ≥ 99.5%	Carl Roth, Karlsruhe, Germany
Albumine, IgG-free	Carl Roth, Karlsruhe, Germany
Biozym LE Agarose	Biozym Scientific, Hessisch Oldendorf, Germany
Brefeldin A	Biolegend, London, United Kingdom
cOMPLETE, EDTA free	Roche Diagnostics, Mannheim, Germany
DAPI	Thermo Fisher Scientific, Planegg, Germany
DMSO	Sigma-Aldrich, Taufkirchen, Germany
Ethanol 96%,	Carl Roth, Karlsruhe, Germany
GelRed Nucleic Acid Gel Stain, 10 000x	Biozol GmbH, Eching, Germany
Glycin	PanReac AppliChem, Darmstadt, Germany
KPL TrueBlueTM Peroxidase Substrate	HiSS Diagnostics GmbH, Freiburg im Breigau, Germany
Methanol ≥ 99%	Carl Roth, Karlsruhe, Germany
MACSQuant FACS buffer	Milenyi Biotec, Bergisch Gladbach, Germany
MACSQuant Perm buffer	Milenyi Biotec, Bergisch Gladbach, Germany
MACSQuant Wash buffer	Milenyi Biotec, Bergisch Gladbach, Germany
Nonfat dried milk powder	PanReac AppliChem, Darmstadt, Germany
Red Blood Cell Lysing Buffer Hybri-Mix	Sigma-Aldrich, Taufkirchen, Germany
Roti-Load 1, reducing, 4x	Carl Roth, Karlsruhe, Germany
Stop Reagent for ELISA	Sigma-Aldrich, Taufkirchen, Germany

Sucrose	Sigma-Aldrich, Taufkirchen, Germany
TMB for ELISA	Sigma-Aldrich, Taufkirchen, Germany
Tris-Ultrapure	PanReac AppliChem, Darmstadt, Germany
Triton-X100	Sigma-Aldrich, Taufkirchen, Germany
Trypan blue	Sigma-Aldrich, Taufkirchen, Germany
Tween20	Sigma-Aldrich, Taufkirchen, Germany
Zombie dye	Biolegend, London, United Kingdom

1.2. Consumables

Material	**Supplier**
6-well tissue culture plates	Sarstedt, Nümbrecht, Germany
24-well tissue culture plates	Sarstedt, Nümbrecht, Germany
96-well tissue culture plates	Sarstedt, Nümbrecht, Germany
Cover slips	Thermo Fisher Scientific, Planegg, Germany
CryoPure tube	Sarstedt, Nümbrecht, Germany
Disposal bag	Sarstedt, Nümbrecht, Germany
Ep T.I.P.S Standard 20-300 µl	Eppendorf AG, Hamburg, Germany
Filter tips (20 µl)	Sarstedt, Nümbrecht, Germany
Filter tips (100 µl)	Sarstedt, Nümbrecht, Germany
Filter tips (200 µl)	Sarstedt, Nümbrecht, Germany
Filtopur S0.45	Sarstedt, Nümbrecht, Germany
Microtest plate 96-well	Sarstedt, Nümbrecht, Germany
MiniCollect vials	Greiner Bio-One, Frickenhausen, Germany
Nitrocelluose Blotting Membrane	GE Healthcare Europe, Freiburg, Germany
Nunc-Immuno Plate	Thermo Fisher Scientific, Planegg, Germany
SafeSeal reaction tube 1.5 ml	Sarstedt, Nümbrecht, Germany
SafeSeal reaction tube 2 ml	Sarstedt, Nümbrecht, Germany
Serological pipette 5 ml	Sarstedt, Nümbrecht, Germany

Serological pipette 10 ml	Sarstedt, Nümbrecht, Germany
Serological pipette 25 ml	Sarstedt, Nümbrecht, Germany
TC flask 25	Sarstedt, Nümbrecht, Germany
TC flask 75	Sarstedt, Nümbrecht, Germany
TC flask 175	Sarstedt, Nümbrecht, Germany
Tube 15 ml	Sarstedt, Nümbrecht, Germany
Tube 50 ml	Sarstedt, Nümbrecht, Germany

1.3. Laboratory equipment

Laboratory equipment	**Supplier**
A.EL.VIS Universal plate reader V3.0	A.EL.VIS GmbH, Hannover, Germany
Avanti J-26 XP Centrifuge	Beckmann Coulter, Krefeld, Germany
Biofuge fresco	Heraeus, Hanau, Germany
Centrifuge 5424	Eppendorf AG, Hamburg, Germany
ChemiDocTMMP, Imaging System	Bio-Rad, Munich, Germany
FACS Calibur cytofluorometer	Becton Dickinson, Heidelberg, Germany
Galaxy 170S Incubator	New Brunswick (Eppendorf), Hamburg, Germany
KEYENCE BZ-X710 All-in one Fluorescence Microscope	KEYENCE Deutschland GmbH, Neulsenburg, Germany
Microplate reader Sunrise	Tecan Trading AG, Männedorf, Switzerland
MJ Research PTC-200 Peltier Thermal Cycler	GMI, Ramsey, USA
Olympus CKX41	Olympus Life Sciences, Hamburg, Germany
OptimaTMLE-80K Ultracentrifuge	Beckman Coulter, Krefeld, Germany
Sonoplus	Bandelin electronic, Berlin, Germany

1.4. DNA and protein marker

Material	Supplier
1 kb DNA ladder	New England Biolabs, Frankfurt, Germany
Pageruler prestained protein ladder	New England Biolabs, Frankfurt, Germany

1.5. Commercial Kits

Material	Supplier
2.5 mM dNTP Mix	Invitrogen, Darmstadt, Germany
MINI-Protean TGX	Bio-Rad, Feldkirchen, Germany
Mouse IFN-y ELISpot^{Plus} kit (ALP)	Mabtech, Nacka Strand, Germany
NucleoBond Xtra Midi	Macherey-Nagel, Düren, Germany
NucleoSpin Blood QuickPure	Macherey-Nagel, Düren, Germany
NucleoSpin Gel and PCR Clean-up	Macherey-Nagel, Düren, Germany
NucleoSpin Plasmid	Macherey-Nagel, Düren, Germany
OneStep RT-PCR Kit	Qiagen, Hilden, Germany
PNGase F	New England Biolabs, Frankfurt, Germany
RNeasy Mini kit	Qiagen, Hilden, Germany
SuperSignal West Dura Extended Duration Substrate	Thermo Fisher Scientific, Planegg, Germany
Taq DNA Polymerase	Invitrogen, Darmstadt, Germany

1.6. Media and supplements for cell culture

Material	Supplier
DMEM	Sigma-Aldrich, Taufkirchen, Germany
DMEM (high glucose)	Sigma-Aldrich, Taufkirchen, Germany
DPBS	Thermo Fisher Scientific, Planegg, Germany
FBS	Thermo Fisher Scientific, Planegg, Germany
HEPES solution	Sigma-Aldrich, Taufkirchen, Germany
L-Glutamine	Thermo Fisher Scientific, Planegg, Germany
MEM	Sigma-Aldrich, Taufkirchen, Germany
MEM non-essential amino acid solution	Sigma-Aldrich, Taufkirchen, Germany
Penicillin-Streptomycin	Sigma-Aldrich, Taufkirchen, Germany
RPMI-1640 medium	Sigma-Aldrich, Taufkirchen, Germany
SFP eggs	VALO BioMedia GmbH, Cuxhaven, Germany
TrypLE™ Select Enzym	Thermo Fisher Scientific, Planegg, Germany
VP-SFM	Thermo Fisher Scientific, Planegg, Germany

1.7. Buffer

Lysis buffer	**Transfer buffer (conc.)**
1% Triton X-100	24 g Tris
25 mM Tris	114.6 g Glycin
1 M NaCl	ad 1l ddH_2O
5x Running buffer	**Transfer buffer (working solution)**
72.5 g Glycin	80 ml Towbin buffer (conc.)
15,2 g Tris	200 ml Methanol
25 ml 20% SDS	ad 1 l ddH_2O
ad 1l ddH_2O	
Vaccine buffer (pH=7.4)	**50x TAE buffer (pH= 7.4)**
10 mM Tris	242 g Tris
140 mM NaCl	57.1 ml acetic acid glacial
	18.6 g EDTA

	ad 1l ddH_2O
LB-Medium (pH= 7.5)	**LB-agar**
5 g NaCl	1,5% Agar-Agar in LB-Medium
5 g Yeast extract	
10 g Trypton	
ad 1l ddH_2O	
10x PBS	
2 g KCl	
2 g KH_2PO_4	
80 g NaCl	
11.5 g Na_2HPO_4	
ad 1l ddH_2O	

1.8. Software

Adobe Reader	Adobe Systems, San Jose, USA
A.EL.VIS V6.1	A.EL.VIS GmbH, Hannover, Germany
BioRender	BioRender, Toronto, USA
DNASTAR Lasergene	DNASTAR, Inc., Madison, Wisconsin, USA
FlowJo LLC	BD Life Sciences, Ashland, USA
GraphPad prism	GraphPad Software, San Diego, USA
Image Lab 5.0 Software	Bio-Rad, Feldkirchen, Germany
Microsoft Office 2016	Microsoft Corp., Redmond, USA
NetNGlyc 1.0 Server	http://www.cbs.dtu.dk/services/NetNGlyc/

XII. DANKSAGUNG

Ich möchte mich ganz herzlich bei all jenen Personen bedanken, die mich während der nicht immer einfachen Zeit der Doktorarbeit unterstützt und motiviert haben.

Mein besonderer Dank gilt meinem Doktorvater Herrn **Prof. Dr. Gerd Sutter** für die Gelegenheit, diese Arbeit am Institut für Infektionsmedizin und Zoonosen durchführen zu können. Vielen Dank für wertvolle und hilfreiche Ratschläge, interessante Fachgespräche und die schnelle Korrektur meiner Arbeit.

Vielen Dank an meine Betreuerin Frau **Prof. Dr. Asisa Volz** für die Betreuung sowie fachliche Unterstützung während der Arbeit. Danke für die Durchsicht meiner Arbeit.

Herzlichen Dank an **Astrid Freudenstein** und **Sylvia Jany** für die tatkräftige Unterstützung während der Laborarbeit. Danke für eure Hilfsbereitschaft, eure gute Laune und vor allem eure Geduld bei all meinen Fragen.

Meinen (ehemaligen) Doktorandenkollegen und Doktorandenkolleginnen- **Dr. Svenja Veit, Dr. Daniela Arndt, Dr. Dominik Forster, Liangliang Nan, Leonard Limpinsel, Stephanie Riederer**- möchte ich für eine schöne und spaßige Zeit im Doktorandenzimmer danken. Danke für eure Unterstützung!

Herzlichen Dank an meinen Bürokollegen **Jan Hendrik Schwarz** für die tolle Zusammenarbeit, motivierende Gespräche und unterhaltsame Zeit!

Danke an **Dr. Georgia Kalodimou** und **Dr. Elke Duell** für die Durchsicht und Korrektur meiner Arbeit, sowie der Unterstützung im Labor.

Vielen lieben Dank an alle anderen Kollegen und Kolleginnen der Virologie- allen voran **Nina Hechtberger, Wanda Schroppa, Dr. Robert Fux, Dr. Katrin Printz, Dr. Michael Lehman**- für euer offenes Ohr bei fachlichen Fragen und eure Hilfsbereitschaft.

Und nicht zuletzt möchte ich meiner lieben Familie ganz herzlich danken. Liebe **Mama**, lieber **Papa,** lieber **Robert**, danke für eure liebevolle und wertvolle Unterstützung aus der Ferne. Ohne euch wäre vieles nicht möglich gewesen!